Geology of the Empire Quadrangle Grand, Gilpin, and Clear Creek Counties Colorado

By WILLIAM A. BRADDOCK

GEOLOGICAL SURVEY PROFESSIONAL PAPER 616

UNITED STATES GOVERNMENT PRINTING OFFICE, WASHINGTON : 1969

UNITED STATES DEPARTMENT OF THE INTERIOR

WALTER J. HICKEL, *Secretary*

GEOLOGICAL SURVEY

William T. Pecora, *Director*

Library of Congress catalog-card No. 78–650 226

For sale by the Superintendent of Documents, U.S. Government Printing Office
Washington, D.C. 20402

CONTENTS

	Page
Abstract	1
Introduction	1
Geologic history	2
Petrographic methods	3
Precambrian metamorphic rocks	3
Biotite gneiss	3
Migmatite	6
Calc-silicate gneiss	6
Microcline gneiss (microcline-quartz-plagioclase-biotite gneiss)	6
Hornblende gneiss and amphibolite	8
Origin of metamorphic rocks	10
Nature of premetamorphic rocks	10
Metamorphic facies	13
Precambrian igneous rocks	14
Quartz diorite of St. Marys Lake	14
Boulder Creek Granite	15
Quartz diorite and hornblendite	17
Hornblende diorite and other metamorphosed basic dikes	18
Granite porphyry	18
Silver Plume Granite	19
Pegmatite	19
Tertiary igneous rocks	19
Granodiorite group	20
Hornblende granodiorite porphyry	20
Biotite granodiorite porphyry	22
Granite aplite	22
Tertiary igneous rocks—Continued	
Monzonite group	22
Feldspathoidal hornblende-pyroxene monzonite	22
Hornblende-pyroxene monzonite	26
Porphyritic hornblende-pyroxene monzonite	31
Monzonite porphyry	32
Quartz-bearing monzonite porphyry	32
Leucocratic monzonite	32
Biotite quartz monzonite porphyry	33
Bostonite porphyry	33
Sanidinite porphyry	35
Age and sequence of intrusion	37
Petrology	37
Definition of rock series	37
Calc-alkali series	40
Alkali-calcic series	41
Undersaturated series	43
Summary of petrologic interpretations	45
Quaternary deposits	45
Structure	45
Older deformation (B_o)	45
Younger deformation (B_y)	49
Relations of intrusive rocks to deformations	49
East-northeast-trending folds of unknown origin	51
Faults	51
References	52
Index	55

ILLUSTRATIONS

		Page
PLATE 1.	Geologic map and sections of the Empire quadrangle	In pocket
2.	Index map of Tertiary igneous rocks in the Empire quadrangle, Grand, Gilpin, and Clear Creek Counties, Colo	In pocket
3.	Foliation and lineation diagrams	In pocket
FIGURE 1.	Index map showing location of the Empire quadrangle and the areas covered by other published geologic maps	2
2.	Photomicrographs of muscovite in biotite gneiss	5
3.	Photographs of migmatite, hornblende gneiss, and amphibolite	7
4.	Triangular plot of quartz, plagioclase, and microcline in the granitic part of migmatite from biotite gneiss and from microcline gneiss	8
5.	Triangular plot of quartz, plagioclase, and microcline in microcline gneiss	8
6.	Graph showing comparison of the mineral composition of biotite gneiss with norms of quartz-rich igneous rocks and with mesonorms of sedimentary rocks	10
7.	Triangular diagrams showing the comparison of modes of biotite gneiss and mesonorms of sedimentary rocks	12
8.	Equilibrium curves related to metamorphism in the Empire quadrangle	14
9.	Photomicrographs of the quartz diorite of St. Marys Lake	16
10.	Triangular plot of plagioclase, quartz, and microcline in the Boulder Creek Granite	17
11.	Triangular plot of plagioclase, quartz, and microcline in the Silver Plume Granite	19
12.	Diagrams showing modal compositions of rocks of the Empire stock	23
13.	Photomicrographs of feldspathoidal hornblende-pyroxene monzonite of the Empire stock	24
14.	Photomicrographs of hornblende-pyroxene monzonite, Empire stock	30

		Page
FIGURE	15. Photomicrographs of leucocratic monzonite, bostonite porphyry, and sanidinite porphyry	34
	16. Diagram showing the known sequence of intrusion of Tertiary igneous rocks in the Empire quadrangle	37
	17. Diagram showing relation between normative anorthite and normative quartz or nepheline in Tertiary igneous rocks	38
	18. Larsen plot of analyses of Tertiary igneous rocks	39
	19. Triangular plot of the calc-alkali series	40
	20. Phase diagrams for the anorthite-albite-orthoclase system compared with the trends of the alkali-calcic and calc-alkali series	41
	21. Triangular plot of alkali-calcic series	42
	22. Triangular plot of the anorthite-poor members of the alkali-calcic series	43
	23. Diagram of quaternary nepheline-anorthite-kalsilite-silica system showing the position of the ternary feldspar plane	44
	24. Addition and subtraction diagram used in testing a theory about the origin of feldspathoidal hornblende-pyroxene monzonite	45
	25. Index map of folds and faults in the Empire and Central City quadrangles and adjacent areas	47
	26. Synoptic diagram showing major maximums of foliation and lineation	48
	27. Photomicrographs of cataclastically deformed rocks	50
	28. Diagram showing the strike of large faults and small faults and veins	52

TABLES

		Page
TABLE	1. Mineral assemblages in several varieties of biotite gneiss	4
	2. Modes of microcline gneiss	9
	3. Modes of amphibolite	9
	4. Chemical and spectrographic analyses of hornblende from amphibolite	10
	5. Mesonorms of sedimentary rocks	11
	6. Probable sedimentary parents of biotite gneisses	13
	7. Modes of quartz diorite of St. Marys Lake	15
	8. Modal composition of Boulder Creek Granite	17
	9. Modal compositions of Silver Plume Granite	19
	10. Correlation of Tertiary igneous rock names as used by Wells (1960) and in this report	20
	11. Chemical and spectrographic analyses and CIPW norms of hornblende granodiorite porphyry, biotite granodiorite porphyry, biotite quartz monzonite porphyry, and granite aplite	21
	12. Chemical and spectrographic analyses and CIPW norms of feldspathoidal hornblende-pyroxene monzonite	26
	13. Chemical and spectrographic analyses and CIPW norms of hornblende-pyroxene monzonite, porphyritic hornblende-pyroxene monzonite, and monzonite porphyry	27
	14. Chemical and spectrographic analyses of pyroxene and amphibole from hornblende-pyroxene monzonite of the Empire stock	29
	15. Variation of the composition of plagioclase and alkali feldspar in the hornblende-pyroxene monzonite of the Empire stock	29
	16. Chemical and spectrographic analyses and CIPW norms of quartz-bearing monzonite porphyry and leucocratic monzonite	32
	17. Chemical and spectrographic analyses and CIPW norms of bostonite porphyry and sanidinite porphyry	36
	18. Chemical analyses and CIPW norms of various Tertiary rocks from the Idaho Springs and Central City areas	39
	19. Chemical compositions and CIPW norms of average hornblende-pyroxene monzonite and two hypothetical magmas that would be produced by the removal of pyroxene	42
	20. CIPW norms of hypothetical rocks produced by the removal of pyroxene from feldspathoidal hornblende-pyroxene monzonite	44

GEOLOGY OF THE EMPIRE QUADRANGLE, GRAND, GILPIN, AND CLEAR CREEK COUNTIES, COLORADO

By William A. Braddock

ABSTRACT

The Empire quadrangle, in the central part of the Front Range, is about 35 miles west of Denver, Colo. The bedrock of the quadrangle is made up predominantly of Precambrian metasedimentary, igneous, and metaigneous rocks. The metasedimentary rocks are composed of calc-silicate gneiss and biotite gneiss. A comparison of the mineralogy of the biotite gneiss with mesonorms of common sedimentary rocks indicates that the original sediments were probably interbedded shale, graywacke, and subgraywacke. The gneisses have been metamorphosed to mineral assemblages typical of the upper part of the amphibolite facies. Microcline gneiss (microcline-quartz-plagioclase-biotite gneiss) may be metamorphosed sodic arkose or metamorphosed lava flows or intrusions. Hornblende gneiss and amphibolite may be metasedimentary or metaigneous rocks.

Prior to the completion of metamorphic recrystallization the rocks were plastically deformed to produce folds in B_o that trend north to northeast. The Lawson syncline and the Loch Lomond anticline are large open folds that form the main structure of the eastern part of the quadrangle. Many B_o folds with shorter wavelengths occur northwest of the Loch Lomond anticline. Lineations in A_o about at right angles to the major folds are common and are believed to be the same age as the B_o folds. The intrusive Boulder Creek Granite and quartz diorite and hornblendite form bodies that are conformable to the B_o folds but that have been plastically deformed and recrystallized during folding in B_o.

The Silver Plume Granite was intruded after the period of B_o folding and forms discordant plutons that cut across the older structures but that do not appear to have caused rotation of the older structures.

A period of Precambrian deformation (B_y) younger than the Silver Plume Granite produced catalastic rocks and well-developed folds that trend east-northeast in areas close to the Empire quadrangle. Within parts of the quadrangle, superposed minor folds and lineations and cataclastically deformed rocks probably also formed at this time. The B_y period of folding did not result in noticeable recrystallization of the rocks in the Empire quadrangle.

The northwestern part of the quadrangle contains many northeast-trending faults that appear to branch from the Berthoud Pass fault. Gouge and breccia are the most common materials along the faults, but flaser gneiss and mylonite also occur along certain ones. The contrasting types of fault material suggest that there have been at least two periods of movement widely separated in time on some of the faults. The gouge and breccia were probably formed during Laramide movement; the other cataclastic materials may have been formed during the Precambrian.

Numerous dikes and small plutons of porphyritic igneous rocks of Tertiary age are exposed. From the study of the chemical compositions and petrography of these rocks it appears that two parent magmas, one monzonite and the other granodiorite, developed beneath the quadrangle at about the same time and that differentiated fractions from these parents were emplaced in an overlapping time sequence. The monzonite parent yielded feldspathoidal hornblende-pyroxene monzonite, hornblende-pyroxene monzonite, leucocratic monzonite, and bostonite. The granodiorite parent yielded granodiorite porphyry and quartz monzonite porphyry.

INTRODUCTION

The Empire quadrangle is about 35 miles west of Denver, Colo. (fig. 1). It straddles the Continental Divide and includes portions of Grand, Gilpin, and Clear Creek Counties. The quadrangle is on the west side of the Front Range and on the northwest side of the Front Range mineral belt—a northeast-trending belt of veins and porphyry intrusions of Tertiary age.

Geologic mapping within the quadrangle and adjacent areas done prior to 1950 has been summarized by Lovering and Goddard (1950). Since 1950 the U.S. Geological Survey has published maps and reports on several mining districts near the Empire quadrangle (Harrison and Wells, 1956 and 1959; Sims and others, 1963; Sims and Gable, 1964; Hawley and Moore, 1967; Moench, 1964) and geologic maps and reports on several nearby quadrangles (Sims, 1964; Sheridan and others, 1958; Wells, 1967; Theobald, 1965; Sims and Gable, 1967). Moench, Harrison, and Sims (1962) summarized the Precambrian structure in the Idaho Springs–Central City area, and Tweto and Sims (1963) discussed the relationships of shear zones and faults in the central Front Range to those of other areas in central Colorado. In addition, Harrison and Moench (1961) investigated the joint pattern in the Precambrian rocks of the Central City–Idaho Springs area; Wells, Sheridan, and Albee (1964) studied the relationship between the thick Precambrian quartzite along Coal Creek and the metamorphic rocks in the adjacent areas; and Wells (1960) classified the Tertiary igneous rocks in the vicinity of Idaho Springs and Central City.

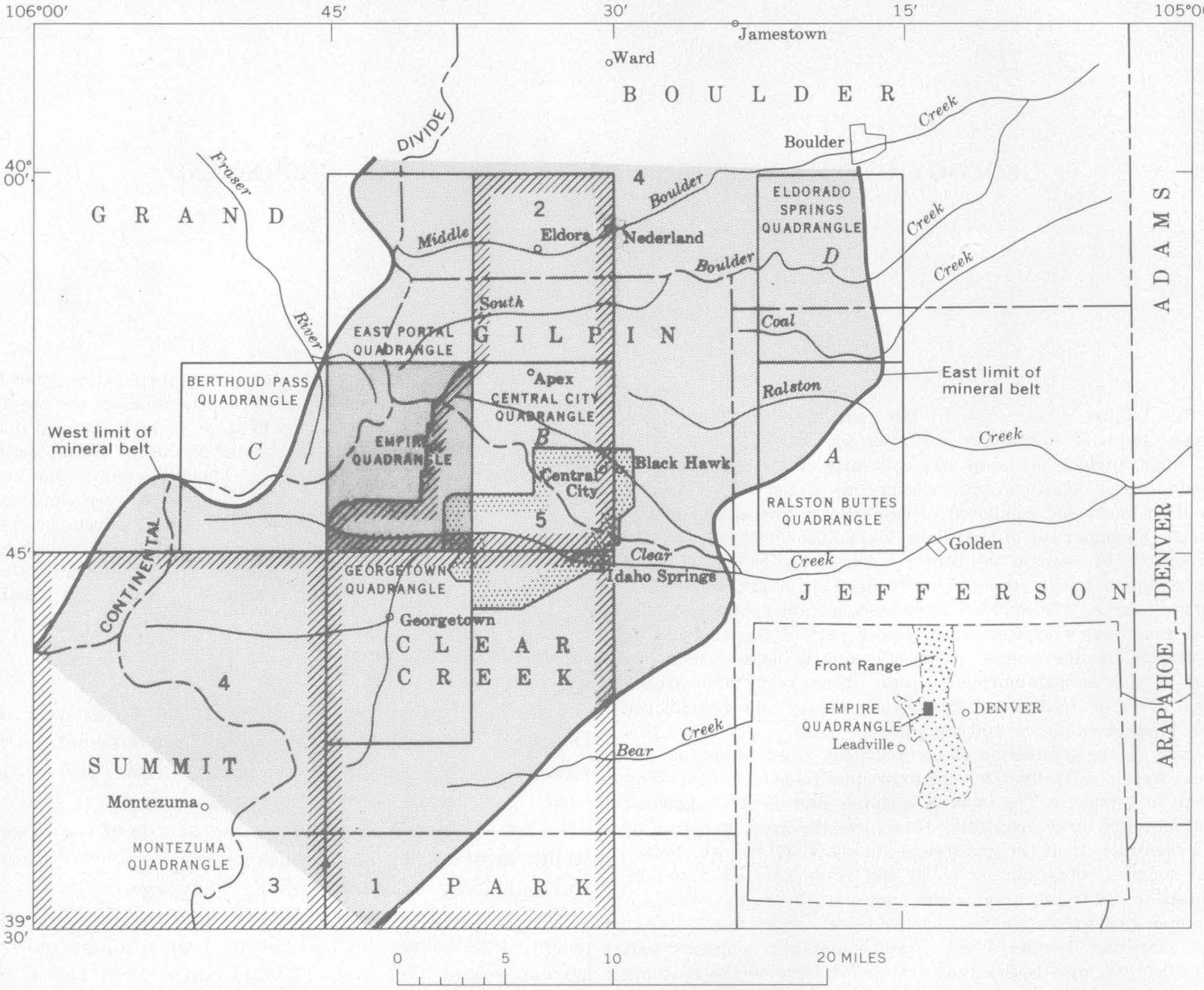

FIGURE 1.—Index map showing location of the Empire quadrangle, Colorado, and the areas covered by other published geologic maps. Quadrangles: *A*, Sheridan, Maxwell, Albee, and Van Horn (1958); *B*, Sims (1964) and Sims and Gable (1967); *C*, Theobald (1965); *D*, Wells (1967). Reports: 1, Spurr and Garrey (1908); 2, Bastin and Hill (1917); 3, Lovering (1935); 4, Lovering and Goddard (1950) (light stipple); 5, Moench, Harrison, and Sims (1962); detailed studies of parts of this area include Harrison and Wells (1956, 1959), Sims, Drake, and Tooker (1963), Moench (1964), Sims and Gable (1964), and Hawley and Moore (1967).

The Empire quadrangle contains the Empire mining district (Lovering and Goddard, 1950, p. 156) and part of the Lawson–Dumont–Fall River district (Hawley and Moore, 1967). No additional studies of the ore deposits of these districts were made in the present investigation.

The Empire quadrangle was mapped during the summers of 1959–62 on a topographic base map (scale of 1:20,000 and a contour interval of 40 ft) made by the U.S. Geological Survey. The writer thanks Melvin Harper and Frederick Files, who assisted with parts of the fieldwork, and Paul K. Sims and Ogden Tweto, who helped the writer become familiar with problems of the geology of the region. He also thanks George Phair, who permitted the inclusion of five chemical analyses of igneous rocks from the Empire stock, and, particularly, Dolores J. Gable and Robert H. Moench for their careful criticism of the manuscript.

GEOLOGIC HISTORY

The earliest event that can be inferred from the study of the rocks of the Empire quadrangle was the deposition of a thick sequence of clastic sediments that perhaps contained interbedded volcanic rocks. The time of deposition and the nature and extent of the depositional environment are unknown. An extended period of intense folding and regional metamorphism that was accompanied by the emplacement of plutons of Boulder Creek Granite and other less abundant igneous rocks occurred about 1.7 billion years ago (Hedge and others, 1967). During this period the sedimentary rocks were converted to gneisses and schists of high metamorphic grade and were deformed into folds trending north-northeast. About 1.4 billion years ago the Silver Plume Granite, which forms extensive bodies throughout the central Front Range, was emplaced (Peterman and others, 1968). Following the intrusion of the Silver Plume, the area was again subjected to strong tectonic forces that produced small folds and shear zones that trend northeast to east-northeast. This later Precambrian deformation, although regionally extensive, was not as intense as the earlier deformation and did not result in noticeable recrystallization of the rocks.

During latest Cretaceous and early Tertiary time the region was faulted, uplifted, and intruded by a series of porphyritic igneous rocks, and vein deposits were formed. Certain faults that were active during the Laramide deformation, however, may have been initiated in late Precambrian time.

Glaciers eroded the region during the Pleistocene and produced the rugged topography, typical of the Continental Divide area, and moraines and outwash deposits along major valleys. Recent deposits of talus, solifluction debris, and alluvium and mine and mill waste occur in many places in the quadrangle.

PETROGRAPHIC METHODS

A substantial part of this study involved the examination of thin sections and selected specimens of igneous and metamorphic rocks. The thin sections were cut perpendicular to any visible foliation or lineation and were stained with sodium cobaltinitrite to facilitate identification of potassium feldspar. Modal mineral compositions were determined by point counting; generally 500–1,000 points were distributed uniformly over a single thin section.

The composition of plagioclase feldspar was determined by several methods. Unzoned, unaltered plagioclase that could be easily separated from the rock was fused, and the refractive index of the resulting glass was measured. Plagioclase that was strongly zoned, somewhat altered, or difficult to separate was identified by measuring the extinction angle in sections cut normal to the *a* crystallographic axis or by measuring the angle between the Z optical direction and the normal to the albite twin plane. The composition of alkali feldspar was determined by measuring the position of the X-ray spectrometer peak for the ($\bar{2}01$) plane of purified material that had been heated at 1,000°C for 40 hours (Orville, 1958). The composition of nepheline was determined from the position of the X-ray spectrometer peak for the (210) plane (Smith and Sahama, 1954).

PRECAMBRIAN METAMORPHIC ROCKS

Well-foliated rocks of high metamorphic grade make up most of the terrain in the Empire quadrangle. These rocks consist of various biotite and sillimanitic biotite gneisses and calc-silicate gneisses called the Idaho Springs Formation by S. H. Ball (in Spurr and Garrey, 1908, p. 37), hornblende gneiss and amphibolite, called the Swandyke Hornblende Gneiss by Lovering and Goddard (1950, p. 20); and microcline gneiss, called quartz monzonite gneiss by S. H. Ball (in Spurr and Garrey, 1908, p. 46). All these rocks have features which clearly indicate that they have been intensely deformed and recrystallized. All geologists who have worked in the area have interpreted most of the biotite gneiss and calc-silicate gneiss as metamorphosed sedimentary rocks. Previous geologists have, however, expressed diverse opinions about the origin of the hornblende gneiss, amphibolite, and microcline gneiss; some believe these rocks to be of igneous origin, whereas others believe them to be of sedimentary origin.

BIOTITE GNEISS

Biotite gneiss is a fine- to medium-grained rock that has a well-developed foliation imparted by the parallel orientation of biotite and by the segregation of the minerals into light and dark layers. It is the most abundant type of metamorphic rock in the quadrangle. The mineralogy is varied: quartz, plagioclase, and biotite are the most abundant minerals; microcline, sillimanite, muscovite, and garnet are less abundant; and magnetite, apatite and sphene form common accessory minerals. Characteristic assemblages of the major minerals are shown in table 1. Alternate layers of gneiss having different mineral assemblages may be only a few millimeters thick or may be several feet thick.

The texture of the most of the gneiss is simple; anhedral grains of quartz and feldspar form a granoblastic matrix that encloses moderately well oriented books of undeformed biotite. Sillimanite commonly occurs in concentrations along quartz-rich laminae, where it forms bundles of very fine fibers, or in concentrations of larger prisms whose long axes lie in the plane of foliation. Sillimanite may also occur in biotite-rich layers where it is included in the biotite. Garnet forms anhedral grains that poikiloblastically enclose quartz and feldspar. No textures were observed that would indicate that the garnets were rotated during growth.

TABLE 1.—*Mineral assemblages in several varieties of biotite gneiss, in volume percent*

[----, not observed]

Mineral assemblage	Biotite-quartz-plagioclase (Common assemblage. Sillimanitic varieties are rare)											
Sample No.	1	2	3	4	5	6	7	8	9	10	11	12
Field No.	9-79B	5-120	1-99D	1-10	4-179A	2-131	2-121B	6-101A	3-20	6-50A	1-92B	9-58
Quartz	≈15	≈35	32	32	≈30	≈25	≈30	≈30	≈65	≈56	35	47
Microcline	----	----	----	----	----	----	----	----	----	----	----	----
Plagioclase	≈75	≈35	30	48	≈50	≈45	≈50	≈50	≈25	≈33	1	19
Sillimanite	----	----	----	----	----	----	----	----	----	----	19	2
Biotite	≈10	≈30	37	18	≈20	≈20	≈20	≈20	≈10	≈11	41	28
Muscovite	----	----	----	1	----	----	----	----	----	----	----	5
Garnet	----	----	----	----	----	----	----	----	----	----	----	----
Other	----	----	1	<1	----	[1] ≈10	≈2	----	----	----	4	<1
Composition of plagioclase	An_{32}	An_{66}	An_{67}	An_{31}	An_{43}	An_{30}	An_{30}	An_{35}	----	An_{37}	----	----
Sample coordinates [2]	3.2–2.7	14.8–26.8	27.2–42.5	33.3–31.2	29.4–15.9	15.6–43.6	15.2–43.7	8.9–18.7	7.4–31.1	1.9–20.8	25.0–37.7	4.6–2.4

Mineral assemblage	Sillimanite-biotite-quartz (Rare assemblage, locally garnetiferous, minor muscovite)					Biotite-quartz-plagioclase-microcline (Common assemblage, minor muscovite)							
Sample No.	13	14	15	16	17	18	19	20	21	22	23	24	25
Field No.	6-129B	3-42	1-91A	5-45	10-108B	1-3	1-29B	6-191	4-104B	10-108C	G-1C	11-106C	4-169
Quartz	≈37	40	48	51	63	27	34	36	46	46	≈50	51	56
Microcline	----	----	----	----	----	12	18	6	17	1	≈5	22	10
Plagioclase	----	----	----	----	----	45	38	28	19	39	≈30	17	23
Sillimanite	≈27	18	14	9	4	----	----	----	----	----	----	----	----
Biotite	≈27	40	34	38	32	15	7	23	16	13	≈5	10	6
Muscovite	≈9	2	----	----	<1	----	<1	----	2	----	----	1	2
Garnet	----	----	----	2	----	----	----	----	----	----	----	----	----
Other	----	----	3	----	<1	<1	2	[3] 7	1	<1	----	<1	2
Composition of plagioclase	----	----	----	----	----	An_{28}	An_{25}	An_{35}	An_{21}	An_{27}	----	----	An_{21}
Sample coordinates [2]	7.1–27.0	5.4–43.7	25.8–38.5	24.0–22.7	34.9–4.3	30.6–32.7	30.3–30.6	4.1–29.3	34.5–28.6	34.9–4.3	15.2–1.8	22.2–42.8	28.6–18.7

Mineral assemblage	Sillimanite-biotite-quartz-plagioclase-microcline-muscovite (Common assemblage. Garnetiferous varieties are rare)										
Sample No.	26	27	28	29	30	31	32	33	34	35	36
Field No.	11-106A	6-147	9-31	13-70	9-143	6-50B	6-199A	9-143A	1-21D	2-182B	1-40
Quartz	≈15	22	26	28	29	31	32	33	35	38	42
Microcline	<5	19	19	8	27	25	8	12	7	12	11
Plagioclase	≈40	9	5	12	8	8	3	14	6	17	8
Sillimanite	<5	12	6	8	11	9	6	7	18	8	2
Biotite	≈15	37	27	35	21	21	40	29	32	20	30
Muscovite	<5	----	15	9	1	6	11	5	1	4	----
Garnet	----	<1	----	----	----	----	----	----	----	----	8
Other	----	----	3	----	2	----	----	<1	1	1	----
Composition of plagioclase	An_{20}	----	----	----	----	An_{26}	----	An_{24}	----	An_{20}	An_{26}
Sample coordinates [2]	22.2–42.8	5.1–28.7	6.7–1.2	10.7–32.3	4.5–8.0	1.9–20.8	5.7–30.3	4.5–8.0	29.8–33.3	14.3–36.1	26.8–31.0

Mineral assemblage	Sillimanite-biotite-quartz-plagioclase-microcline-muscovite (Common assemblage. Garnetiferous varieties are rare)—Continued										
Sample No.	37	38	39	40	41	42	43	44	45	46	47
Field No.	11-54	2-79	9-54C	1-91B	2-69	6-185B	2-182A	9-78	6-101B	6-185A	6-199B
Quartz	45	44	46	50	50	54	58	59	61	65	73
Microcline	11	4	8	13	3	8	9	7	<1	8	4
Plagioclase	11	6	10	20	16	4	22	15	22	13	15
Sillimanite	10	14	14	4	1	14	<1	2	<1	<1	1
Biotite	20	31	19	12	20	18	8	12	13	13	5
Muscovite	2	1	4	----	10	2	1	3	3	<1	1
Garnet	----	----	----	----	----	----	----	----	----	----	----
Other	2	<1	----	2	<1	----	1	1	----	----	----
Composition of plagioclase	An_{26}	An_{27}	An_{26}	An_{26}	----	An_{20}	----	An_{24}	An_{20}	An_{24}	An_{20}
Sample coordinates [2]	22.2–36.2	15.9–36.1	4.8–1.9	25.8–38.5	15.4–43.5	1.7–29.1	14.3–36.1	4.5–2.9	8.9–18.7	1.7–29.1	5.7–30.3

[1] Sphene.
[2] Sample coordinates are given in thousands of feet east and north of the southwest corner of the Empire quadrangle. The first number is the east coordinate, and the second number is the north coordinate.
[3] Contains 5 percent hornblende.

NOTE.—All modes showing specific amounts of minerals represent 500 points over a single thin section. For these the amounts have been rounded to the nearest percent. Those modes showing approximate amounts of minerals were visually estimated.

Muscovite occurs as sericite in the alteration products of plagioclase and sillimanite, as small books intergrown with biotite, and as coarse poikiloblastic grains replacing sillimanite and adjacent minerals. The sericite commonly occurs in rocks showing indications of hydrothermal alteration such as chloritized biotite, and much of the sericite probably was produced by the Tertiary hydrothermal activity that formed the Front Range mineral belt. The muscovite that forms small books associated with biotite (fig. 2*A*) does not show any textural evidence indicating that it is a late mineral, and it occurs with sillimanite and microcline. It appears to have been a stable member of the mineral assemblage. This type of muscovite has been found at scattered localities throughout the quadrangle. The poikiloblastic muscovite is concentrated in layers rich in sillimanite (fig. 2*B*, *C*), and it encloses sillimanite grains, some of which are clearly rounded. Commonly (001) of the muscovite

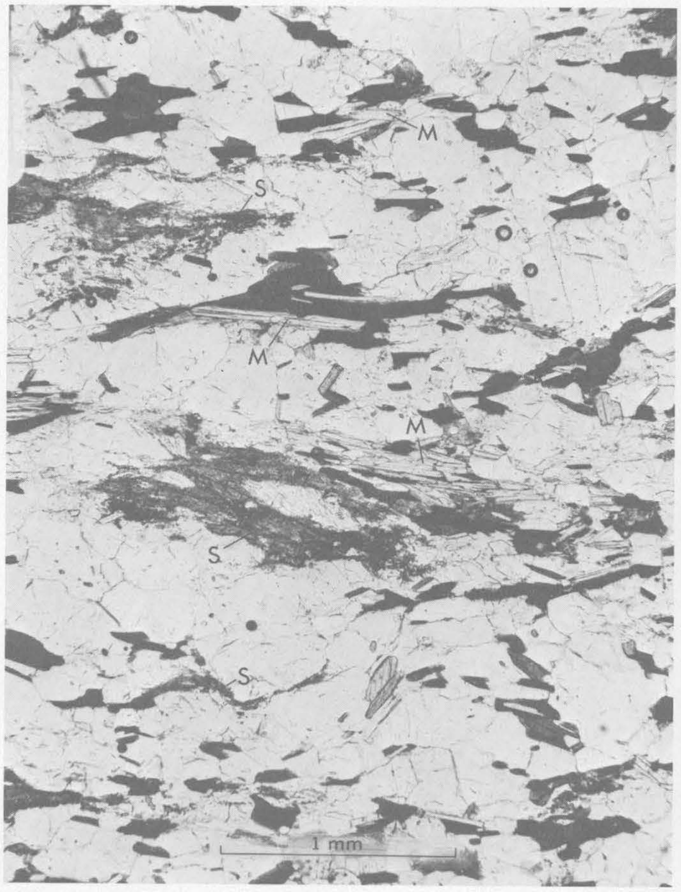

A

B

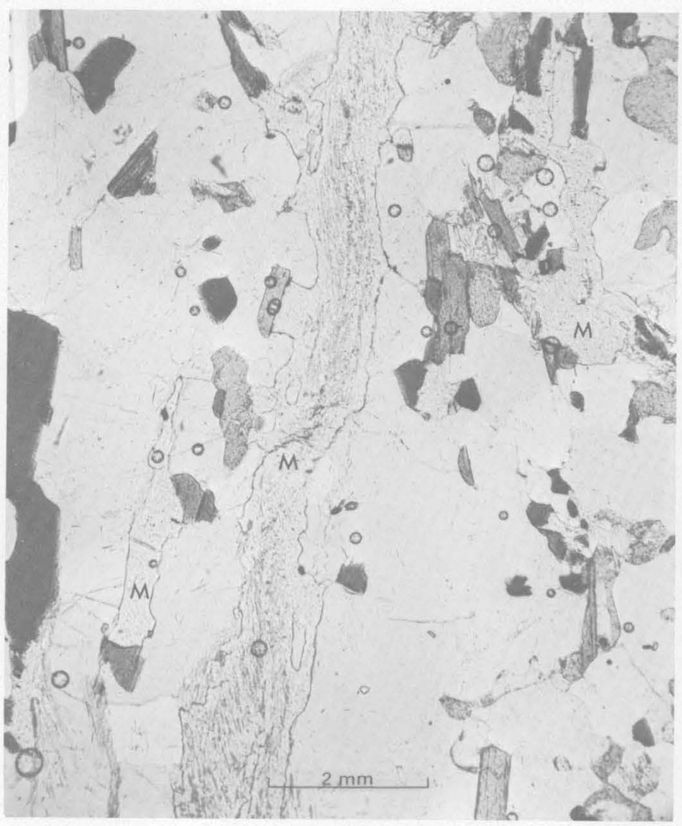

C

FIGURE 2.—Photomicrographs of muscovite in biotite gneiss. *A*, Small books of muscovite (M) associated with biotite (black). Bundles of fibrous sillimanite (S) are not replaced by muscovite. Plain light. *B*, Large poikiloblasts of muscovite (M) containing remnants of bundles of sillimanite. Plain light. *C*, Large poikiloblasts of muscovite (M). The large central area of muscovite is a single crystal that has developed along a sillimanite layer, and contains residual needles of sillimanite. Plain light.

is nearly perpendicular to the foliation, even though the grains are elongate along sillimanite layers parallel to the foliation. The poikiloblastic muscovite apparently is a late mineral that has formed because potassium and water were introduced into the sillimanite-bearing rocks. Late muscovite of this type is not spatially related to Tertiary veins but, on the contrary, is most abundant in sillimanitic rocks in the southwestern part of the quadrangle and in the northeast-trending zone of faults in the northern and western parts of the quadrangle. In the western part the late muscovite has commonly been moderately to strongly deformed and contains well-formed kink bands (fig. 27*B*).

Microcline is a common mineral in several varieties of biotite gneiss. The particularly signficant sillimanite-biotite-quartz-plagioclase-microcline mineral assemblage, in which the sillimanite and microcline appear

332-862 O—69——2

to be in equilibrium, occurs throughout the quadrangle. The microcline in this assemblage is noticeably perthitic, whereas the microcline in the biotite-quartz-plagioclase-microline assemblage is weakly perthitic to nonperthitic.

Plagioclase occurs in most mineral assemblages. Its composition is extremely variable in the simpler assemblages, ranging from An_{30} to An_{67} (table 1). In the more complex assemblages the plagioclase is dominantly oligoclase, and in the sillimanite-biotite-quartz-plagioclase-microcline-muscovite assemblage the average composition is An_{24}.

MIGMATITE

Well-foliated biotite gneiss is very commonly mixed with thin to thick layers of poorly foliated granitic gneiss forming migmatite (fig. 3*A*). The amount of granitic material ranges from a few percent to nearly 100 percent of the volume of large outcrops. In adjacent areas, Harrison and Wells mapped migmatite where there are moderate amounts of interlayered granitic material (1956, p. 49), and granite gneiss and pegmatite where the granitic material predominates (1956, p. 50; 1959, p. 11). Within the Empire quadrangle, similar, but less abundant, layers of granitic gneiss also occur in the microcline gneiss and in hornblende gneiss.

The granitic part of the migmatite is fine to coarse grained or pegmatitic and is most commonly found as conformable layers, although local crosscutting relationships have been observed at many locations. (See lowest horizontal granitic layer shown in fig. 3*A*). Biotite is generally very sparse in the granitic part, although sporadic wisps of biotite-rich material commonly delineate the foliation. Quartz, microcline, and oligoclase usually make up more than 90 percent of the granitic part of the gneiss, and biotite, muscovite, sillimanite, and opaque oxides occur in small amounts. The relative abundance of the principal minerals of 18 samples of the granitic part is shown in figure 4. The texture of the rock is typically xenomorphic granular; the microcline is slighly to moderately perthitic and is commonly enclosed by myrmekite.

CALC-SILICATE GNEISS

Calc-silicate gneiss is a minor rock unit occurring in mappable bodies at only two places in the quadrangle. At the extreme south edge of the quadrangle, south of Empire, there is a layer of calc-silicate gneiss more than 100 feet thick that is interlayered with biotite gneiss to the south. Similar calc-silicate gneiss interlayered with biotite gneiss crops out on the top of the ridge between Silver Creek and Cumberland Gulch. The principal minerals are quartz, hornblende, diopside, plagioclase, garnet, epidote, scapolite, and sphene, which occur in layers that impart a distinct gneissic structure to the rock. The proportions of the different minerals vary noticeably from layer to layer. Commonly, thin layers of quartz gneiss alternate with hornblende-plagioclase-sphene layers or with diopside-quartz-scapolite layers. Garnetiferous layers are common and have been observed to consist of quartz-garnet-diopside and quartz-epidote-garnet-sphene.

MICROCLINE GNEISS (MICROCLINE-QUARTZ-PLAGIOCLASE-BIOTITE GNEISS)

Microcline gneiss is a light- to yellowish-gray granitic-looking rock that occurs in comformable layers throughout the quadrangle. It is abundant in the southern and eastern parts of the quadrangle and sparse elsewhere. Quartz, plagioclase, and microcline make up more than 75 volume percent of the rock and average about 92 percent (compositions are based on 62 modes from single thin sections; table 2). The proportions of these three minerals vary widely (fig. 5). The average volumes of other constituents are biotite, 4.6 percent; muscovite, 1.0 percent; opaque oxides, 0.9 percent; and miscellaneous minerals, 0.5 percent. Hornblende occurs in some samples, where it ranges from a trace to 9 percent.

A weak to moderate gneissic layering due to minor variations in the proportions of the major minerals is apparent on most outcrops. A semischistose structure due to a crude dimensional alinement of biotite, quartz, and feldspar is visible in hand specimens.

Quartz forms anhedral grains with weak to moderate undulatory extinction. Plagioclase forms subhedral to anhedral grains. The composition of the plagioclase ranges from An_{14} to An_{33} and averages An_{23}. Microcline is anhedral and occurs as irregular grains interstitial to quartz and plagioclase, as large grains, and as rectangular patches in the plagioclase resembling antiperthite. The microcline is characteristically intensely grid-twinned and very slightly perthitic. Myrmekitic intergrowths of plagioclase and quartz that replace microcline are present in nearly all thin sections. Biotite is distributed uniformly throughout the rock and shows poor dimensional orientation parallel to the foliation. Muscovite occurs in most samples either as subhedral tablets irregularly intergrown with biotite or as large poikiloblastic grains. Hornblende may be present in those layers which are closely associated with hornblende gneiss or amphibolite.

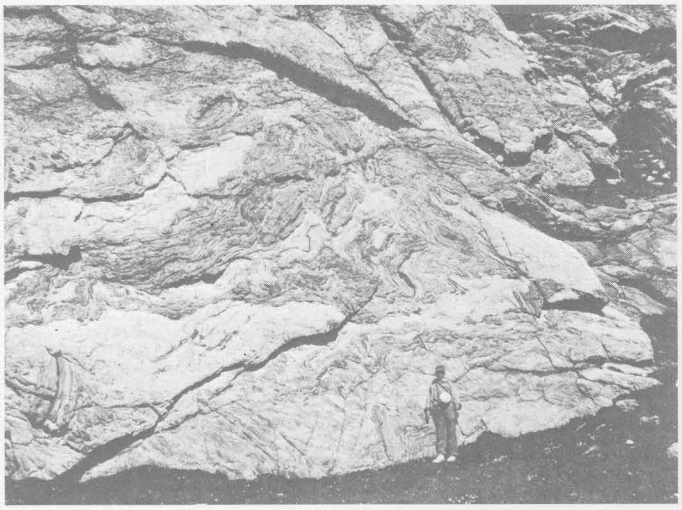

A

B

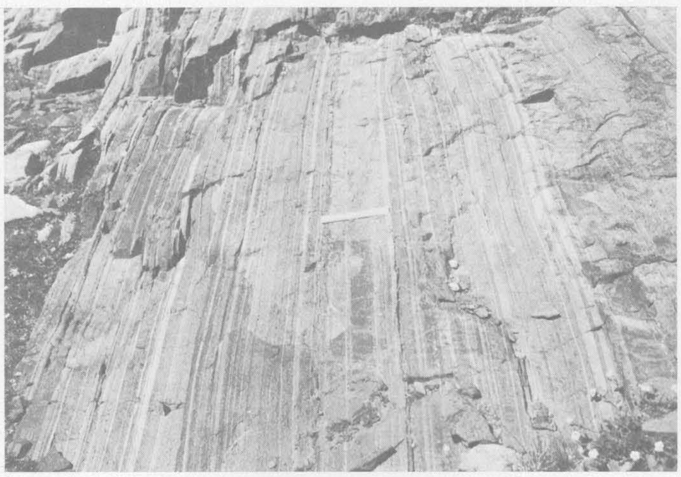

C

FIGURE 3.—Migmatite, hornblende gneiss, and amphibolite. *A*, Intensely migmatized biotite gneiss on the west shore of Reynolds Lake. White layers are the granitic part of the migmatite. *B*, Interlayered microcline gneiss, hornblende gneiss, and amphibolite. The light-colored layers are microcline gneiss, and the darkest layers are amphibolite. The gray layers are quartz-plagioclase-hornblende gneiss. Several of the amphibolite layers have been boudinaged and plastically thinned by rock flow. The outcrop is on the west side of Ohman Lake. The 12-inch hammer shows the scale. *C*, Hornblende gneiss. White layers are plagioclase-quartz rock; gray to black layers are hornblende-plagioclase-quartz rock in which the proportions of the three minerals vary widely. The outcrop is at an altitude of about 11,600 feet on the headwaters of the Fall River, just west of the Bancroft microcline gneiss layer. Six-inch ruler gives the scale.

The thick layer of microcline gneiss on the east side of the quadrangle extends at least 7 miles northeast through the Central City 7½-minute quadrangle (Sims, 1964) and has been named the Lawson layer by Moench, Harrison, and Sims (1962, p. 39). This thick unit apparently pinches out just north of the Fall River. (See cross section C–C′, pl. 1.) The microcline gneiss layer that extends north-northeast on the east flank of Mount Bancroft is here named the Bancroft layer and is believed to be stratigraphically equivalent to the Lawson layer. These two layers have similar mineralogies (fig. 5), and both are associated with hornblendic rocks. The Lawson layer contains lenses of amphibolite; the Bancroft layer contains thin unmapped layers of amphibolite and is overlain and underlain in part by hornblende gneiss. The contacts of the Lawson and Bancroft layers appear to be conformable with the foliation in the adjacent biotite and hornblende gneisses. No crosscutting relations were observed.

The large body of microcline gneiss that lies west of (and apparently stratigraphically below) the Lawson layer on Red Elephant Hill is variable in composition, texture, and structure. Much of the rock along the irregular southwest margin of this body is coarser grained than typical microcline gneiss and lacks foliation. The thin layers of gneiss in the central and northeastern parts of the quadrangle also have variable composition, but they characteristically are foliated and appear to be conformable with overlying and underlying biotite gneiss.

The discontinuous microcline gneiss layers in the southwestern part of the quadrangle and on Breckinridge Peak contain as much as 68 percent quartz and in part could be classed as feldspathic quartzite.

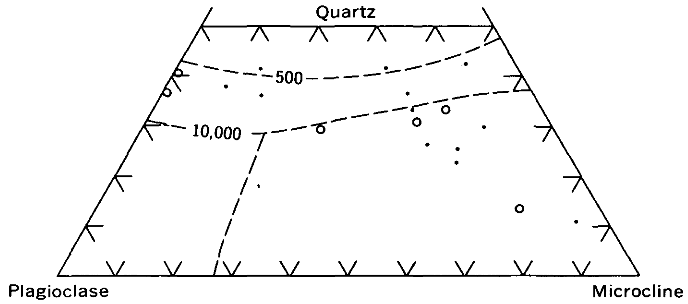

FIGURE 4.—Triangular plot of quartz, plagioclase, and microcline in the granitic part of migmatite from biotite gneiss (dots) and from microcline gneiss (circles). Modal volume percent. All samples contain more than 90 percent quartz and feldspar. Dashed lines are the cotectics between quartz and alkali feldspars at various water pressures (Tuttle and Bowen, 1958, p. 75; Luth and others, 1964, p. 766).

HORNBLENDE GNEISS AND AMPHIBOLITE

Hornblende gneiss and amphibolite are greenish-black to black and white fine- to medium-grained gneisses composed principally of hornblende, plagioclase, and quartz. Amphibolite (table 3) does not contain numerous layers marked by different mineral composition. It occurs as separate layers a few inches to 100 feet thick interlayered with hornblende gneiss or microcline gneiss or biotite gneiss. Internally the amphibolite has a semischistose structure due to the elongation of the amphibole and plagioclase in the plane of foliation. Hornblende gneiss is a mixed rock containing alternating layers of hornblende-plagioclase-quartz rock, plagioclase-quartz rock, and amphibolite and characteristically has a pronounced layered structure (fig. 3*B*, *C*).

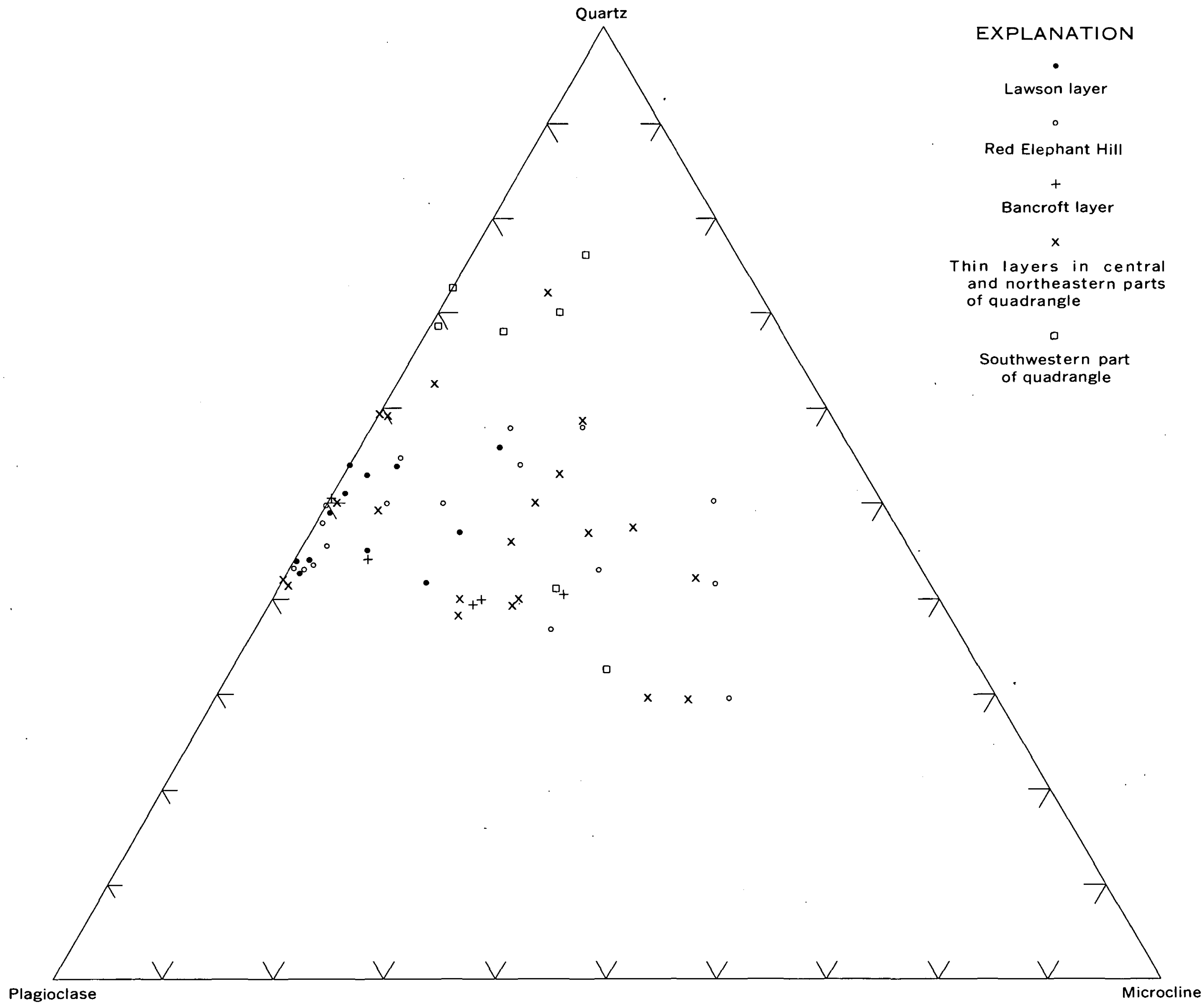

FIGURE 5.—Triangular plot of quartz, plagioclase, and microcline in microcline gneiss. Modal volume percent.

TABLE 2.—*Modes, in volume percent, of microcline gneiss*

[Number of samples analyzed is shown in parentheses. Tr., trace; ----, not observed]

	Lawson layer (13)		Bancroft layer (5)		Red Elephant Hill (17)		Central and northeastern parts of quadrangle (20)		Southwestern part of quadrangle (7)	
	Range	Average	Range	Average	Range	Average	Range	Average	Range	Average
Quartz	39 -55	45	35 -45	39	29 -55	44	26 -61	42	29 -68	56
Microcline	Tr.-13	5	Tr.-24	12	1 -45	14	Tr.-38	15	Tr.-30	11
Plagioclase	31 -53	44	32 -45	39	14 -55	38	16 -56	32	12 -30	24
Biotite	.3- 6.6	2.3	3.6- 7.1	5.5	.1- 6.4	2.6	.7-14.0	7.2	3.2- 9.8	5.7
Hornblende	0 - 9	1.4	0 - 7.5	1.5	----	----	----	----	----	----
Muscovite	0 - 2.0	.5	0 - 1.0	.3	0 - 3.4	.3	0 - 6.6	1.6	0 - 4.4	2.0
Opaque	Tr.- 2.3	.9	.3- 1.2	.8	Tr.- 2.4	1.0	Tr.- 2.3	.8	.1- 2.1	1.0
Others [1]	Tr.- .9	Tr.	.3- 2.9	1.0	Tr.- 1.8	.4	Tr.- 4.5	.4	----	Tr.

[1] Includes epidote, sillimanite, garnet, zircon, apatite, and sphene.

TABLE 3.—*Modes, in volume percent, of amphibolite*

[----, not observed; Tr., trace]

	1				2		
Sample No.	C5-10	C10-52B	C6-35	C7-26	2-18B	[1] 11-61A	Va
Plagioclase	33	54	47	28	45	38	47
Hornblende	41	31	44	60	33	46	49
Pyroxene	6	----	8	----	----	----	----
Quartz	16	6	1	8	20	16	2
Biotite	----	9	----	1	----	----	Tr.
Opaque	1	Tr.	----	2	Tr.	Tr.	----
Accessory	3	Tr.	Tr.	1	2	Tr.	2

[1] Amphibolite layer in hornblende gneiss.

1. Amphibolites associated with the Lawson layer of microcline gneiss (C. C. Hawley, written commun., 1962).
2. Amphibolites associated with the Bancroft layer of microcline gneiss.

Internally the layers of the gneiss have a semischistose structure.

The largest grains of hornblende, plagioclase, or quartz in thin sections commonly have an average diameter of about 0.5 mm, although unusually coarse-grained layers may have grains 2.75 mm in diameter. Quartz forms anhedral grains, elongated in the plane of foliation, which commonly show moderate undulatory extinction. Plagioclase forms anhedral to subhedral grains also elongated in the foliation planes. The composition of the plagioclase in five samples ranges from An_{30} to An_{38}. Hornblende forms anhedral to subhedral grains elongated in the foliation plane. It also appears that the long dimensions of the crystals (the *c* crystallographic axis) are roughly parallel to macroscopic lineations. Chemical analyses of two hornblende samples (table 4) indicate that the amphibole can be classed as common hornblende. Apatite, zircon, epidote, chlorite, and sericite occur as accessory minerals or alteration products. The structural formulas of two samples of hornblende analyzed in table 4 are as follows:

Structural formulas

$A_{0\to1}X_2Y_5Z_8O_{22}(OH, F, O)_2$
[Number of ions on the basis of 24 (O, OH, F, Cl)]

	1		2	
Si	6.39	8.00=Z	6.71	8.00=Z
Al	1.61		1.29	
Al	.47	4.99=Y	.38	5.02=Y
Ti	.13		.08	
Fe^{+3}	.69		.50	
Mg	1.98		2.61	
Fe^{+2}	1.66		1.40	
Mn	.06		.05	
Ca	1.86	2.47=$A+X$	1.91	2.37=$A+X$
Na	.33		.25	
K	.28		.21	
OH	1.72	1.88	1.83	1.97
F, Cl	.16		.14	
100 Mg: (Mg+Fe^{2}+Fe^{3}+Mn)	45.1		57.2	

1. Field No. 11-61C; lab. No. I4055.
2. Field No. V; lab. No. I4056.

Hornblende gneiss and amphibolite occur dominantly as conformable sheets interlayered with microcline gneiss. This relation is widespread in the central Front Range and adjacent areas (Moench and others, 1962, p. 39; Bergendahl, 1963, p. D5–D6). In the Empire quadrangle, amphibolite is most common in the outcrop areas of the Lawson layer of microcline gneiss, and hornblende gneiss is most common in the outcrop areas of the Bancroft layer of microcline gneiss. A few thin layers of amphibolite are interbedded with biotite gneiss on James Peak and southwest of Mount Eva.

Apparently hornblende gneiss and amphibolite were relatively competent rocks during the major period of deformation. Thin layers have been pulled apart to form boudinage structures or compressed into simple folds that are disharmonic relative to the complex folds of adjacent layers of microcline gneiss. Thick layers of hornblende gneiss and amphibolite have simple internal structures and do not show the complex small folds that are common to microcline gneiss and biotite gneiss. At no place in the Empire quadrangle was hornblende gneiss or amphibolite found to crosscut the structures of adjacent rocks.

TABLE 4.—*Chemical and spectrographic analyses of hornblende from amphibolite*

[Chemical analyses by D. F. Powers; spectrographic analyses by J. C. Hamilton]

Chemical analyses, in weight percent					
	1	2		1	2
SiO_2	42.35	45.37	H_2O+	1.71	1.85
TiO_2	1.09	.71	H_2O-	.04	.02
Al_2O_3	11.73	9.59	F	.17	.19
Fe_2O_3	6.03	4.50	Cl	.32	.17
FeO	13.14	11.34	P_2O_5	.04	.01
MnO	.52	.37			
MgO	8.83	11.85	Subtotal	100.12	99.96
CaO	11.52	12.04	Less O=F, Cl	.14	.12
Na_2O	1.15	.88			
K_2O	1.48	1.07	Total	99.98	99.84

Spectrographic analyses, in weight percent [1]					
Ba	0.005	0.003	Sc	0.005	0.003
Co	.003	.002	Sr	.005	.003
Cr	.007	.02	V	.02	.02
Cu	.002	0.	Y	.005	.003
Ga	.003	.002	Yb	.0005	.0003
Ni	.005	.007	Zr	.005	.0015

[1] Looked for but not detected: Ag, As, Au, B, Be, Bi, Cd, Ce, Ge, Hf, Hg, In, La, Li, Mo, Nb, Pb, Pd, Pt, Re, Sb, Sn, Ta, Te, Th, Tl, U, W, Zn, Pr, Nd, Sm, Eu.

1. Field No. 11–61C; lab. No. I4055. Hornblende from amphibolite layer in hornblende gneiss 1,300 ft S. 25° W., from south end of James Peak Lake at altitude 12,000 ft. Mode of enclosing rock given in table 3, sample 11–61A.
2. Field No. V; lab. No. I4056. Hornblende from amphibolite at the south end of Ohman Lake. Mode of enclosing rock given in table 3, sample Va.

ORIGIN OF METAMORPHIC ROCKS

NATURE OF PREMETAMORPHIC ROCKS

The biotite gneiss of the Empire quadrangle is almost certainly the product of metamorphism of sedimentary rocks. This conclusion is based on several facts: in the northeastern Front Range similar gneisses can be traced into areas of lower metamorphic grade where their sedimentary nature is clearly visible (Nutalaya, 1966); the well-developed layering formed by the alternation of strata of different compositions is most reasonably interpreted as relict bedding; the mineral composition of the gneiss is unlike that which would be produced by the metamorphism of common igneous rocks but is similar to that which would be produced from common sedimentary rocks. The validity of this last statement is shown in figure 6, where the composition of the gneiss is compared with the mesonorms (discussed below) of quartz-rich igneous rocks and sedimentary rocks.

Relict bedding is the only sedimentary feature that has been preserved in the gneiss, so attempts to relate the gneiss to particular sedimentary rock parents must be based on comparisons of chemical compositions. Such comparisons are difficult to make, however, because combined chemical and petrographic data on sedimentary rocks are few and because it is not known how much metasomatism may have accompanied metamorphism. Further, as no chemical analyses of the gneiss in the

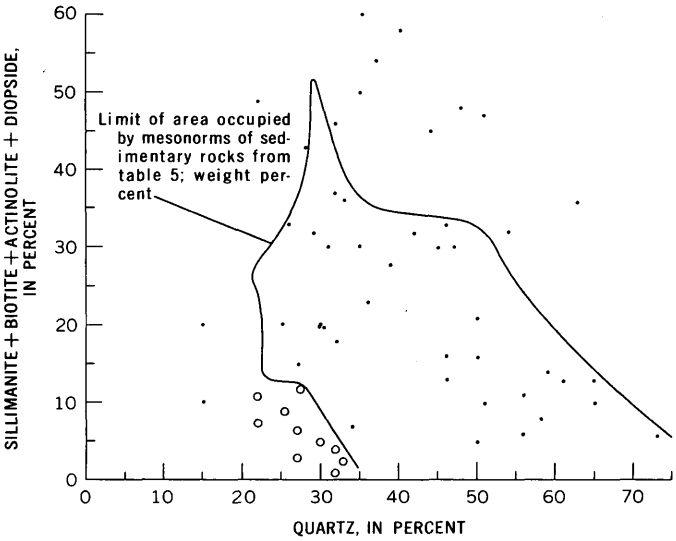

FIGURE 6.—Comparison of the mineral composition of biotite gneiss with norms of quartz-rich igneous rocks and with mesonorms of sedimentary rocks. Dots, modes of biotite gneiss given in table 1, in volume percent. Open circles, mesonorms of average igneous rocks containing more than 10 percent quartz, in weight percent (Nockolds, 1954, p. 1012–1015).

quadrangle have been made, the chemical analogies made between the gneiss and the sedimentary rocks must be based on similar mineralogies.

To provide the necessary basis for comparison, the chemical compositions of several different types of sedimentary rocks were used to compute a hypothetical mineral assemblage called the mesonorm (table 5). The mesonorm is an approximation of the mineralogy that the sedimentary rock would attain if metamorphosed to a degree equivalent to the silliminate-almandine-orthoclase subfacies of Turner and Verhoogen (1960, p. 594). The method of calculating the mesonorm is virtually that of Barth (1962, p. 339–342), with the following modifications; Calcite has not been calculated unless CaO is present in quantities too large to assign to anorthite, actinolite, and diopside; excess Al_2O_3 has been calculated as sillimanite instead of corundum; and the amounts of the normative minerals are given in weight percent rather than in molecular amounts. The results of these calculations for 51 sedimentary rocks are shown in table 5. For several reasons the computed minerals shown will depart somewhat from the actual minerals that would be produced from isochemical metamorphism of these sediments. Garnet and muscovite are not included in the mesonorm. The oxidation state of the iron would probably change (Shaw, 1956, p. 929), and this change would affect the proportions of biotite and iron oxides. The formula for the biotite that was computed is $K_2(Fe, Mg, Mn)_6(Al_2Si_6O_{20})\cdot(OH)_4$, whereas biotite from metamorphic rocks commonly contains additional Al that substitutes for Si, Al, Ti, and Fe^{+3} that substitute for Fe^{+2} and Mg, and Ca and Na that substitute for K. These substitutions would probably result in a higher percentage of biotite in the actual rock than in the mesonorm, and a lower percentage of orthoclase and sillimanite. That this effect would be small even in a rock with abundant biotite can be seen by comparing the mesonorm of the slate (table 5, No. 49) with the values calculated using a biotite whose formula is $K_2(Fe, Mg, Mn)_{5.5}(Al)_{0.5}(Al_{2.5}Si_{5.5}O_{20}).(OH)_2$:

Minerals	*Mesonorm with normal biotite*	*Mesonorm with aluminous biotite*
Quartz	29.6	30.6
Orthoclase	12.6	12.0
Albite	11.3	11.3
Anorthite	1.5	1.5
Sillimanite	18.2	16.3
Biotite	18.5	20.0
All others unchanged	8.5	8.5

TABLE 5.—*Mesonorms of sedimentary rocks, in weight percent*

[Q, quartz; Or, orthoclase; Ab, albite; An, anorthite; Sill, sillimanite; Bi, biotite; Act, actinolite; Diop, diopside; Hy, hypersthene; Mt, magnetite; Il, ilmenite; Hm, hematite; Ti, sphene; Ap, apatite; Cc, calcite. Tr., trace]

Reference: Author	Reference: Year	Table No.	Table Col.	Sample No.	Q	Or	Ab	An	Sill	Bi	Act	Diop	Hy	Mt	Il	Hm	Ti	Ap	Cc	Total	Remarks
Arkose																					
Pettijohn	1957	56	E	1	59.3	28.2	5.3		2.4	Tr.				3.3	0.6	0.70	.2			100.0	
	1957	56	B	2	57.5	30.7	4.2		5.2	0.7						1.2		0.3		99.8	
	1963	8	A	3	49.5	23.8	18.7	1.1	1.5	3.4				1.4			.6			100.0	
	1957	56	C	4	45.5	16.9	21.3	5.1	3.0	5.5				1.2			1.0	.7		100.2	
	1963	8	J	5	44.5	15.8	20.4	9.6		7.6				1.2			.6	.4		100.1	
	1949	68	D	6	39.8	33.6	16.9	5.6				1.2				2.4			0.4	99.9	Average of 3 analyses.
	1957	56	D	7	34.8	37.3	20.2	2.0				1.3		2.4		1.9			.1	100.0	
Protoquartzite, quartzite, and subarkose																					
Pettijohn	1963	8	G	8	85.5	3.3	1.1	6.1	1.9	1.1				0.7						99.7	Subarkose.
	1963	8	H	9	79.7	11.3	2.0			.9						0.7			5.5	100.1	Calcareous subarkose.
	1963	2	B	10	93.5	1.7			3.8	Tr.						.1				99.1	Quartzite.
	1957	54	E	11	91.6			1.1	5.6				1.4	.2						99.9	Protoquartzite.
	1963	4	A	12	78.4	5.2	1.6	3.7				4.0		.2					6.7	99.8	Do.
	1963	2	F	13	83.0	1.4						.2				.1			15.1	99.8	Sandstone.
	1957	54	C	14	42.1	8.7	18.6	13.1				2.5		2.4					12.5	99.9	Sandstone of Frio Formation, average of 10 analyses.
Subgraywacke																					
Pettijohn	1957	54	D	15	62.6	5.7	16.1	2.9		1.7	8.1			2.1			0.8			100.0	
	1963	54	H	16	60.5	5.9	10.5		12.1	4.9						4.9	1.2			100.0	
	1957	54	A	17	55.0	2.3	14.0	2.3	9.8	13.2				1.2			2.0	0.3		100.1	
	1957	54	B	18	52.4	2.8	21.8	3.6	7.4	11.1				.9						100.0	
	1963	4	C	19	36.0	9.4	11.6	13.5				7.1				1.7	.2		20.5	100.0	Calcareous.
	1963	4	F	20	21.4	6.7	11.0	10.1				26.6				2.6	.6	.4	20.5	99.9	
Graywacke																					
Pettijohn	1963	6	F	21	54.5	2.8	14.0	2.8	9.3	12.9				1.2			2.0	0.3		99.8	
	1963	6	C	22	52.0	3.4	21.8	3.6	7.4	10.9				.9						100.0	
	1957	51	L	23	47.2		13.5		16.5	17.1			0.9	.2	1.3		.6	1.1		100.2	
	1957	51	I	24	45.4		31.0	6.3	1.2	13.7			1.0	.7				.4		99.7	
	1957	51	J	25	41.7	.6	28.4	3.2	4.9	17.4				2.2			1.6			100.0	
	1957	51	H	26	38.0	12.2	27.4	7.9	1.3	5.4				3.6		1.8	.8	1.4		99.8	
	1957	51	A	27	37.8	6.3	21.0	10.5	10.5	12.8							.8	.3		100.0	
	1957	51	M	28	34.8	2.4	37.9	3.2	3.8	13.3				4.3			.2	.4		100.3	Average of 3 analyses.
	1957	51	E	29	34.9	1.7	36.5	7.7	3.1	13.9				.9			1.0	.3		100.0	Do.
	1957	51	B	30	32.2	3.4	23.7	16.4	12.5	7.4				4.5						100.0	Do.
	1963	6	H	31	31.1	9.1	33.7	9.9	2.5	11.8				.9			.6	.3		99.9	
	1957	51	G	32	29.1	8.7	28.2	21.2		.5	10.4			1.0			1.1			100.2	
	1957	51	F	33	28.8		21.8	5.8	12.3	22.4			4.3	1.0			2.2	.7	(1)	100.1	
	1957	51	C	34	27.8	1.7	23.6	21.6	.2	23.0				.9			1.2			100.0	Average of 3 analyses.
	1963	6	B	35	26.1		24.4	13.8	10.0	13.2			9.9	.7			1.6	.3		100.0	
	1957	51	D	36	24.6	2.3	33.2	14.1		18.3	3.1			2.7			1.6			99.9	Average of 3 analyses.
	1957	51	K	37	22.9	2.5	20.3	27.4	6.7	13.7				3.9			2.2	.7		100.3	
Shale, slate, and argillite																					
Shaw	1956	2	L10	38	47.5	11.8	7.2		20.3	8.2				2.7	1.9		0.4			100.0	Slate.
	1956	2	L1	39	42.1	16.7	1.6		19.0	16.0				2.6	1.4		.2	0.3		99.9	Black shale.
	1956	2	L3	40	41.8	14.6	4.9		22.1	12.2				2.2	2.2					100.0	Black slate.
	1956	2	L8	41	40.0	13.9	6.0		23.5	11.5				2.7	2.1			.4		100.1	Do.
Tourtelot	1962	6	1st	42	39.6	11.2	10.6	5.6	16.0	8.6				3.6		2.7	1.8	.4		100.1	Pierre Shale, average of 17 analyses.
Pettijohn	1957	61	C	43	35.2	15.5	9.0	3.6	16.7	11.3				6.2			2.1	.4		100.0	Composite of 51 shales.
Shaw	1956	2	L11	44	33.9	9.8	14.2		17.2	18.9				4.3	1.1		.2	.4		100.0	Slate.
Pettijohn	1957	61	D	45	33.3	13.0	10.6	5.6	16.0	16.2				3.4			1.9			100.0	Slate, average of 36 analyses.
	1957	61	A	46	32.2	13.5	12.1	13.5	9.3	11.0				6.4			1.8	.4		100.2	Shale, average of 2 composites.

[1] Pyrite=0.8

TABLE 5.—*Mesonorms of sedimentary rocks, in weight percent*—Continued

Reference: Author	Year	Table No.	Table Col.	Sample No.	Q	Or	Ab	An	Sill	Bi	Act	Diop	Hy	Mt	Il	Hm	Ti	Ap	Cc	Total	Remarks
Shale, slate, and argillite—Continued																					
Shaw	1956	2	L9	47	31.2	13.9	6.6		21.4	22.6				1.9	1.9		.2	.4		100.1	Gray shale.
Pettijohn	1957	62	E	48	31.0	32.8	10.0		10.0	10.4				4.2	.5		.6	.3		99.8	Argillite.
	1957	61	E	49	29.6	12.6	11.3	1.5	18.2	18.5				6.0			2.1	.4		100.2	Slate, average of 33 analyses.
Shaw	1956	2	L2	50	29.1	6.9	9.8		24.9	27.2				.5	.5		1.0			99.9	Black slate.
Pettijohn	1957	61	B	51	22.4	16.0	16.8	23.7		3.0	10.1			6.2		.2	1.3	.4		100.1	Composite of 27 shales.

The mesonorms of the sedimentary rocks were plotted on several diagrams on a trial basis. The two triangular plots in figure 7 were selected for further use because the fields occupied by the various rock types are reasonably distinct. The modes of the gneisses given in table 1 were plotted in figure 7 after first eliminating muscovite in the modes according to the relation: muscovite + 2 quartz → microcline + 2 sillimanite. The results of comparison of the positions of the plotted modes relative to the field boundaries are shown in table 6.

The biotite gneiss, therefore, may have formed from a sequence of sedimentary rocks predominantly having the chemical character of shales, graywackes and subgraywackes. Moench (1964, p. A32) and Sims and Gable (1964, p. C27) reached similar conclusions for the biotite gneisses in the Idaho Springs and Central City areas.

The calc-silicate gneiss is interlayered with biotite gneiss and with quartz gneiss and, judging from the abundance of calcium-bearing minerals, may be the product of metamorphism of calcareous sedimentary rocks.

Lovering and Goddard (1950, p. 23–25) and S. H. Ball (in Spurr and Garrey, 1908, p. 46–49) believed that the rock unit which they called quartz monzonite gneiss and that is here called microcline gneiss was the oldest intrusive igneous rock of the region and that its texture had been modified by deformation. By contrast, Moench, Harrison, and Sims (1962, p. 37–38) regarded "the microcline - quartz - plagioclase - biotite gneiss (microcline gneiss) as metasedimentary, for its structure and lithology are more consistent with this interpretation than with that of a metamorphosed granitic rock." It is most difficult to establish conclusively which of these points of view is correct. Proponents of an igneous parentage have been impressed by the similarity between the composition of the gneiss and the composition of common igneous rocks. The modes show that microcline gneiss could represent a metamorphosed sequence of igneous rocks (pyroclastic, extrusive, or plutonic) ranging from dacite to quartz latite. The modes also show that some microcline gneiss layers (particularly those in the southwest corner of the quadrangle) cannot be a product of igneous rocks because the quartz content of the gneiss is too high.

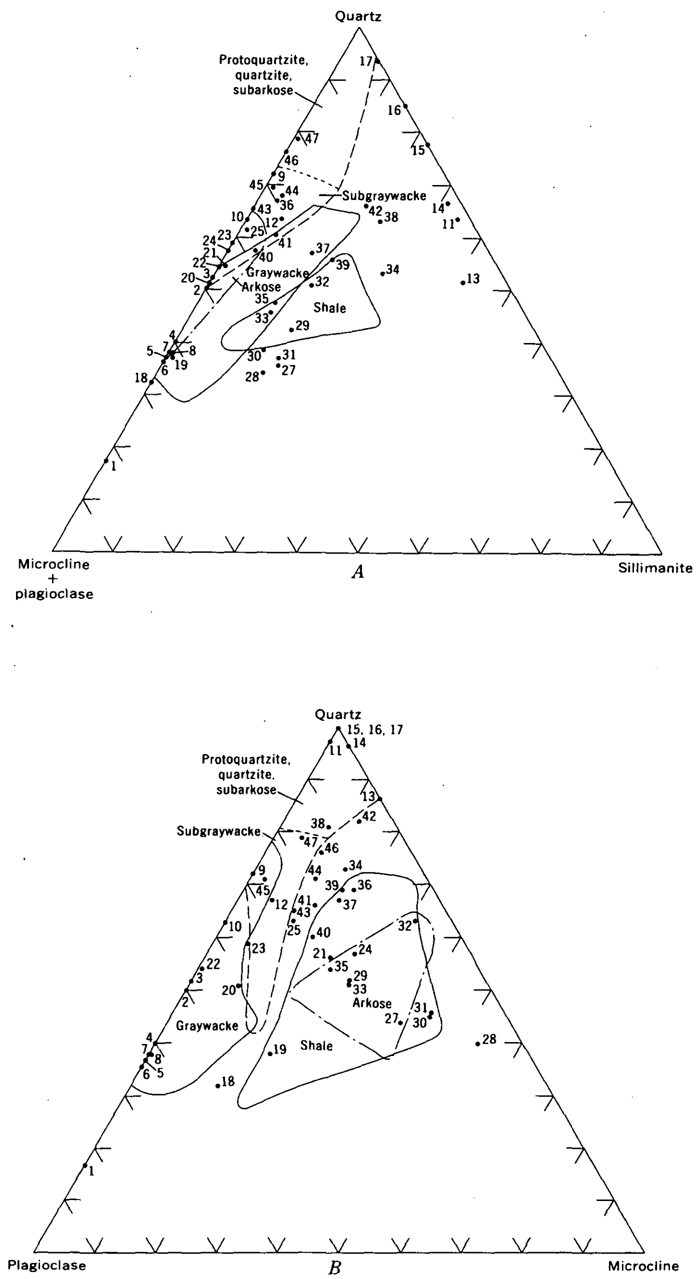

FIGURE 7.—Comparison of modes of biotite gneiss and mesonorms of sedimentary rocks. Sedimentary rock fields defined by mesonorms of table 5. Numbered points are biotite-gneiss samples of table 1, except sample 26 is not plotted. Volume percent.

TABLE 6.—*Probable sedimentary parents of biotite gneisses*

[Numbers are sample numbers in table 1. Question marks indicate uncertain correlation]

	Biotite-quartz-plagioclase	Sillimanite-biotite-quartz	Biotite-quartz-plagioclase-microcline	Sillimanite-biotite-quartz-plagioclase-microcline-muscovite
Subgraywacke	9, 10?, 12	----------	23, 25	36?, 40, 41, 43, 44, 45, 46, 47.
Arkose	----------	----------	21, 24,	----------
Graywacke	1?, 2, 3, 4, 5, 6, 7, 8,	----------	18, 19?, 20, 22,	----------
Shale	----------	----------	----------	27?, 28?, 29, 30, 31, 32, 33, 34, 35, 37, 39.
Not like common sedimentary rocks.	11	13, 14, 15, 16, 17	----------	38, 42.

Those favoring a sedimentary origin for the gneiss have been influenced by the observations that the gneiss has a layered structure resembling bedding, that it is distributed as comformable sheets of considerable extent, and that it lacks small-scale crosscutting structures or inclusions. Because of the high content of feldspar and the low content of mica, one would suppose that the probable sedimentary parent would have been an arkose. Mesonorms of common arkoses contain a relatively high proportion of potassium feldspar (table 5; fig. 7*B*). A comparison of figures 5 and 7*B* shows that only about 25 percent of the microcline gneiss modes would plot in the arkose field. Those microcline gneiss layers that contain appreciable microcline would closely match the rock that would form from the metamorphism of a typical arkose. However, those gneiss layers that contain minor microcline would apparently represent rather unusual arkoses. Pettijohn (1963, p. S 8) has shown that arkoses typically contain more K_2O than Na_2O. In fact, two-thirds of the analyses considered by him have a K_2O-Na_2O ratio greater than 3:2. At a 3:2 ratio the equivalent molecular amounts of K_2O and Na_2O are equal and the normative orthoclase and albite would be about equal. Thus arkoses that would yield a metamorphic rock containing abundant plagioclase and minor orthoclase are apparently not common, but they do exist.

Certain bodies of gneiss have structural peculiarities that are difficult to explain as being of sedimentary origin. As previously mentioned, the Lawson layer, which is more than 2,500 feet thick immediately east of the Empire quadrangle (Moench and others, 1962, p. 39), pinches out abruptly on the west limb of the Lawson syncline. The microcline gneiss body that has an apparent thickness of about 2,000 feet on Red Elephant Hill pinches out a short distance to the northwest and southeast. Thick bodies of gneiss on Montana Mountain in the adjacent Central City quadrangle (Sims, 1964) and on Nebraska Hill just north of the Empire quadrangle (Lovering and Goddard, 1950, pl. 2) exhibit similar rapid variations in thickness.

These pinchouts might be the crests or troughs of complex folds older than any folds now recognized in the area. This structural interpretation, however, cannot be made with any certainty from the data now available. Unless such a structural interpretation is made, though, the shape of the microcline gneiss bodies will remain an argument against their sedimentary origin.

In conclusion, some quartz-rich layers mapped as microcline gneiss are probably metamorphosed arkosic sandstones and the bulk of the gneiss could have either a sedimentary or volcanic origin.

The hornblende gneiss and amphibolite may be either orthogneiss dervied from the metamorphism of basic igneous rocks or paragneiss derived from the metamorphism of carbonate-shale or carbonate-graywacke mixtures. The conformable relations of both hornblende gneiss and amphibolite with the bordering rocks and the alternation of layers of different mineralogy in the hornblende gneiss are indicative of a sedimentary origin.

Several amphibolites showing crosscutting relations have been found in the central Front Range (S. H. Ball, in Spurr and Garrey, 1908, p. 45; R. B. Taylor, oral commun., 1962), which suggests that they may have been intrusive bodies. The data are not sufficient to indicate the origin of the amphibolites in the Empire quadrangle.

METAMORPHIC FACIES

The metamorphic rocks of the Empire quadrangle contain mineral assemblages that are characteristic of the almandine-amphibolite facies (Turner and Verhoogen, 1960, p. 544–553). Biotite gneiss throughout the quadrangle contains both sillimanite and microcline, which apparently represent a stable mineral pair, and indicate that the metamorphic rocks in the entire quadrangle are within the sillimanite-potassium feldspar isograd (Guidotti, 1963). Thus the mineral assemblage of the rocks belongs to the sillimanite-almandine-orthoclase subfacies. The same conclusion was reached by Sims and Gable (1964, p. C40) for the metamorphic rocks in the Central City area just east of the Empire quadrangle.

332-862 O—69——3

The pressure-temperature level at the peak of metamorphism cannot be determined exactly from the present data. However, the limits of the pressure-temperature range can be inferred from certain experimentally determined equilibrium curves (fig. 8).

The limits of stability of sillimanite have been investigated by several workers who have had varying results. The limits as determined by Newton (1966) are shown by curves 1*a* and 1*b* (fig. 8). If one assumes that these curves are correct and that the sillimanite in the gneisses formed stably, the pressure-temperature conditions at the peak of metamorphism must have been within the sillimanite field. The upper limit of stability of muscovite plus quartz is shown by curves 3*a* and 3*b*, and because muscovite plus quartz occurs throughout the quadrangle, the pressure-temperature conditions must have been to the left of these curves.

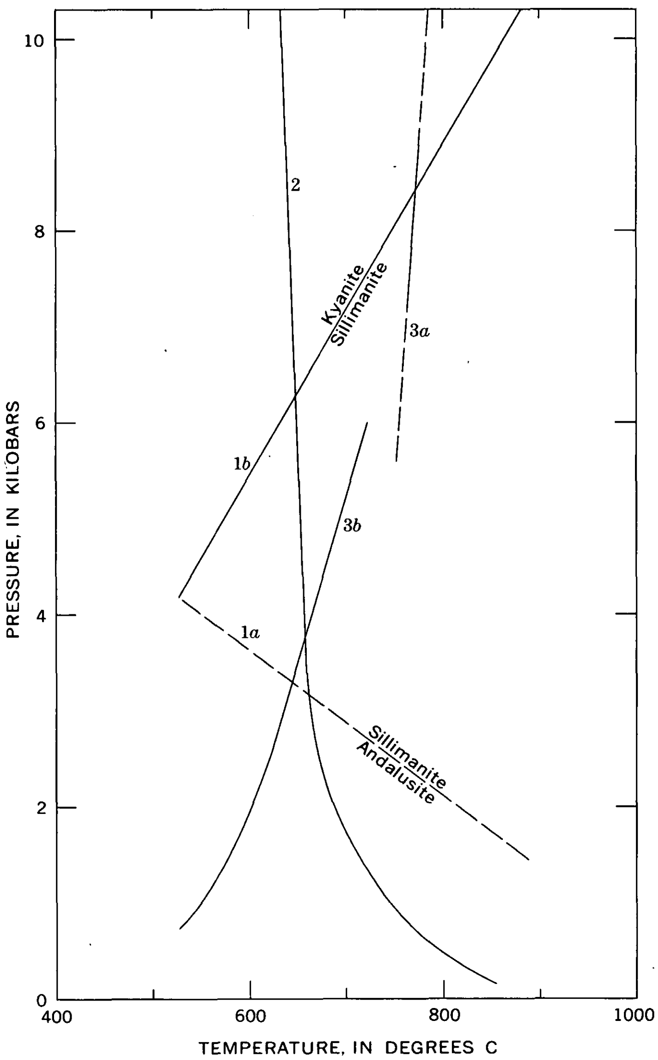

FIGURE 8.—Equilibrium curves related to metamorphism in the Empire quadrangle. 1*a*, andalusite ⇌ sillimanite (Newton, 1966); 1*b*, kyanite ⇌ sillimanite (Newton, 1966); 2, minimum melting in the system $NaAlSi_3O_8$–$KAlSi_3O_8$–SiO_2–H_2O (Luth and others, 1964); 3*a*, beginning of melting of mixtures and muscovite and quartz (Segnit and Kennedy, 1961); 3*b*, muscovite plus quartz ⇌ potassium feldspar plus Al_2SiO_5 plus H_2O (vapor pressure equals total pressure) (Evans, 1965).

The minimum temperature at which quartzo-feldspathic rocks would begin to melt is shown by curve 2. The crosscutting relation (fig. 3) and the mineral compositions (fig. 4) of the granitic part of the migmatite suggest that the biotite gneiss was partially melted at the peak of metamorphism. If this is so, the pressure-temperature conditions would lie to the right of curve 2. These considerations suggest that the maximum temperature attained was 750°±50°C and that the pressure was 4–8 kilobars.

The origin of the poikiloblastic muscovite that replaces sillimanite in the western part of the quadrangle is not clearly understood, but it may be related to metasomatism accompanying the emplacement of a large batholith of Silver Plume Granite in the Berthoud Pass quadrangle to the west.

PRECAMBRIAN IGNEOUS ROCKS

Precambrian intrusives occupy a large area of the Empire quadrangle. The oldest intrusives are the quartz diorite of St. Marys Lake, the Boulder Creek Granite, and the quartz diorite and hornblendite that commonly form concordant bodies and have been foliated and recrystallized to varying degrees. The Silver Plume Granite intrudes the older plutonic rocks and forms discordant plutons and irregular dikes, which commonly have primary flow structures but do not have secondary foliation due to recrystallization. Hornblende diorite and granite porphyry are minor rock types which form short dikes in the older metamorphic rocks. Pegmatite spatially related to Silver Plume Granite forms small irregular bodies in parts of the quadrangle.

QUARTZ DIORITE OF ST. MARYS LAKE

At St. Marys Lake a small pluton of quartz diorite is exposed in contact with Boulder Creek Granite and biotite gneiss, and about 0.3 mile west of Alice a thin sill of porphyritic quartz diorite is exposed. These two bodies constitute the quartz diorite of St. Marys Lake.

The rock of the pluton is dark gray, very fine to fine-grained, and generally structureless. In a few outcrops a weak foliation is visible. Scattered indistinct feldspar phenocrysts occur in the finer grained parts. White biotite-bearing pegmatites that range in length from a few feet to several hundred feet are common within the pluton just north of the lake.

The rock is composed principally of quartz, plagioclase, biotite, and hornblende (table 7). Most of the plagioclase occurs as small subhedral grains, but some occurs as larger grains that resemble phenocrysts. These larger grains are anhedral and have very irregular borders and contain numerous small inclusions of quartz and laths of biotite (fig. 9*A*, *B*). The plagioclase ranges in composition from An_{45} to An_{63}. Hornblende forms anhedral grains that commonly exhibit a sieve texture and that contain irregular feldspar inclusions. Hornblende, quartz, and magnetite form unusual intergrowths (fig. 9*E*). Quartz forms anhedral grains that are largely interstitial to the other components, and in some thin sections it forms very large poikilitic grains that enclose all other minerals. Biotite occurs as anhedral unoriented grains distributed uniformly in the rock.

TABLE 7.—*Modes, in volume percent, of quartz diorite of St. Marys Lake*

	Pluton at St. Marys Lake				Sill west of Alice
Sample No.	1-24B	4-118A	4-118B	4-124B	4-140
Quartz	31	18	29	27	22
Plagioclase	32	35	38	36	45
Biotite	24	27	22	25	19
Hornblende	11	17	5	9	8
Opaque oxides	2	2	2	3	6
Other minerals	<1	<2	<4	<1	<1
Composition of plagioclase	An_{57}–An_{63}	An_{45}	An_{45}	An_{60}	An_{62}

The quartz diorite sill west of Alice is about 30 feet thick. Where exposed at the north end, it conforms to a small fold in the biotite gneiss. The rock is weakly foliated parallel to its contacts and to the foliation in the biotite gneiss. Tabular phenocrysts of plagioclase 1–2 cm long are conspicuous and show only a slight tendency to be oriented. The plagioclase in the phenocrysts has a composition of about An_{60}. The phenocrysts have very irregular boundaries, and many are cut by fractures which have been healed by the growth of biotite and small amounts of quartz and hornblende (fig. 9*C*, *D*). The dark-gray groundmass is very fine grained and texturally resembles the quartz diorite from the pluton.

The growth of biotite along fractures in phenocrysts, the occurrence of relict phenocrysts containing abundant quartz and biotite, the unusual hornblende-quartz-magnetite intergrowths, and the sieve and poikilitic textures of hornblende and quartz suggest that the original texture and mineralogy of the quartz diorite has been considerably modified by recrystallization. Plastic flowage of the rock during recrystallization was apparently not intense, as foliation is not well developed.

In the good exposures north of St. Marys Glacier the quartz diorite appears to grade into Boulder Creek Granite through a gradational zone in which the grain size increases and the content of dark minerals decreases. Mixed rocks eastward along this contact contain fragments of fine-grained diorite that appear to be inclusions in Boulder Creek. On the knob east of St. Marys Lake a tabular body of Boulder Creek separates the quartz diorite from biotite gneiss, and numerous irregular dikes of Boulder Creek cut the quartz diorite. These relations indicate that the quartz diorite is older than the Boulder Creek Granite.

BOULDER CREEK GRANITE

Bodies of fine- to medium-grained rock having the average composition of granodiorite but including quartz diorite and quartz monzonite are abundant in the quadrangle. The name Boulder Creek Granite is applied to these rocks in accordance with the usage of Lovering and Goddard (1950, p. 27). This rock is semischistose to granular and is generally concordant with the layering in adjacent metamorphic rocks. Similar rocks south of the Empire quadrangle were called Archean quartz monzonite by S. H. Ball (in Spurr and Garrey, 1908, p. 51–54). Boos and Boos (1934, p. 305–306) applied the name "Boulder Creek granite gneiss" to a body of similar rock west of Boulder, Colo. The Boulder Creek Granite has been called granodiorite, granodiorite and associated rocks, and granodiorite and quartz diorite in recent publications (Harrison and Wells, 1959; Moench, 1964; Sims and Gable, 1964).

Bodies of Boulder Creek Granite have sharp contacts that are generally concordant with adjacent units, but the ends of some sills and parts of the borders of more irregular bodies are discordant. Foliation marked by the parallel alinement of biotite grains and biotite-rich layers is weak to strong and is parallel to the foliation in adjacent wallrocks. Lenticular inclusions of biotite gneiss and migmatite are common. The layering in the inclusions is contorted to about the same degree as that in the wallrock, and the foliation and lineation within inclusions is apparently parallel to the lineation and foliation in adjacent metamorphic rocks.

Gneissic quartz diorite in the trough of the Lawson syncline just north of Lawson and in the small bodies in Mammoth Gulch northeast of James Peak are sills that are characteristically moderately to strongly foliated throughout. The sill in the Lawson syncline contains lenticular to subangular inclusions of amphibolite and biotite gneiss. Along the east side of the quad-

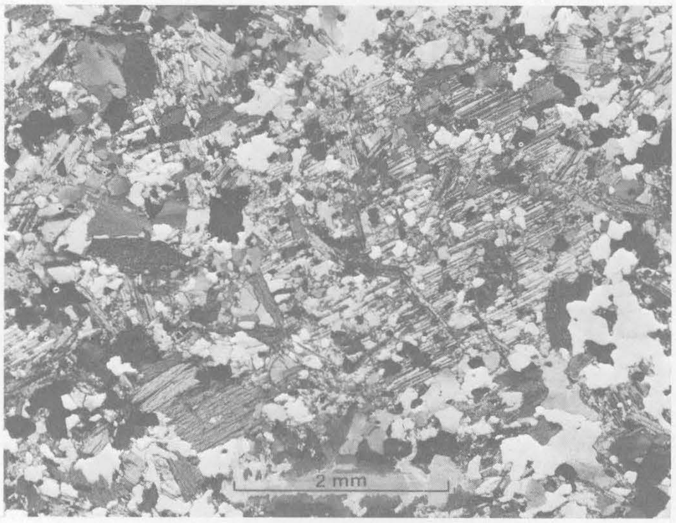

A

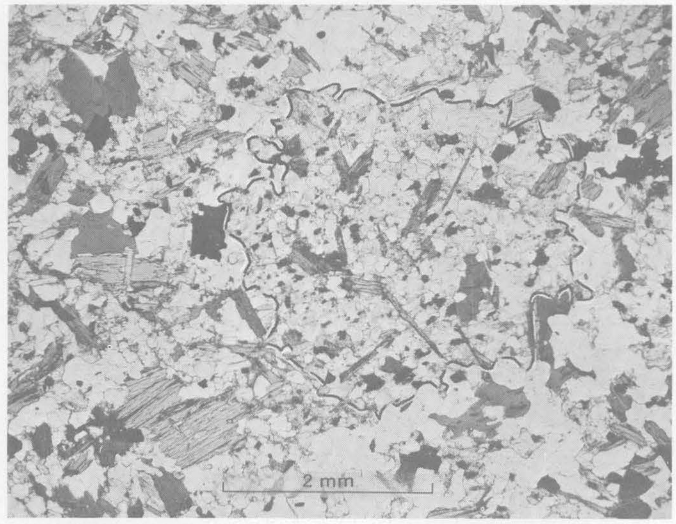

B

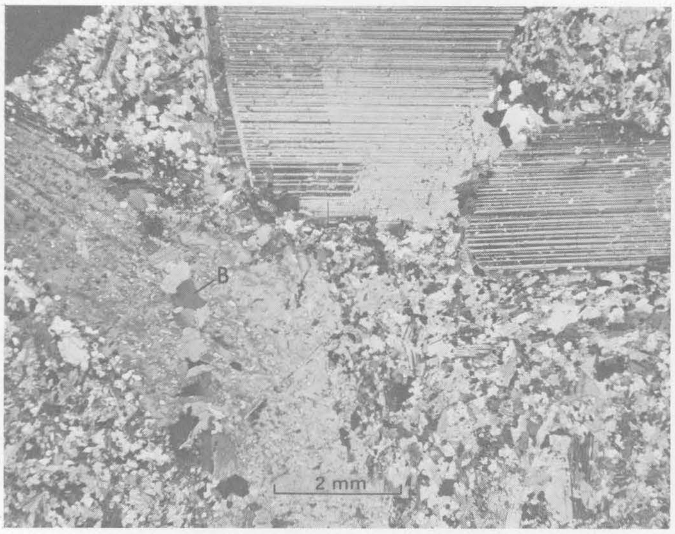

C

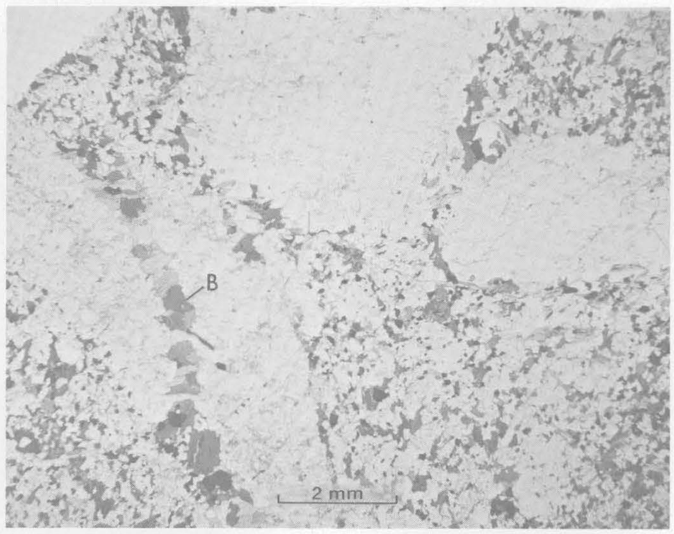

D

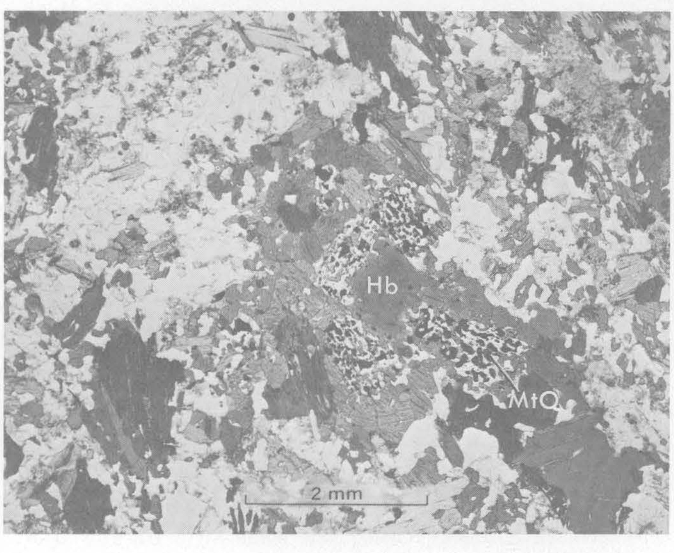

E

FIGURE 9.—Photomicrographs of the quartz diorite of St. Marys Lake. *A*, Quartz diorite from St. Marys Lake pluton. The large irregular plagioclase grain in the center of the picture contains inclusions of quartz, hornblende, and biotite. Crossed nicols. *B*, Same, plain light. The dashed line encloses the large plagioclase grain. *C*, Porphyritic quartz diorite from a sill 0.3 mile west of Alice. Groundmass is quartz, plagioclase, biotite, and hornblende. Phenocryst of plagioclase has been broken and coarse biotite (B) has formed along fracture. Crossed nicols. *D*, Same, plain light. *E*, Quartz diorite from St. Marys Lake pluton showing unusual intergrowth of hornblende (Hb) and quartz and magnetite (M+Q). Plain light.

rangle, Boulder Creek forms many sills in which foliation is poor except near the margins. North of James Peak coalescing sills of Boulder Creek form a phacolithic body that is concordant with a large fold in the metamorphic rocks. The Boulder Creek here is virtually nonfoliated.

The average modes of Boulder Creek Granite from the Empire quadrangle are given in table 8, and the proportions of plagioclase, quartz, and microcline are shown in figure 10. These quartz dioritic, granodioritic, the quartz monzonitic rocks have no regular geographic distribution in the area.

TABLE 8.—*Modal composition of Boulder Creek Granite, in volume percent*

[Tr., trace; number in parentheses is number of samples averaged]

	Gneissic quartz diorite		Quartz diorite		Granodiorite		Quartz monzonite	
	Range	Average (3)	Range	Average (13)	Range	Average (19)	Range	Average (5)
Quartz	21–26	25	17–37	31	21–34	28	18–42	28
Microcline	0	0	0–6	1	8–21	13	19–25	22
Plagioclase	52–58	55	37–53	45	29–55	43	27–40	35
Biotite	16–21	19	4–34	20	2–21	12	3–17	10
Muscovite	0	0	0–3	<1	0–5	1	1–4	2
Other minerals	Tr.–1.0	<1.0	1–6	3	0.5–5.5	2	Tr.–4	2
Composition of plagioclase		An_{50}	An_{30-45}		An_{25-35}		An_{30-35}	

The Boulder Creek is fine to medium grained, and commonly seriate porphyritic with some coarse feldspar phenocrysts. The feldspars are typically white, and biotite is sufficiently abundant to make the fresh rock gray to mottled black and white. On weathered surfaces the rock is typically mottled black and red brown. The texture is dominantly xenomorphic granular, and the minerals in the semischistose varieties show no more evidence of granulation than those in massive rocks. Plagioclase ranges in composition from An_{25} to An_{50} and probably averages An_{35}. Zoning is rare. Plagioclase is commonly slightly to strongly altered to sericitic mica. Weakly perthitic or nonperthitic microcline is commonly embayed by myrmekite. Quartz occurs as irregular masses interstitial to the feldspars and as medium to coarse composite grains made up of a mosaic of smaller units. The quartz generally shows moderate to strong undulatory extinction. Biotite forms anhedral grains that are roughly alined in semischistose rock and unalined in massive rock. Muscovite occurs sparingly in subhedral grains commonly intergrown with biotite. Apatite, epidote, magnetite, sphene, and allanite are present as accessory minerals generally associated with biotite. Common alteration products of biotite include epidote, chlorite, and opaque oxides. The only evidence of mechanical deformation of biotite, even in semischistose rocks, is the presence of a few bent grains.

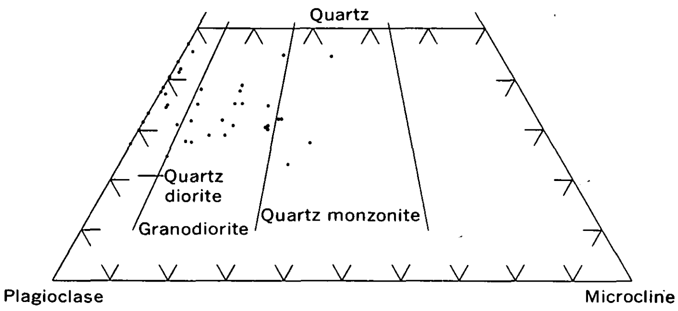

FIGURE 10.—Triangular plot of plagioclase, quartz, and microcline in the Boulder Creek Granite. Modal volume percent; dots are the 40 modes summarized in table 8.

QUARTZ DIORITE AND HORNBLENDITE

Quartz diorite is a black to mottled black and white fine- to medium-grained rock consisting principally of plagioclase, hornblende, biotite, and quartz. Hornblendite is a black to dark-green rock composed principally of hornblende and minor amounts of plagioclase and quartz. Both rock types may be either massive or weakly to strongly foliated.

These rocks form small intrusive bodies distributed along two linear zones. One zone extends at least 11 miles N. 45° E. from where the West Fork of Clear Creek enters the quadrangle to the vicinity of Elk Park in the adjacent Central City quadrangle. The other zone crosses the southeast corner of the quadrangle and extends at least 10 miles N. 45° E. across the Central City quadrangle (Sims, 1964). The zones are about half a mile wide and are about 4 miles apart. Individual bodies within these zones vary from elliptical plugs 100–800 feet in diameter to sill-like bodies as much as 200 feet thick and more than 2,000 feet long. Foliation, where present, is commonly parallel to the foliation in adjacent biotite gneiss.

The quartz diorite intrusives in the southeast corner of the quadrangle are mostly massive but are locally foliated along their margins. Plagioclase (andesine-labradorite) is typically the most abundant mineral; commonly it has irregular mottled zones, and the anorthite content of different zones varies as much as 15 percent. Quartz, which occurs in minor amounts, commonly forms subgraphic intergrowths with hornblende or biotite or is poikilitically included in zoned plagioclase. Biotite is less abundant than hornblende in the massive bodies but is the only ferromagnesian mineral in the foliated margins of several bodies. Opaque oxide minerals, apatite, and sphene are common accessory minerals.

The quartz diorite intrusive bodies in the linear zone crossing the center of the quadrangle are predominantly well foliated. Both biotite and hornblende are abundant.

Plagioclase (andesine) commonly forms anhedral grains with a sieve texture in which round inclusions of quartz are abundant. Most of the plagioclase has been altered to sericitic mica.

The thick hornblendite sills adjacent to the West Fork of Clear Creek on the west side of the quadrangle are massive to weakly foliated. The rock is composed of medium-grained anhedral hornblende, less than 10 percent quartz and sericitized plagioclase, and traces of opaque oxide minerals and apatite. A small apophysis from the northern sill cuts across the layering of the adjacent biotite gneiss, but it is weakly foliated parallel to the layering in the gneiss. The hornblendite in this apophysis contains a moderate amount of biotite.

The five small intrusives in a cluster half a mile northwest of St. Marys Lake show marked variations in composition. The northern two bodies are medium-grained quartz diorite composed primarily of hornblende, plagioclase, and quartz and minor amounts of opaque oxide minerals, apatite, and sphene. Diopside, partly replaced by hornblende, is common in some samples. The composition of plagioclase ranges from unzoned labradorite to bytownite that has mottled zones (An_{65}–An_{75}). The larger central body ranges in composition from sericitized quartz diorite to hornblende composed of very pale green to colorless amphibole and minor opaque oxides and spinel. One sample of this hornblendite contains moderate amounts of an orthorhombic pyroxene which probably is hypersthene.

Dikes of both hornblendite and quartz diorite cut across Boulder Creek Granite, and dikes of Silver Plume Granite cut hornblendite and quartz diorite southeast of the Empire quadrangle. No age relations between hornblendite and quartz diorite and Boulder Creek were observed in the Empire quadrangle, but at several localities Silver Plume Granite clearly intrudes both quartz diorite and hornblendite.

Harrison and Wells (1956, p. 45; 1959, p. 16–17) discussed the petrographic evidence for metamorphism of the foliated varieties of quartz diorite and hornblendite. They concluded that the mineralogic changes that probably were caused by metamorphism are (1) reduction of the amount of hornblende, (2) reduction of the anorthite content of the plagioclase, (3) increase in the amount of biotite, (4) formation of microcline, and (5) a change in texture from hypautomorphic granular to allotriomorphic granular with poikilitic textures. Similar mineralogic changes were observed in transitions from massive to foliated quartz diorite in the Empire quadrangle, except that no microcline was found.

Several gabbro plutons in the central Front Range are younger than the Boulder Creek Granite, have been slightly to moderately recrystallized, and are cut by biotite-muscovite granite similar to the Silver Plume (Taylor and Sims, 1962). One of these gabbro bodies, the Elk Creek pluton just east of the Empire quadrangle, appears to grade into quartz-amphibolite-bearing rocks similar to some of the quartz diorites of the Empire quadrangle. The small bodies of quartz diorite and hornblendite may be genetically related to the gabbroic magma that produced the larger gabbro plutons.

HORNBLENDE DIORITE AND OTHER METAMORPHOSED BASIC DIKES

Scattered throughout the quadrangle are thin discontinuous dikes of hornblende or biotite-rich rock, most of which are too small to show on the geologic map. Such dikes are probably most abundant in the northwestern part of the quadrangle. One body of hornblende diorite is shown on the northern slope of Parry Peak. The dikes are 1–20 feet thick, are strongly foliated, have metamorphic rather than igneous textures, and are cut by discordant pegmatites. The metamorphic foliation is parallel to the dike walls, although the trend of the dikes is at a high angle to the foliation in the wallrocks. Some of the dikes are folded, although less intensely than the wallrocks, and some have lineation marked by elongate clots of hornblende or biotite which are parallel to the mineral alinement in the wallrocks.

The mineralogy of the dikes is extremely varied. Many dikes consist of abundant well-oriented biotite and abundant plagioclase (An_{30}) and quartz; others contain, in addition, moderate amounts of hornblende. The mapped hornblende diorite is composed of medium-grained hornblende, fine-grained sericitized plagioclase, and sparse amounts of microcline and biotite.

The dikes were apparently intruded after most of the folding of the metasedimentary rocks had occurred but before the end of regional metamorphism. The dikes may be related in age to the magmatic episode that produced the Boulder Creek Granite and the quartz diorite.

GRANITE PORPHYRY

Dikes of granite porphyry were mapped at three localities: on the ridge extending west from Mount Eva, near the top of Parry Peak, and just south of the large pegmatite body in the northwest corner of the quadrangle. In addition, on the west side of Mount Flora an oval patch of biotite gneiss about 300 feet in diameter, which is surrounded by Silver Plume Granite, is cut by an unmapped granite porphyry dike, but the dike could not be traced into the Silver Plume. It is possible, therefore, that the granite porphyry is older than the Silver Plume. The other granite porphyry dikes are cut by coarse-grained pegmatites.

The granite porphyry contains abundant mediumsized phenocrysts of plagioclase (An_{30}), quartz, and subordinate microcline that are embedded in a fine-grained matrix of quartz, microcline, biotite, and subordinate plagioclase. The rock varies from granodiorite to quartz monzonite.

SILVER PLUME GRANITE

Bodies of fine- to medium-grained granitic rock which have the average composition of quartz monzonite crop out throughout the quadrangle and are particularly abundant in the southwestern part. Similar rocks a few miles to the south in the Georgetown quadrangle were called Silver Plume Granite by S. H. Ball (in Spurr and Garrey, 1908, p. 58), and this name is retained in this report. The term "biotite-muscovite granite" has been used in recent reports of the U.S. Geological Survey for equivalent rocks (Harrison and Wells, 1959; Moench and others, 1962).

The Silver Plume Granite is a gray to buff fine- to meduim-grained rock composed principally of quartz, microcline, and plagioclase. Most of the granite is massive, but parts of some large bodies and the entire thickness of some dikes and sills are well foliated owing to the parallel alinement of crystals of microcline. This foliation parallels discordant contacts of the granite and has been widely interpreted as a primary magmatic flow layering.

Some bodies of the granite are sills that are conformable to the layering in the adjacent metamorphic rocks, but most are dikes or irregular discordant bodies that range in width from a few hundred feet to several miles. Small inclusions are rare. Within the Empire quadrangle the granite cuts across Boulder Creek Granite, quartz diorite, and hornblendite.

A zone about 2,500 feet wide in which thin Silver Plume sills are very abundant extends west-southwest from Sherwin Lake across Witter Peak. To the southwest, rocks in the zone grade into homogeneous Silver Plume. Throughout much of this zone the sills have sharp boundaries with the metamorphic rocks, and granite and metamorphic rocks are clearly distinct from each other. Near Sherwin Lake, however, assimilation of the metamorphic rocks has been extensive, and the granite–metamorphic-rock complex becomes more like a migmatite.

In the Empire quadrangle typical Silver Plume is fine to medium grained, seriate porphyritic to equigranular, and hypidiomorphic. The proportions of the major minerals—quartz, microcline, and plagioclase—are relatively constant (table 9 and fig. 11), and most of the rocks examined have the mineralogic composition of quartz monzonite. Quartz forms anhedral single grains or mosaics and shows weak to moderate undulatory extinction. Microcline is nonperthitic or slightly microperthitic and commonly is embayed by myrmekite. Unzoned plagioclase ranges in composition from An_{30} to An_{17} but is generally about An_{25}; it is commonly slightly altered to sericite. Biotite, commonly slightly altered to ‘ .lorite, and primary muscovite are minor constituents. The accessory minerals are zircon, apatite, monazite, and magnetite.

TABLE 9.—*Modal compositions of Silver Plume Granite, in volume percent*

[Tr., trace; number in parentheses indicates number of samples averaged]

	Granodiorite		Quartz monzonite		Granite	
	Range	Average (5)	Range	Average (41)	Range	Average (8)
Quartz	17–34	28	16–39	28	26–33	31
Microcline	14–23	19	20–44	31	35–64	46
Plagioclase	33–43	39	20–40	30	0–19	15
Biotite	8–15	10	1–13	7	1–18	4
Muscovite	1–4	2	Tr.–8	3	Tr.–7	3
Other minerals	1–3	2	Tr.–3	1	Tr.–4	1
Composition of plagioclase	An_{27-31}	An_{30}	An_{24-35}	An_{26}	An_{17-27}	An_{23}

PEGMATITE

Coarse-grained rocks of pegmatitic texture occur throughout the quandrangle and commonly are associated with migmatized biotite gneiss. This type of pegmatite has not been mapped. The mapped bodies of pegmatic are in the northwest corner of the quadrangle and are not associated with migmatite. They form discordant dikes, sills, and irregular pluglike bodies.

The pegmatites are white to pink and are composed of quartz, perthite, albite-oligoclase, and muscovite. A few appear to be zoned and have massive quartz cores. Many are granulated, and the largest mass shown has a well-developed cataclastic foliation that is parallel to the foliation in adjacent biotite gneiss.

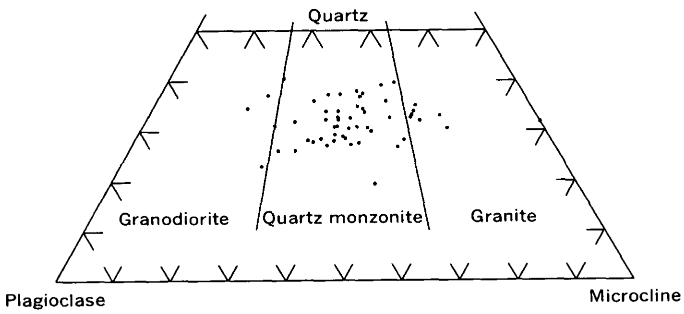

FIGURE 11.—Triangular plot of plagioclase, quartz, and microcline in the Silver Plume Granite. Modal volume percent; dots are the 54 modes summarized in table 9.

TERTIARY IGNEOUS ROCKS

Tertiary igneous rocks in the central part of the Front Range of Colorado are concentrated in a belt that extends northeast from Montezuma to Boulder (Tweto and Sims, 1963, pl. 1). As the Empire quadrangle is on the northwest side of this belt, Tertiary igneous rocks are common in the southern and eastern parts of the quadrangle and absent in the northwestern part (pl. 2).

Within the Empire quadrangle, small stocks, plugs, and dikes of a variety of igneous rocks crop out. The rocks of the Empire stock (pl. 2) are phaneritic or porphyritic phaneritic, whereas most of the other Tertiary igneous rocks are porphyries with very fine grained to aphanitic groundmasses. Wells (1960, p. 234–235) has presented a detailed petrographic classification of the Tertiary igneous rocks that occur in the Lawson–Central City–Idaho Springs area, which is just east and southeast of the Empire quadrangle. In the present study, the same classification was used with considerable success, and additional rock types were identified. Table 10 shows the correlation between the names of rock types used in this report and those used in the report by Wells and shows the rock types that are not common to both areas.

TABLE 10.—*Correlation of Tertiary igneous rock names as used by Wells (1960) and in this report*

Wells (1960)	This report
No equivalent	Monzonite group:
	Feldspathoidal hornblende-pyroxene monzonite.
	Hornblende-pyroxene monzonite.
	Porphyritic hornblende-pyroxene monzonite.
	Quartz-bearing monzonite porphyry.
	Monzonite porphyry undivided.
Light-colored granodiorite group:	
Light-colored granodiorite porphyry.	No equivalent.
Albite granodiorite porphyry	Leucocratic monzonite.
Alkalic syenite porphyry	
Quartz monzonite group:	No equivalent.
Quartz monzonite porphyry.	
Granite porphyry.	
Alaskite porphyry.	
Bostonite group:	Bostonite porphyry undivided.
Bostonite porphyry.	
Garnetiferous bostonite porphyry.	
Trachytic granite porphyry.	
Quartz bostonite porphyry.	
No equivalent	Sanidinite porphyry.
Hornblende granodiorite group:	
Hornblende granodiorite porphyry.	Hornblende granodiorite porphyry.[1]
Biotite granodiorite porphyry.	Biotite granodiorite porphyry.[1]
Biotite quartz monzonite porphyry.	Biotite quartz monzonite porphyry.
Biotite quartz latite porphyry.	No equivalent.

[1] Granodiorite group.

GRANODIORITE GROUP

The rocks of the granodiorite group are characterized by a large modal and normative quartz content, by more plagioclase than alkali feldspar, and by moderately abundant ferromagnesian minerals. Plagioclase, alkali feldspar, quartz, hornblende, and biotite occur as phenocrysts. These rocks form several small stocks or plugs and numerous dikes in the southern and eastern parts of the quadrangle.

The granodiorite group has been divided, according to the dominant ferromagnesian mineral, into hornblende granodiorite porphyry and biotite granodiorite porphyry. Many of the dikes have been so intensely altered that the characteristic primary ferromagnesian mineral cannot be recognized. Such dikes are classified as granodiorite porphyry, undivided.

HORNBLENDE GRANODIORITE PORPHYRY

Hornblende granodiorite porphyry forms a small plug about 1¼ miles north of Empire, part of the small stock west of Alice, and several dikes, one of which is near the Mammoth Gulch fault in the northern part of the quadrangle. One dike north of Empire is cut by a bostonite porphyry dike, and this is the only indication of relative age of the hornblende granodiorite found in the Empire quadrangle.

The hornblende granodiorite porphyry plugs are phaneritic and seriate porphyritic. They consist of about 17 percent quartz, 30 percent orthoclase, 40 percent plagioclase, 5–10 percent hornblende, and minor amounts of opaque oxides, sphene, and apatite. The dikes contain phenocrysts of plagioclase, alkali feldspar, quartz, and hornblende and have xenomorphic granular to aphanitic groundmasses composed of quartz and feldspar.

The plagioclase phenocrysts are moderately to strongly zoned and commonly range from An_{40} in the cores to An_{25} in the rims. Weakly perthitic alkali feldspar forms phenocrysts and forms mantles on plagioclase phenocrysts. Myrmekite is common at plagioclase-alkali feldspar contacts. The hornblende is pale green and occurs as short subhedral prisms.

The chemical compositions and CIPW norms of four samples of hornblende granodiorite porphyry are shown in table 11.

TABLE 11.—*Chemical and spectrographic analyses and CIPW norms of hornblende granodiorite porphyry, biotite granodiorite porphyry, biotite quartz monzonite porphyry, and granite aplite, in weight percent*

[--, constituent was not analyzed. Sample localities shown on pl. 2]

	Hornblende granodiorite porphyry				Biotite granodiorite porphyry				Biotite quartz monzonite porphyry	Granite aplite
Field No.	[1] 1-107	[1] 4-165B	[2] 4-165D	[1] 5-2	[1] 4-164B	[2] 4-196	[2] 10-1	[1] 10-31B	[3] 8-133	[1] 4-165A
Lab No.	158280	158288	H3250	158289	158286	H3251	H3252	158294	160972	158287
Chemical analyses										
SiO_2	58.1	63.8	62.09	63.6	65.4	66.32	68.62	69.4	65.7	76.4
Al_2O_3	18.4	16.2	17.62	16.6	16.8	16.22	15.82	16.2	15.4	12.4
Fe_2O_3	4.3	2.7	2.66	2.7	2.6	2.23	1.20	1.5	1.5	1.4
FeO	2.8	2.4	2.09	3.0	2.0	1.99	1.34	.93	1.2	.72
MgO	2.0	1.5	1.35	1.6	1.08	1.05	.67	.57	.76	.18
CaO	4.6	5.0	5.29	3.8	3.23	2.35	2.98	1.6	2.8	.64
Na_2O	4.1	3.5	4.34	3.0	3.3	3.76	3.75	4.6	4.0	2.3
K_2O	1.7	3.2	2.81	3.1	3.6	3.76	3.66	3.8	3.6	5.9
H_2O+ }	2.4	.44	.35	}1.2	.94	1.10	.45	} .98	.45	} .50
H_2O- }			.12			.29	.11		1.0	
TiO_2	.79	.58	.51	.50	.39	.38	.27	.30	.29	.08
P_2O_5	.48	.44	.29	.32	.29	.23	.14	.18	.18	.02
MnO	.08	.10	.14	.02	.02	.05	.03	.02	.16	.00
CO_2	.05	.01	.02	.00	.00	.01	.31	.01	2.6	.00
Cl	.02	.03	.02	.03	.03	.01	.02	.00	--	.02
F	.12	.08	.07	.06	.08	.04	.06	.04	--	.01
S	.00	.00	.07	.00	.10	.00	.03	.00	--	.00
Subtotal	--	--	99.84	--	--	99.79	99.46	--	--	--
Less O=F,Cl	--	--	.07	--	--	.02	.05	--	--	--
Total	100	100	99.77	99	100	99.77	99.41	100	100	100
Spectrographic analyses [4]										
Ba	0.15	0.3	0.15	0.2	0.15	0.15	0.2	0.3	--	0.2
Be	.01	.0005	.0002	.002	.0007	.00015	.00015	.0003	--	.0007
Ce	.03	.02	.02	.02	.02	0	.03	.015	--	0
Co	.0007	.0007	.001	0	.0007	.0007	.002	.0007	--	0
Cr	.0007	.0005	.0007	.0015	.0007	.0003	.001	.0005	--	0
Cu	.005	.002	.003	.007	.007	.007	.007	.0005	--	.005
Ga	.003	.002	.003	.003	.003	.003	.003	.003	--	.002
La	.02	.015	.015	.01	.01	.01	.015	.007	--	0
Nb	.007	.005	.005	.003	.003	.005	.003	.005	--	0
Ni	.002	0	0	.001	.0007	0	0	0	--	0
Pb	.005	.0015	.0015	.003	.002	.003	.002	.002	--	.0015
Sc	.0015	.0015	.0015	.0015	.0015	.001	.0007	.0007	--	0
Sr	.2	.15	.2	.15	.2	.15	.15	.3	--	.15
V	.02	.007	.007	.01	.007	.007	.005	.005	--	.002
Y	.007	.005	.005	.003	.005	.002	.002	.0015	--	0
Yb	.0007	.0005	.0005	.0003	.0005	.0002	.0002	.00015	--	0
Zr	.03	.015	.02	.015	.015	.01	.01	.01	--	.007
Nd	.015	.015	.015	.015	.015	.015	0	0	--	--
CIPW norms [5]										
Q	16.6	19.3	14.2	23.8	24.8	23.7	26.5	24.5	--	39.0
or	10.0	19.6	16.6	18.3	21.3	22.2	21.6	22.4	--	34.8
ab	34.5	29.4	36.6	25.1	27.7	31.7	31.6	38.9	--	19.3
an	18.6	18.8	20.4	16.4	13.6	9.9	11.5	6.5	--	3.0
C	3.0	0	0	2.3	2.5	2.4	1.5	2.2	--	1.2
di	0	2.2	2.7	0	0	0	0	0	--	0
hy	5.4	2.7	3.0	6.5	3.4	3.9	2.7	1.4	--	.5
mt	6.2	3.9	3.9	3.9	3.8	3.2	1.7	2.2	--	2.0
il	1.5	1.1	1.0	1.0	.7	.7	.5	.6	--	.2
ap	1.1	1.0	.7	.8	.7	.5	.3	.4	--	0
cc	.1	0	0	0	0	0	.7	0	--	0
fr	.2	.1	.1	.1	.1	.1	.1	.1	--	0

[1] Chemical analyses are rapid-rock analyses by P. L. D. Elmore, I. H. Barlow, S. D. Botts, G. W. Chloe, J. C. Hamilton, 1961; F, Cl, S separate analyses by V. C. Smith,, 1961.
[2] Chemical analyses are standard rock analyses by C. L. Parker, 1961.
[3] Chemical analyses are rapid-rock analyses by P. L. D. Elmore, S. D. Botts, G. W. Chloe, L. Artis, H. Smith, 1963.
[4] Analyst, J. C. Hamilton, 1961. Looked for but not detected: Ag, As, Au, B, Bi, Cd, Ge, Hf, Hg, In, Li, Mo, Pd, Pt, Re, Sb, Sn, Ta, Te, Th, Tl, U, W, Zn, Pr, Sm, Eu. Gd, Tb, Dy, Ho, Er, Tm. Biotite quartz monzonite porphyry not analyzed.
[5] CO_2 content was too high to permit calculation of meaningful norms for biotite quartz monzonite porphyry.

BIOTITE GRANODIORITE PORPHYRY

Biotite granodiorite porphyry forms a small irregular stock on the north side of Clear Creek between Lawson and Empire, part of the small stock west of Alice, a plug or stock of unknown size that extends southward from beneath glacial moraine on the south side of Mill Creek, and several dikes in the southeast part of the quadrangle. Biotite granodiorite porphyry dikes are cut by bostonite porphyry dikes at three localities.

In plugs and stocks the biotite granodiorite porphyry is seriate porphyritic and contains 15–30 percent quartz, 45–55 percent plagioclase, 7–28 percent alkali feldspar, 2–11 percent biotite, and minor amounts of opaque oxides, sphene, and apatite. Phenocrysts of quartz, plagioclase, alkali feldspar, and biotite are surrounded by a fine-grained to very fine grained, xenomorphic granular groundmass of quartz and feldspar. In dikes the rock is porphyritic, has a very fine grained to aphanitic groundmass, and contains the same phenocrysts as in the plugs except for alkali feldspar.

The plagioclase phenocrysts are moderately to strongly zoned and appear to range from An_{30} in the cores to An_{15} in the rims. The alkali feldspar phenocrysts are untwinned and slightly perthitic. Alkali feldspar commonly forms mantles on the plagioclase phenocrysts, and myrmekite is common at plagioclase–alkali feldspar contacts. Quartz forms euhedral phenocrysts, rounded phenocrysts, and coarse anhedral grains between feldspar phenocrysts. Biotite occurs as small subhedral crystals.

The chemical composition and CIPW norms of four samples of biotite granodiorite porphyry are shown in table 11.

GRANITE APLITE

Granite aplite dikes a few inches wide cut hornblende and biotite granodiorite porphyry in the composite stock west of Alice (pls. 1, 2). The aplite is a xenomorphic granular rock composed of quartz, oligoclase, orthoclase perthite, and minor amounts of opaque oxides. Chemical and spectrographic analyses and CIPW norm of the aplite are given in table 11.

MONZONITE GROUP

The rocks of the monzonite group are characterized by the scarcity or absence of modal or normative quartz, by approximately equal proportions of plagioclase and potassium feldspar, and by the presence of pyroxene and amphibole. The following varieties have been recognized: feldspathoidal hornblende-pyroxene monzonite, hornblende-pyroxene monzonite, porphyritic hornblende-pyroxene monzonite, monzonite porphyry, quartz-bearing monzonite porphyry, and leucocratic monzonite. These rocks occur in the Empire stock, in the Lincoln Mountain stock, and as dikes in the southwestern part of the quadrangle and on the divide between Mill Creek and Fall River.

FELDSPATHOIDAL HORNBLENDE-PYROXENE MONZONITE

Three small bodies of feldspathoidal rock, in the western and southern parts of the Empire stock (pl. 2), are shown as feldspathoidal hornblende-pyroxene monzonite on the geologic map, but the southernmost body is a hybrid rock of mixed monzonite and feldspathoidal syenite.

The feldspathoidal hornblende-pyroxene monzonite is medium to dark gray and very fine grained. The ferromagnesian minerals are generally coarse enough that they stand out as small black specks, and they commonly have a weak to distinct parallel alinement of the prism zones. The rock has a greasy luster due to the presence of nepheline; it also contains hornblende, pyroxene, opaque oxides, plagioclase, alkali feldspar, sodalite, apatite, and sphene. The range of modal compositions of 11 samples is shown in figure 12.

Subhedral phenocrysts of pale-green nonpleochroic pyroxene constitute 10–20 percent of the feldspathoidal hornblende-pyroxene monzonite. Inclusions of apatite and opaque oxides are common in the pyroxene, but inclusions of feldspars or feldspathoids are sparse. The pyroxene is generally rimmed and irregularly replaced by green amphibole (fig. 13*B*). The pyroxenes are generally weakly zoned and the optical properties vary: $ny=1.70\text{–}1.71, y=b, 2V_z = 55°$ (core)–65° (rim), $Z<c=50°$. The pyroxene appears to be the same as that in the hornblende-pyroxene monzonite for which chemical analyses are given in table 12.

The hornblende content ranges from trace amounts to 23 percent. Much of the hornblende is present as uralite surrounding and embaying pyroxene, and a large amount occurs as anhedral grains that poikilitically enclose subhedral grains of plagioclase and alkali feldspar. The total amount of hornblende and pyroxene ranges from 13 to 35 percent in samples of the feldspathoidal hornblende-pyroxene monzonite, and the ratio of pyroxene to hornblende is very erratic, ranging from very large to about 0.6. This erratic variation of the ratio of pyroxene to hornblende is also characteristic of the hornblende-pyroxene monzonite.

Plagioclase makes up 16–26 percent of the rock and occurs in two textural varieties. One variety occurs as subhedral to anhedral well-twinned grains and ranges in composition from about An_{25} to An_{30}. Most grains are weakly zoned and have albite-rich margins. The second variety is fine-grained poorly twinned plagioclase that occurs as mantles on nepheline (fig. 13*A*). This

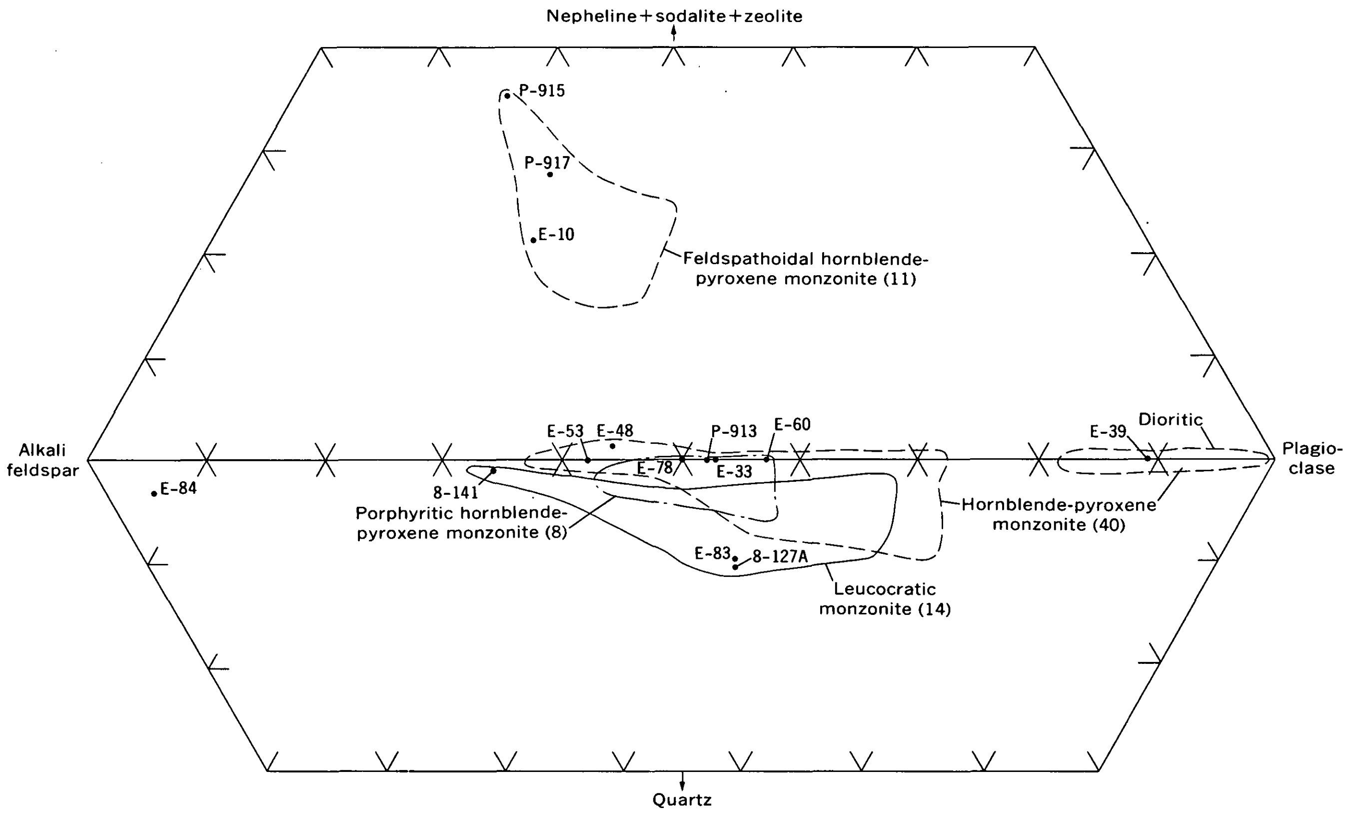

A

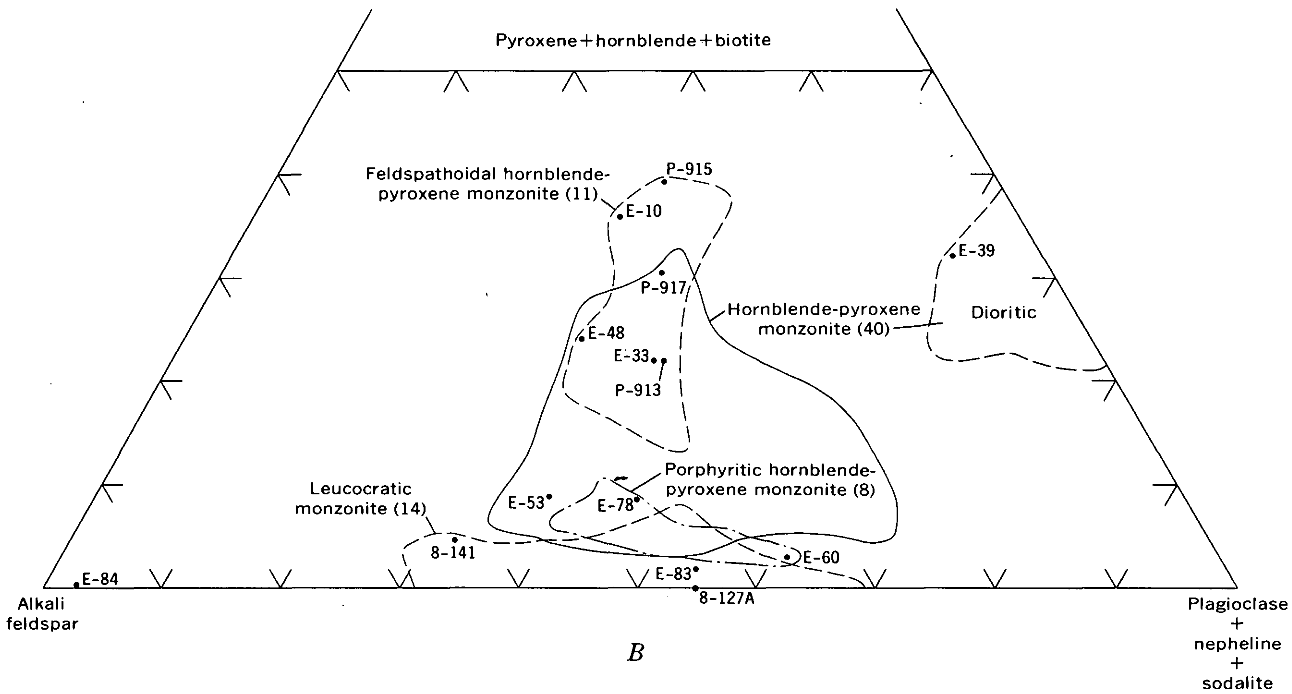

B

FIGURE 12.—Modal compositions of rocks of the Empire stock. The number of modes for each rock type is indicated in parentheses. Chemically analyzed samples listed in tables 12, 13, and 16 are shown by numbered dots. *A*, Proportions of quartz, feldspars, and feldspathoids. *B*, Proportions of ferromagnesian minerals, feldspars, and feldspathoids.

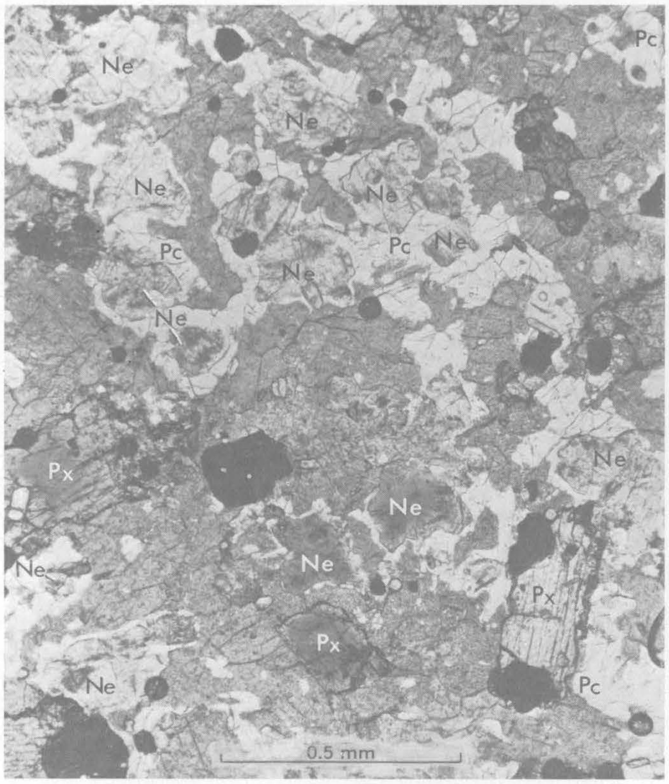

A

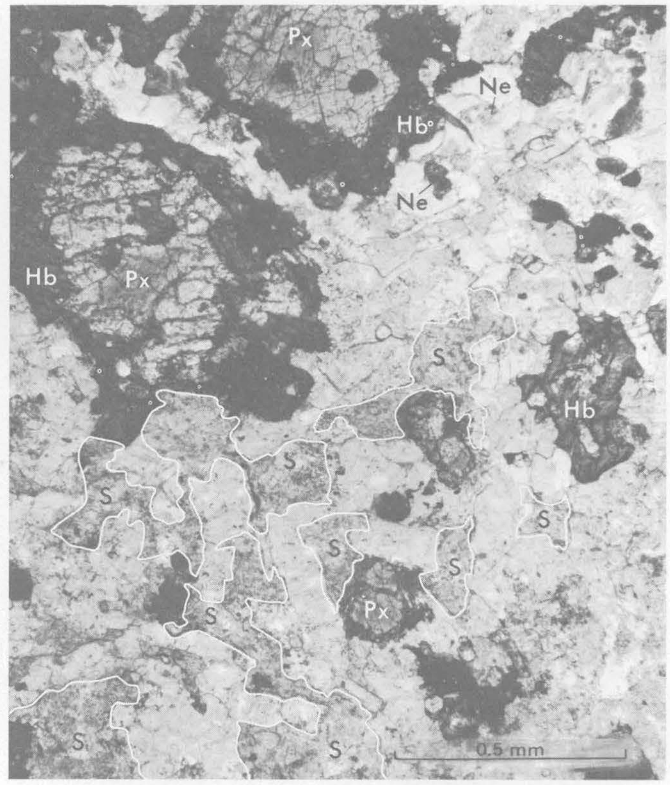

B

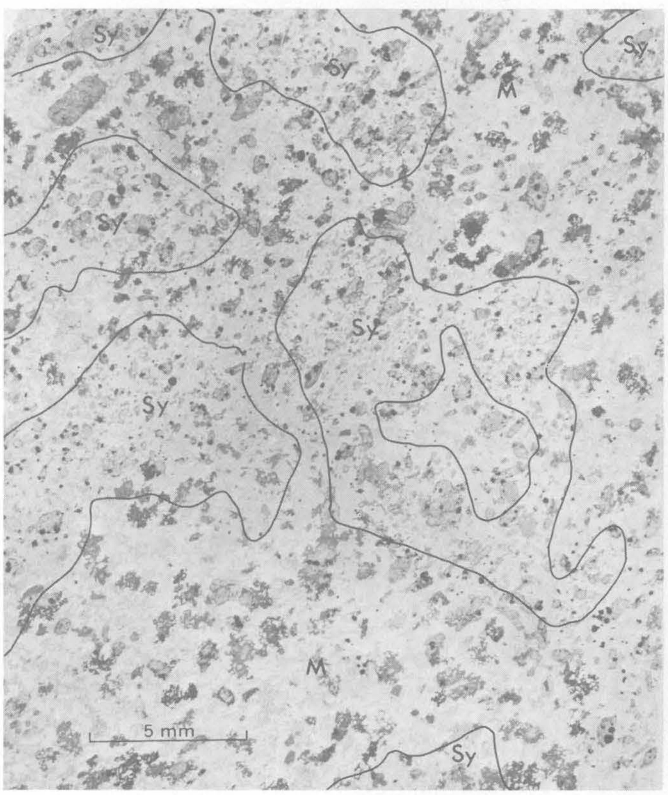

C

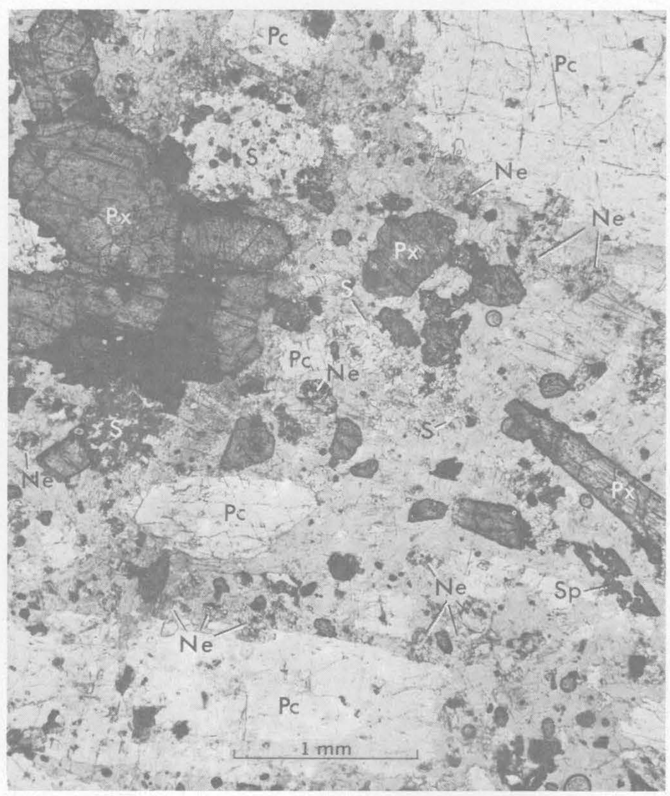

D

FIGURE 13.—Photomicrographs of feldspathoidal hornblende-pyroxene monzonite of the Empire stock. *A*, Nepheline (Ne) is surrounded by thin to thick rims of plagioclase (Pc), and pyroxene (Px) is slightly uralitized. Alkali feldspar is medium gray. The thin section was stained with sodium cobaltinitrite and malachite green. Plain light. *B*, Hornblende (Hb) forms uralitic rims on pyroxene (Px) and also occurs as anhedral grains surrounding feldspars. Anhedral masses of sodalite (S) occur in a portion of the rock in which nepheline (Ne) is sparse. Plagioclase is white: alkali feldspar is light gray. The thin section was stained with sodium cobaltinitrite and malachite green. Plain light. *C*, Most of a thin section of hybrid feldspathoidal monzonite. The outlined areas are syenite (Sy) and consist of alkali feldspar, nepheline, sodalite, minor plagioclase, pyroxene, and minor hornblende. The surrounding areas are monzonite (M) and contain plagioclase, alkali feldspar, hornblende, and minor amounts of pyroxene. Plain light. *D*, Porphyritic feldspathoidal monzonite from the contact zone between hybrid feldspathoidal monzonite and hornblende-pyroxene monzonite. The phenocrysts consist of plagioclase (Pc), pyroxene (Px), sodalite (S), and sphene (Sp). The groundmass consists principally of alkali feldspar (medium gray) accompanied by nepheline (Ne) and minor amounts of sodalite (S), plagioclase, and pyroxene. The thin section was stained with sodium cobaltinitrite. Plain light.

plagioclase is probably more sodic, perhaps An_{15}, than the separate grains of plagioclase. In some samples practically all the plagioclase occurs as rims around nepheline, whereas in other samples the amount of plagioclase occuring as rims is a small part of the total plagioclase.

Nepheline makes up 6–13 percent of the rock and occurs as anhedral to subhedral grains of about the same size as the associated plagioclase. The nepheline grains commonly develop a weak yellow stain when treated with hydrofluoric acid and then with sodium cobaltinitrite. This stain indicates a substantial potassium content. The composition is determined by X-ray is Ne_{62} Ks_{38} weight percent.

Alkali feldspar, which makes up 24–37 percent of the rock , is nonperthitic, untwinned, and anhedral, and it forms a matrix to all of the other minerals. The composition of the alkali feldspar in analyzed sample E–10, as determined by X-ray measurement is $Or_{75}Ab_{25}$ weight percent. Phair and Fisher (1962) reported that the alkali feldspar in three samples of the nepheline monzonite had compositions between $Or_{71}Ab_{29}$ and $Or_{73}Ab_{26}$.

Sodalite, which makes up 1–4 percent of the rock, forms anhedral patches that are irregularly distributed throughout the rock (fig. 13*B*), and it occupies microscopic areas in which nepheline is sparse. The sodalite was identified by X-ray and by qualitative chemical tests for chlorine.

Clots of fibrous zeolites make up as much as 5 percent of the rock. The zeolites are clearly the alteration product of sodalite and, to a lesser degree, nepheline.

Thin leucocratic veinlets, principally of alkali feldspar and sodalite, cut the feldspathoidal hondblende-pyroxene monzonite in the roadcuts along U.S. Highway 40. These veinlets are paper thin to 1 inch thick and can be traced for a few tens of feet. The feldspar is nonperthitic to very weakly perthitic and is subhedral. The sodalite forms coarse anhedral patches and irregular masses interstitial to the feldspar. Some veins contain minor amounts of hornblende and sphene and traces of magnetite as the only other minerals. Other veins, however, contain alkali feldspar and sodalite as the main minerals accompanied by hornblende, biotite, brown garnet, sphene, minor nepheline, and as much as 4 percent cancrinite. The garnet forms skeletal to poikilitic intergrowths with the feldspar, and the cancrinite is intergrown with sodalite or interstitial to the feldspar.

The chemical compositions and CIPW norms of representative samples of the feldspathoidal hornblende-pyroxene monzonite are shown in table 12.

Hybrid feldspathoidal monzonite, which occurs in the Empire stock south of the West Fork of Clear Creek, is readily distinguishable from the surrounding hornblende-pyroxene monzonite because it is much finer grained. The northwestern contact of the body obliquely crosses a small ridge, and at an altitude of about 9,100 feet is well exposed and sharp for a distance of about 60 feet. Elsewhere the contact is covered.

The rock is classified as a hybrid monzonite because it consists of an intimate mixture of feldspathoidal syenite and hornblende-pyroxene monzonite, which are visible in hand specimens and thin sections. Figure 13*C* shows most of a thin section of a sample of the hybrid rock. The boundaries of nepheline syenite have been drawn to show the fine scale of the intermixture. The monzonite part of the rock contains plagioclase, alkali feldspar, uralitized pyroxene, and abundant primary hornblende. The syenite part of the rock contains alkali feldspar, nepheline, sodalite, minor plagioclase, and uralitized pyroxene (hornblende is abundant only at the boundary with monzonite).

Boulders that mantle the northwest contact of the hybrid rock below an altitude of 9,100 feet also show an intermixture of rock types, but here the monzonite part of the mixture is much coarser, and the mixture is also coarser. Patches several inches across of feldspathoidal rock are mixed in a swirled pattern with medium-grained hornblende-pyroxene monzonite. The feldspathoidal rock contains large phenocrysts of zoned plagioclase (An_{30-35}), seriate phenocrysts of slightly

332-862 O—69——4

TABLE 12.—*Chemical and spectrographic analyses and CIPW norms of feldspathoidal hornblende-pyroxene monzonite*

[All amounts in weight percent. ----, constituent was not analyzed. Sample localities shown on pl. 2]

Field No.	[1] E-10	[2] P-915	[2] P-917	[2] P-570
Chemical analyses				
SiO_2	50.04	50.7	52.0	49.4
Al_2O_3	17.36	17.3	17.8	15.6
Fe_2O_3	4.07	4.2	4.0	6.1
FeO	4.63	4.2	3.9	5.1
MgO	3.19	3.0	2.3	3.7
CaO	8.19	7.3	6.5	8.6
Na_2O	4.99	5.5	6.0	4.1
K_2O	4.65	4.6	4.8	4.0
H_2O+	.52	} .46	.54	[3] .80
H_2O-	.05			
TiO_2	.93	.90	.84	1.0
P_2O_5	.69	.68	.56	.83
MnO	.22	.22	.22	.24
CO_2	.11	.20	.22	----
Cl	.14	----	----	----
F	.11	----	----	----
S	.03	----	----	----
Subtotal	99.92	----	----	----
Less O=F, Cl	.10	----	----	----
Total	99.82	99	100	100
Spectrographic analyses [4]				
Ba	0.2	----	----	----
Be	.00015	----	----	----
Ce	.03	----	----	----
Co	.002	----	----	----
Cr	.001	----	----	----
Cu	.007	----	----	----
Ga	.003	----	----	----
La	.015	----	----	----
Nb	.005	----	----	----
Ni	.001	----	----	----
Pb	.003	----	----	----
Sc	.003	----	----	----
Sr	.3	----	----	----
V	.03	----	----	----
Y	.003	----	----	----
Yb	.0003	----	----	----
Zr	.01	----	----	----
Nd	.015	----	----	----
CIPW norms				
or	27.5	27.2	28.4	23.6
ab	15.2	18.9	21.9	20.3
an	11.8	8.9	7.5	12.4
ne	14.0	15.0	15.6	7.8
hl	.2	----	----	----
di	18.7	17.4	16.0	20.0
ol	2.1	1.6	.6	2.0
mt	5.9	6.1	5.8	8.8
il	1.8	1.7	1.6	1.9
ap	1.6	1.6	1.3	2.0
fr	.2	----	----	----
cc	.2	.5	.5	----

[1] Chemical analyses are standard rock analyses by C. L. Parker, 1961. Lab. No. H3253.
[2] Chemical analyses from unpublished rapid-rock analyses from George Phair. Analysts, P. L. D. Elmore, K. E. White, and S. D. Botts. P-915, P-917 analyzed in 1955; P-570 in 1952. Exact locality of P-570 not known, not shown on plate 2.
[3] Loss on ignition.
[4] Analyst, J. C. Hamilton, 1961. Looked for but not detected: Ag, As, Au, B, Bi, Cd, Ge, Hf, Hg, In, Li, Mo, Pd, Pt, Re, Sb, Sn, Ta, Te, Th, Tl, U, W, Zn, Pr, Sm, Eu, Gd, Tb, Dy, Ho, Er, Tm.

uralitized pyroxene, and equant phenocrysts of sodalite in a matrix of alkali feldspar and nepheline (fig. 13*D*). The nepheline has thin rims of plagioclase (An_{20}).

HORNBLENDE-PYROXENE MONZONITE

The main part of the Empire stock consists of phaneritic hornblende-pyroxene monzonite. This rock is medium to light gray and fine grained and even grained. Prisms and irregular grains of hornblende and pyroxene are abundant and conspicuous; they are commonly alined, and this alinement imparts a steeply plunging flow lineation to the rock. In many outcrops the rock has a weak to strong compositional layering in which ferromagnesian mineral-rich layers alternate with feldspar-rich layers.

Small inclusions of Precambrian rocks are distributed sparsely throughout much of the hornblende-pyroxene monzonite. These inclusions are dominantly foliated hornblende-rich rocks that resemble the Precambrian hornblende gneiss, amphibolite, calc-silicate gneiss, or hornblendite. Biotite gneiss and microcline gneiss inclusions occur in the southern part of the stock.

A sharp contact between the feldspathoidal hornblende-pyroxene monzonite and the surrounding hornblende-pyroxene monzonite is exposed in the highway cuts at the west side of the western body. This contact is very sinuous, and rounded lobes of hornblende-pyroxene monzonite extend into the feldspathoidal hornblende-pyroxene monzonite; thus, wedges of the feldspathoidal monzonite are isolated. Within a few centimeters of the contact the hornblende-pyroxene monzonite contains very small irregular patches of rock that have the same mineralogy and texture as the feldspathoidal hornblende-pyroxene monzonite. At one place a rounded inclusion of the feldspathoidal hornblende-pyroxene monzonite was found within the hornblende-pyroxene monzonite. These relations clearly indicate that the hornblende-pyroxene monzonite intruded the feldspathoidal hornblende-pyroxene monzonite, and the sinuous contact suggests that the feldspathoidal hornblende-pyroxene monzonite was not completely solid at the time it was invaded by the hornblende-pyroxene monzonite.

The hornblende-pyroxene monzonite is a fine-grained hypautomorphic granular rock composed principally of plagioclase, hornblende, pyroxene, and alkali feldspar. Opaque oxides, apatite, and sphene are ubiquitous accessory minerals, and biotite occurs in small amounts in some in some specimens. Quartz is sparse or absent in most of the samples examined, although it makes up 9 percent of one sample. Small irregular clots of fibrous to cryptocrystalline material, probably zeolites, make up from trace amounts to 6 percent of some samples. In a few thin sections, parts of these aggregates appeared to be isotropic and were deeply stained by H_3PO_4 and methyl blue, suggesting that the zeolite aggregates are replacements of sodalite. Quartz and the zeolite aggregates do not occur in the same samples.

Figure 12 shows the range of modal compositions of the hornblende-pyroxene monzonite samples examined, and table 13 gives the chemical composition and CIPW norms of six samples.

Ferromagnesian minerals compose 4–27 percent of the hornblende-pyroxene monzonite. They are most abundant in the southern part of the monzonite body and become less abundant outward from this area. They compose 4–13 percent of the northern part of the body.

TABLE 13.—*Chemical and spectrographic analyses and CIPW norms of hornblende-pyroxene monzonite, porphyritic hornblende-pyroxene monzonite, and monzonite porphyry, in weight percent*

[----, constituent was not analyzed. Sample localities shown on pl. 2]

	Hornblende-pyroxene monzonite							Porphyritic hornblende-pyroxene monzonite	Monzonite porphyry
Field No.	[1] E-33	[2] E-39	[1] E-48	[1] E-53	[2] E-78	[3] P-913	[3] P-914	[2] E-60	[1] 5-51
Lab. No.	158297	H3254	158298	158299	H3256			H3255	158291
Chemical analyses									
SiO_2	54.7	47.00	53.9	57.0	58.13	54.4	54.2	57.73	58.2
Al_2O_3	18.5	16.56	17.6	17.6	19.09	18.5	18.5	20.31	17.4
Fe_2O_3	4.1	6.19	3.2	4.0	3.17	3.6	3.7	3.05	4.2
FeO	3.4	5.36	3.8	2.8	1.79	3.3	3.4	1.35	2.8
MgO	2.3	4.54	2.6	1.8	1.11	2.1	1.9	.75	2.0
CaO	6.4	11.93	7.0	5.3	4.79	6.5	6.4	5.30	5.3
Na_2O	4.6	3.29	4.4	4.6	5.14	4.3	5.2	5.28	4.5
K_2O	4.2	1.50	4.5	4.8	5.02	4.3	4.1	4.22	3.3
H_2O+	.69	.65	.90	.58	.27	----	.76	.33	.57
H_2O-		.15			.17	[4] .80		.27	
TiO_2	.89	1.31	.90	.86	.68	.81	.70	.73	.84
P_2O_5	.49	.87	.49	.45	.21	.50	.40	.16	.50
MnO	.19	.24	.20	.16	.19	.16	.18	.16	.13
CO_2	.01	.19	.02	.01	.01	----	.40	.03	.01
Cl	.03	.02	.08	.04	.02	----	----	.02	.05
F	.08	.10	.11	.10	.09	----	----	.07	.11
S	.00	.02	.00	.00	.01	----	----	.01	.00
Subtotal								99.77	----
Less O=F, Cl	----	.05	----	----	.05	----	----	.04	----
Total	100.0	99.87	100.0	100.0	99.84	100.0	100.0	99.73	100.0
Spectrographic analyses [5]									
Ba	0.3	0.15	0.2	0.2	0.3	----	----	0.3	0.2
Be	.0002	0	.0003	.0002	.00015	----	----	.00015	.0002
Ce	.03	.03	.03	.03	.05	----	----	.05	.02
Co	.0015	.0015	.0015	.0015	.0007	----	----	.0007	.0015
Cr	.0005	.0015	.0015	.0005	.00015	----	----	0	.0015
Cu	.003	.007	.005	.003	.003	----	----	.007	.005
Ga	.003	.003	.003	.003	.003	----	----	.003	.003
La	.015	.01	.015	.015	.02	----	----	.02	.015
Nb	.003	0	.003	.005	.005	----	----	.005	.005
Ni	0	.001	.0007	0	0	----	----	0	.0007
Pb	.002	.0015	.003	.002	.003	----	----	.002	.002
Sc	.0015	.003	.002	.0015	.001	----	----	.0007	.002
Sr	.5	.3	.3	.3	.3	----	----	.5	.3
V	.02	.03	.03	.02	.02	----	----	.02	.02
Y	.003	.003	.005	.003	.003	----	----	.005	.003
Yb	.0003	.0003	.0005	.0003	.0005	----	----	.0005	.0005
Zr	.007	.007	.015	.015	.01	----	----	.007	.015
Nd	.015	.015	.015	.015	.015	----	----	.015	.015
CIPW norms									
Q	0	0	0	1.3	0	0	0	0.4	7.8
or	24.8	8.9	26.6	28.4	29.7	25.4	24.2	24.9	19.5
ab	36.4	24.6	30.6	38.6	42.8	35.4	35.5	44.5	37.7
an	17.5	26.1	15.3	13.4	14.3	18.5	15.0	19.3	17.7
ne	1.2	1.7	3.3	0	.3	.5	4.6	0	0

See footnotes at end of table.

TABLE 13.—*Chemical and spectrographic analyses and CIPW norms of hornblende-pyroxene monzonite, porphyritic hornblende-pyroxene monzonite, and monzonite porphyry, in weight percent*—Continued

[----, constituent was not analyzed. Sample localities shown on pl. 2]

	Hornblende-pyroxene monzonite							Porphyritic hornblende-pyroxene monzonite	Monzonite porphyry
Field No.	[1] E-33	[2] E-39	[1] E-48	[1] E-53	[2] E-78	[3] P-913	[3] P-914	[2] E-60	[1] 5-51
Lab. No.	158297	H3254	158298	158299	H3256			H3255	158291
	CIPW norms—Continued								
hl	0	0	.1	.1	0	----	----	0	.1
di	8.4	20.5	12.5	7.4	5.8	8.4	9.4	4.0	3.6
hy	0	0	0	1.7	0	0	0	0	3.8
ol	2.5	3.2	2.6	0	.1	2.3	1.8	0	0
mt	5.9	9.0	4.6	5.8	4.4	5.2	5.4	2.7	6.1
hm	0	0	0	0	.1	0	0	1.2	0
il	1.7	2.5	1.7	1.6	1.3	1.5	1.3	1.4	1.6
ap	1.2	2.1	1.2	1.1	.5	1.2	1.0	.4	1.2
fr	.1	.1	.2	.2	.2	0	0	.1	.2
cc	0	.4	0	0	0	0	.9	.1	0

[1] Chemical analyses are rapid rock analyses by P. L. D. Elmore, I. H. Barlow, S. D. Botts, and G. W. Chloe, 1961. Separate analyses for F, Cl, S by V. C. Smith, 1961.
[2] Chemical analyses are standard rock analyses by C. L. Parker, 1961.
[3] Chemical analyses are unpublished analyses from George Phair. Rapid rock analyses by P. L. D. Elmore, K. E. White, and S. D. Botts, 1955.
[4] Ignition.
[5] Analyst, J. C. Hamilton, 1961. Looked for but not detected: Ag, As, Au, B, Bi, Cd, Ge, Hf, Hg, In, Li, Mo, Pd, Pt, Re, Sb, Sn, To, Te, Th, Tl, U, W, Zn, Pr, Sm, Eu, Gd, Tb, Dy, Ho, Er, Tm.

Pyroxene, which forms 0–20 percent of the rock, is generally rimmed and irregular replaced by green amphibole (fig. 14*A*, *B*). The chemical analyses of pyroxenes separated from samples E–23 and E–119 are given in table 14. Calculation of the structural formulas for these pyroxenes indicates that they are aluminous salites containing about 9–15 percent acmite, as shown below:

Structural formulas

	$W_{(1-P)}(X,Y)_{(1+P)}Z_2O_6$ (Number of ions on basis of 6 oxygen [1]) 1		2		$A_{0\rightarrow 1}X_2Y_5Z_8O_{22}(OH,F,O)_2$ Number of ions on basis of 24(OH,F,Cl,O) 3	
Si	1.77	2.00 = Z	1.80	2.00 = Z	6.21	8.00 = Z
Al	.23		.20		1.79	
Al	.10	1.05 = X,Y	.05	1.02 = X,Y	.34	4.84 = Y
Ti	.04		.05		.22	
Fe^{+3}	.15		.15		.92	
Mg	.54		.56		1.76	
Fe^{+2}	.20		.19		1.52	
Mn	.02		.02		.08	
Ca	.81	0.95 = W	.88	0.97 = W	1.99	= X
Na	.11		.08		.75	1.02 = A
K	.03		.01		.36	
O	6.00		6.00		22.00	
OH					1.14	2.00
F					.19	
O					.70	

[1] 0.08 [$Ca_5(PO_4)_3(Cl, F)$] removed from sample 1 and 0.05 [$Ca_5(PO_4)_3(Cl, F)$] removed from samples 2 and 3 before calculating structural formulas.

1. Field No. E–23; lab. No. I4052. Pyroxene.
2. Field No. E–119; lab. No. I4054. Pyroxene.
3. Field No. E–68; lab. No. I4053. Amphibole.

Hornblende, which forms 0–20 percent of the rock, occurs as rims and replacement of pyroxene and as anhedral grains that poikilitically enclose feldspar grains (fig. 14*A*, *B*). The chemical analysis and formula of hornblende from sample E–68 are shown in table 14. This amphibole can be loosely classified as pargasite.

Whereas the total amount of pyroxene plus amphibole varies regularly from place to place within the stock, the ratio of amphibole to pyroxene is very erratic.

Biotite, which ranges in content from 0 to 9 percent, generally occurs as small subhedral crystals disseminated uniformly throughout a particular rock. In a few samples biotite appears to have replaced pyroxene and amphibole. The distribution of biotite-bearing hornblende-pyroxene monzonite is very irregular within the Empire stock. Many of the biotite-bearing samples were collected from near the contact of the stock with Precambrian rocks or near inclusions of Precambrian rock.

The feldspars make up the bulk of the monzonite. The ratio of alkali feldspar to total feldspar ranges from 0.25 to 0.62. No clear relation between the feldspar ratio and position of feldspar in the stock or amount of ferromagnesian minerals is apparent.

The plagioclase crystals in the hornblende-pyroxene monzonite are subhedral and commonly alined (fig. 14, *C*), such that the rock has a flow layering. Compositional zoning is weak but of the normal type. The anorthite content of the plagioclase decreases as the normative anorthite of the rock decreases and as the relative abundance of the plagioclase decreases (table 15).

The alkali feldspar of the monzonite is anhedral and slightly to moderately perthitic. The variation in the texture of the monzonite as the relative amount of alkali feldspar increases relative to the total feldspar is shown in figures 14*D*, *E*. and *F*. Alkali feldspars mantle the plagioclase and form anhedral grains that fill the small spaces between plagioclase grains. Where abundant, alkali feldspar also forms anhedral to subhedral

TABLE 14.—*Chemical and spectrographic analyses of pyroxene and amphibole from hornblende-pyroxene monzonite of the Empire stock*

[Sample localities shown on pl. 2]

	Pyroxene		Amphibole
Field No.	E-23	E-119	E-68
Lab. No.	I4052	I4054	I4053
Chemical analyses, in weight percent [1]			
SiO_2	45. 87	47. 09	39. 83
TiO_2	1. 46	1. 60	1. 87
Al_2O_3	7. 03	5. 50	11. 68
Fe_2O_3	5. 19	5. 25	7. 87
FeO	6. 59	6. 11	11. 68
MnO	. 49	. 64	. 60
MgO	9. 38	9. 83	7. 59
CaO	20. 50	22. 09	12. 60
Na_2O	1. 51	1. 11	2. 49
K_2O	. 61	. 19	1. 84
H_2O+	. 26	. 07	1. 10
H_2O-	0	. 02	. 01
Cl	. 03	. 01	. 05
F	. 11	. 04	. 40
P_2O_5	. 72	. 45	. 49
Subtotal	100. 02	100. 00	100. 02
Less O=F,Cl	. 06	. 02	. 18
Total	99. 96	99. 98	99. 84
Spectrographic analyses, in weight percent [2]			
Ba	0. 007	0. 005	0. 01
Be	. 0003	. 0002	. 0007
Ce	. 02	. 03	. 02
Co	. 005	. 003	. 007
Cr	. 0005	. 0003	. 002
Cu	. 007	. 002	. 005
Ga	. 003	. 003	. 007
La	. 015	. 015	. 015
Nb	. 007	. 002	. 01
Ni	. 001	0	. 003
Sc	. 007	. 005	. 005
Sr	. 07	. 05	. 03
V	. 03	. 02	. 05
Y	. 005	. 005	. 003
Yb	. 0005	. 0005	. 0005
Zr	. 02	. 01	. 03
Nd	. 03	. 03	. 03

[1] Analyst, D. F. Powers, 1962.
[2] Analyst, J. C. Hamilton, 1962.

TABLE 15.—*Variation of the composition of plagioclase and alkali feldspar in the hornblende-pyroxene monzonite of the Empire stock*

Sample No.	Modal alkali feldspar / total feldspar	Normative anorthite (weight percent)	Mean composition of plagioclase by optical methods	Composition of alkali feldspar by (201) spacing
E-39	0. 11	26. 4	An_{35}	----------
P-913	. 47	18. 4	An_{36} [1]	Or_{75} [1]
E-33	. 48	17. 5	An_{25}	Or_{68}
E-48	. 56	15. 6	An_{25}	----------
E-78	. 50	14. 5	An_{22}	Or_{69}
E-53	. 58	13. 6	An_{20}	Or_{65}

[1] Data from Phair and Fisher (1962, p. 490, 502).

grains of the same size as the plagioclase. As shown in table 15, the orthoclase content of the alkali feldspar decreases as the relative abundance of alkali feldspar increases.

Dioritic rock, in the form of small fine-grained, probably cognate, inclusions, occurs in the monzonite at several localities (fig. 12). This rock, which is composed of alined crystals of pyroxene and plagioclase, differs from the enclosing monzonite only in grain size and in the absence of alkali feldspar. Other samples of hornblende-pyroxene monzonite having a dioritic composition show well to poorly developed flow layering and glomeroporphyritic textures. These rocks probably are local accumulations of early-formed pyroxene and plagioclase. The chemical composition of one such dioritic sample (E-39) is shown in table 13.

Small bodies of pyroxenite occur in the hornblende-pyroxene monzonite, near its contact with the feldspathoidal hornblende-pyroxene monzonite, about 4,000 feet west of the junction of Mad and Clear Creeks. The pyroxenite bodies have very irregular contacts—lobes extend outward into monzonite and isolated patches of monzonite occur within pyroxenite. The pyroxenite consists of about 80 percent clinopyroxene, 15 percent opaque oxides, and 5 percent apatite. Variable amounts of coarse amphibole and sphene occur in some samples. The amphibole and sphene are associated in all samples and appear to be late minerals for they poikilitically enclose the other minerals. In some specimens the clinopyroxene prisms are alined parallel to the contact between pyroxenite and hornblende-pyroxene monzonite.

Several lamprophyre dikes, 1–4 inches thick, cut both the feldspathoidal hornblende-pyroxene monzonite and the hornblende-pyroxene monzonite in exposures along U.S. Highway 40 at the western contact of the feldspathoidal hornblende-pyroxene monzonite. Slightly uralitized clinopyroxene forms the only phenocrysts. The groundmass consists of subhedral amphibole and apatite prisms poikilitically enclosed in medium-grained weakly perthitic alkali feldspar.

Contact metamorphic effects of the Empire stock were not studied in detail but have been recognized as much as 500 feet from the border of the stock. In a sample of biotite gneiss collected about 300 feet from the contact of the monzonite, the alkali feldspar has been converted from grid-twinned microcline typical of the Precambrian rocks to untwinned orthoclase, and biotite has reacted with quartz to form cordierite and magnetite. Sillimanite in a sillimanitic biotite gneiss about 500 feet from the contact has been partly converted to coarse andalusite.

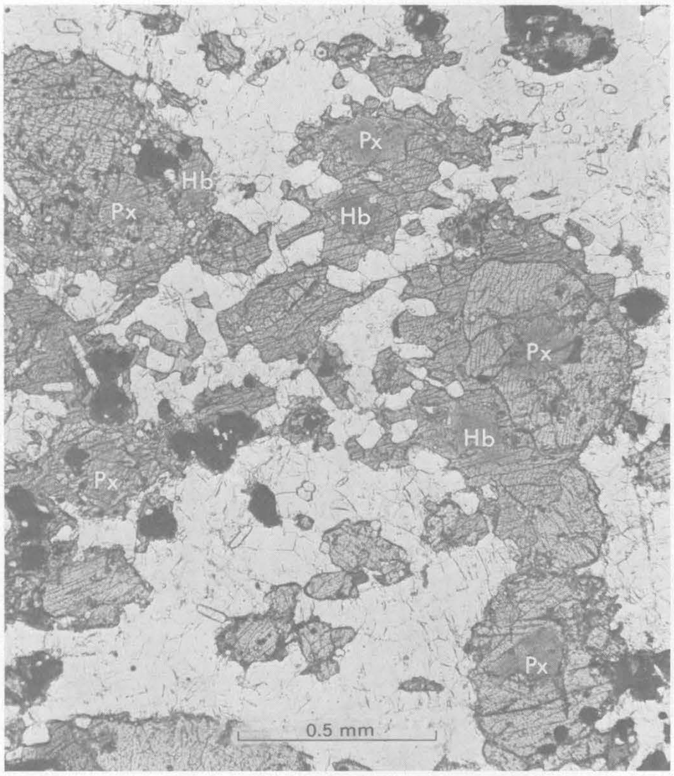

A

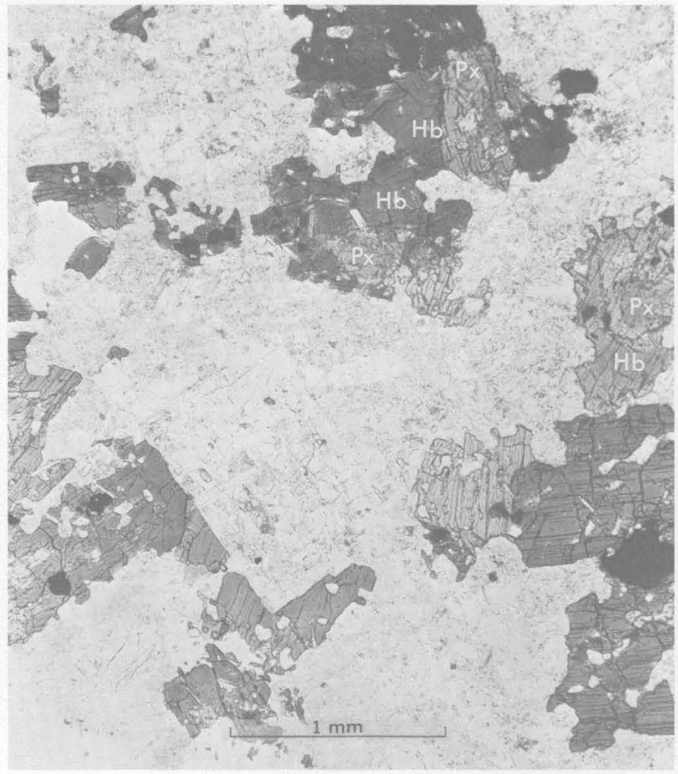

B

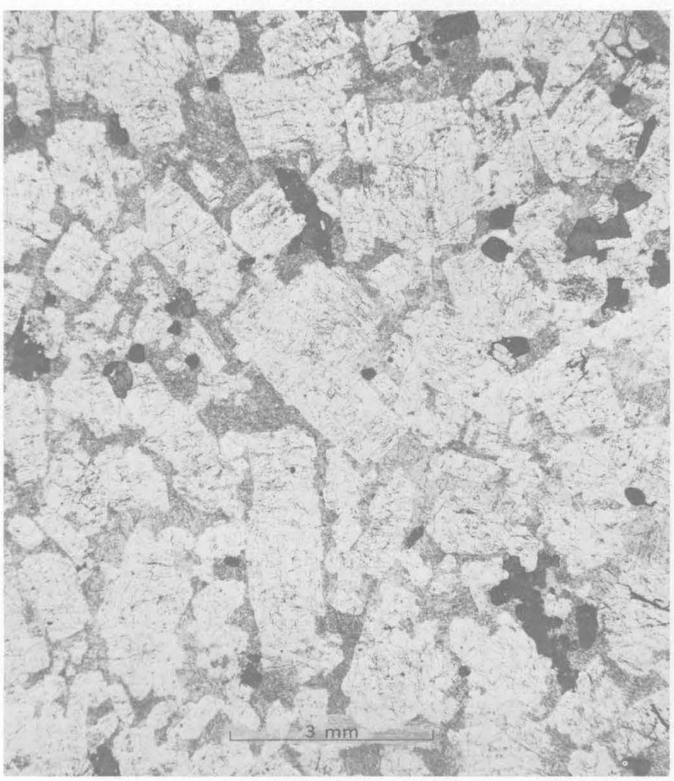

D

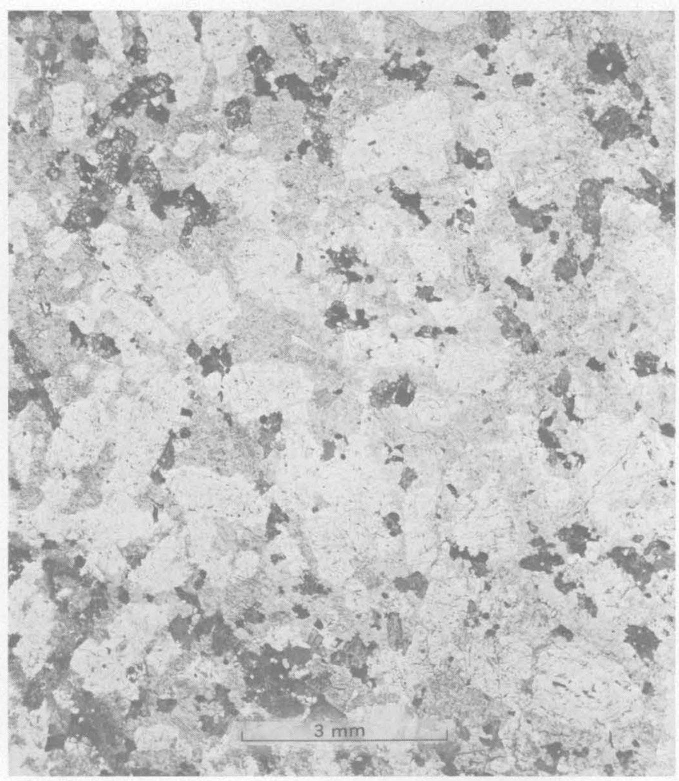

E

C

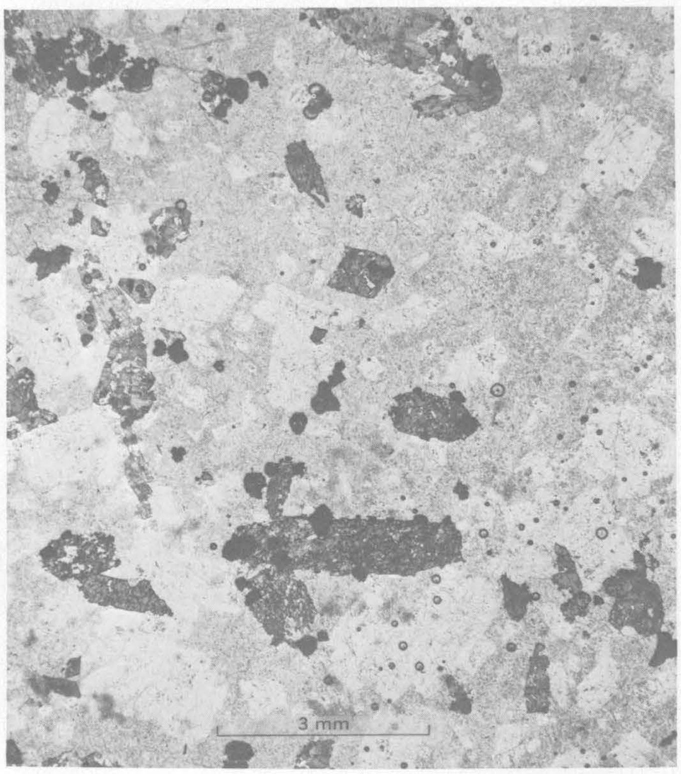

F

FIGURE 14.—Photomicrographs of hornblende-pyroxene monzonite, Empire stock. *A*, Pyroxene phenocrysts (Px) are partially mantled by hornblende (Hb), and the hornblende poikilitically encloses feldspar (white). Also visible are opaque oxides and apatite (hexagonal prisms). Plane light *B*. Pyroxene phenocrysts (Px) are mantled and largely replaced by hornblende (Hb), but most of the hornblende is unrelated to pyroxene and poikilitically encloses feldspar. Alkali feldspar is light gray, plagioclase is white. One large rectangular plagioclase phenocryst is partly surrounded by hornblende. Thin section stained with sodium cobaltinitrite. Plain light. *C*, Plagioclase grains are roughly alined imparting a flow layering. The *C* axes of pyroxene crystals are mostly perpendicular to the plane of the thin section showing the flow lineation that is common in the monzonite. Crossed nicols. *D*, *E*, and *F*, These photomicrographs show the change in texture that occurs as the proportion of alkali feldspar (gray) to plagioclase (white) changes. Where alkali feldspar is sparse (*D*) it forms mantles on plagioclase and fills interstices between plagioclase. Where alkali feldspar is abundant (*F*) it forms some subhedral phenocrysts. Thin sections stained with sodium cobaltinitrite. Plain light.

PORPHYRITIC HORNBLENDE-PYROXENE MONZONITE

Four small bodies of porphyritic hornblende-pyroxene monzonite are shown on plate 1 near the west and south margins of the Empire stock. This rock is medium to light gray, phaneritic, and distinctly porphyritic. Alined phenocrysts of alkali feldspar impart a crude flow layering to the rock. The porphyritic monzonite intrudes the adjacent hornblende-pyroxene monzonite, but its age relative to other igneous rocks is not known.

The porphyritic monzonite is composed principally of plagioclase and alkali feldspar and contains minor amounts of pyroxene, amphibole, sphene, apatite, magnetite, and quartz. Figure 12 shows the range of the modal compositions of the sample studied, and table 11 gives the chemical composition and CIPW norm of one sample (E–60).

Plagioclase, which makes up 17–50 percent of the rock, is subhedral and weakly zoned and ranges in mean composition from An_{20} to An_{35}. Alkali feldspar, which makes up 31–77 percent of the rock, forms phenocrysts that have weakly perthitic cores and moderately perthitic margins and forms anhedral moderately perthitic mantles on plagioclase. The mean composition of alkali feldspar from sample E–60 as determined by X-ray is Or_{69} weight percent. Ferromagnesian minerals make up 2.5–10 percent of the rock and consist of uralitized clinopyroxene and anhedral amphibole. Sphene occurs as large anhedral grains, and quartz occurs as anhedral grains that are interstitial to the feldspars.

MONZONITE PORPHYRY

Monzonite porphyry forms several dikes in the southwestern part of the quadrangle and one dike on the ridge between Fall River and Mill Creek (pl. 2). These rocks are mostly porphyritic and have aphanitic groundmasses. The phenocrysts, which generally are moderately altered, consist mostly of plagioclase that is noticeably zoned from about An_{35} in the core to An_{25} on the margins. Sanidine forms sparse phenocrysts in some samples. The ferromagnesian phenocrysts typically are completely altered to chlorite, epidote, and calcite, but clinopyroxene or biotite occurs in a few unaltered samples. The groundmass consists of feldspar laths, which commonly have a subtrachytic texture, and trace amounts of quartz. The small amount of quartz in these rocks was verified by examination with the X-ray spectrometer.

The chemical composition and CIPW norm of monzonite porphyry sample 5–51 are given in table 13.

QUARTZ-BEARING MONZONITE PORPHYRY

A small part of the Lincoln Mountain stock extends into the southwestern part of the quadrangle. This stock and the two dikes immediately north of it are classed as quartz-bearing monzonites to distinguish them from other monzonites which contain much less quartz and from quartz monzonite which contains more quartz. Both the stock and the dikes are light-gray porphyries that have very fine grained to aphanitic xenomorphic granular groundmasses. The phenocrysts are mostly plagioclase, but some are sanidine, clinopyroxene, amphibole, and biotite. The groundmass consists principally of plagioclase, alkali feldspar, and quartz, and it contains minor amounts of fluorite. No field relationships were observed that would indicate the relative age of the quartz-bearing monzonite.

The fine grain size of the matrix of the quartz-bearing monzonites precludes accurate modal analysis. The chemical composition and CIPW norms of two samples are given in table 16.

The plagioclase phenocrysts are moderately zoned. Large parts of the centers of the phenocrysts have compositions between An_{30} and An_{40}, and the margins are as sodic as An_5. The alkali feldspar in analyzed sample P–912 was reported by Phair and Fisher (1962, table 6) to have a composition Or_{58}. The alkali feldspar commonly forms mantles around the plagioclase.

Clinopyroxene, amphibole, and biotite all occur as phenocrysts, but the total amount of ferromagnesian minerals is less than 10 percent. Clinopyroxene is rare and is largely altered to pale-green amphibole. Prisms of pale-green amphibole are common. Anhedral crystals of brown biotite occur in most samples. Commonly the amphibole is highly altered to chlorite and calcite and the biotite is bleached or chloritized.

TABLE 16.—*Chemical and spectrographic analyses and CIPW norms of quartz-bearing monzonite porphyry and leucocratic monzonite, in weight percent*

[Tr., trace; ----, constituent was not analyzed. Sample localities shown on pl. 2]

	Quartz-bearing monzonite porphyry		Leucocratic monzonite			
Field No.	[1] P–912	[2] 9–33A	[3] E–83	[4] E–84	[2] 8–127A	[2] 8–141
Lab. No.	----	160973	158300	H–3257	160970	160971
Chemical analyses						
SiO_2	62.3	62.4	65.9	65.44	66.6	61.5
Al_2O_3	16.4	16.8	17.5	18.06	17.4	18.2
Fe_2O_3	2.6	3.6	2.2	1.62	1.7	3.0
FeO	1.7	2.0	.78	.52	.42	1.5
MgO	1.2	1.2	1.0	.08	.14	.65
CaO	3.0	2.5	1.3	.46	1.9	2.4
Na_2O	4.9	5.1	5.7	5.57	5.6	4.5
K_2O	3.8	3.8	4.7	7.43	4.4	6.6
H_2O+	1.2	.80	.59	.30	.52	.48
H_2O-		.35		.13	.26	.14
TiO_2	.52	.64	.30	.16	.24	.60
P_2O_5	.30	.44	.10	.01	.06	.28
MnO	.10	.14	.06	.03	.03	.12
CO_2	.94	.11	.02	.01	.39	<.05
Cl	----	----	.01	.02	----	----
F	----	----	.05	.01	----	----
Subtotal	----	----	----	99.85	----	----
Less O=F, Cl	----	----	----	.00	----	----
Total	99	100	100	99.85	100	100
Spectrographic analyses [5]						
Ba	----	----	0.3	0.07	----	----
Be	----	----	.0002	.00015	----	----
Ce	----	----	.03	0	----	----
Cr	----	----	.0002	0	----	----
Cu	----	----	.01	.0015	----	----
Ga	----	----	.003	.005	----	----
La	----	----	.03	.007	----	----
Nb	----	----	.007	.005	----	----
Pb	----	----	.0015	.002	----	----
Sr	----	----	.3	.15	----	----
V	----	----	.007	.007	----	----
Y	----	----	.003	.0015	----	----
Yb	----	----	.0003	.00015	----	----
Zr	----	----	.015	.02	----	----
Nd	----	----	.015	0	----	----
CIPW norms						
Q	14.3	12.6	11.0	3.7	14.2	4.8
or	22.4	22.4	27.8	43.9	26.0	39.0
ab	41.4	43.1	48.1	47.0	47.4	38.1
an	7.0	8.8	5.3	2.1	6.6	10.0
C	1.7	1.1	1.1	.1	1.0	0
di	0	0	0	0	0	.1
hy	3.3	3.0	2.5	.2	.4	1.6
mt	3.8	5.0	1.8	1.3	.8	3.5
hm	0	.1	.9	.7	1.2	.6
il	1.0	1.2	.6	.3	.5	1.1
ap	.7	1.0	.2	Tr.	.1	.7
cc	2.1	.2	Tr.	Tr.	.9	0

[1] Chemical analyses are unpublished rapid-rock analyses from George Phair by P. L. D. Elmore, K. E. White, S. D. Botts, 1955. Sample from north part of Lincoln Mountain stock. Not shown on plate 2.
[2] Chemical analyses are rapid-rock analyses by P. L. D. Elmore, S. D. Botts, G. W. Chloe, L. Artis, H. Smith, 1963.
[3] Chemical analyses are rapid-rock analyses by P. L. D. Elmore, I. H. Barlow, S. D. Botts, G. W. Chloe, 1961. Separate analysis for Cl and F by V. C. Smith, 1961.
[4] Chemical analyses are standard rock analyses by C. L. Parker, 1961.
[5] Analyst, J. C. Hamilton, 1961. Looked for but not detected: Ag, As, Au, B, Bi, Cd, Co, Ge, Hf, Hg, In, Li, Ni, Mo, Pd, Pt, Re, Sb, Sc, Sn, To, Te, Th, Ti, U, W, Zn, Pr, Sm, Eu, Gd, Tb, Dy, Ho, Er, Tm.

LEUCOCRATIC MONZONITE

Leucocratic monzonite occurs in the eastern part of the Empire stock and forms a dike on the north side of Mammoth Gulch in the extreme northeast corner of the quadrangle. The rock is light gray and consists predominantly of oligoclase and alkali feldspar, less than 8 percent ferromagnesian minerals, and less than 11 percent quartz. The variations of modal compositions are shown in figure 12.

On the ridge between Clear Creek and Mad Creek and just above their junction, the hornblende pyroxene monzonite is cut by numerous steeply dipping 1 inch thick to 2-foot-thick dikes of leucocratic rock that is texturally and mineralogically similar to the leucocratic monzonite exposed on the northeast side of Mad Creek. The area in which the leucocratic dikes are abundant has been indicated on plate 1 as a hornblende-pyroxene monzonite veined by leucocratic monzonite.

The leucocratic monzonite is a seriate to strongly porphyritic rock (fig. 15*A*); the phenocrysts are alkali feldspar ($Or_{60}Ab_{40}$), oligoclase and minor amounts of clinopyroxene; the matrix is phaneritic alkali-feldspar perthite, oligoclase, and quartz and minor amounts of sphene, apatite, and opaque ovides. The oligoclase phenocrysts are commonly mantled by alkali feldspar, and these mantles, as well as the alkali-feldspar phenocrysts, are strongly perthitic (fig. 15*B*) in places. Pale-green nonpleochroic pyroxene forms short prisms that are partly altered to pale-green amphibole. The pyroxene is probably a salite containing minor acmite ($2V_z$ about 65°, $z<c$ is 50°–58°). Leucocratic monzonite porphyry (fig. 15*C*) with a very fine-grained to aphanitic groundmass is locally present. Some phaneritic nonporphyritic samples are syenite (fig. 15*D*) composed predominantly of perthitic alkali feldspar ($Or_{56}Ab_{44}$) and resemble the matrix of the typical leucocratic monzonite. The chemical analyses and CIPW norms of four samples of leucocratic monzonite are given in table 16; E–84 is a syenite sample.

BIOTITE QUARTZ MONZONITE PORPHYRY

Biotite quartz monzonite porphyry occurs only in the south-central part of the quadrangle, where it forms a plug on the east side of the Empire stock complex, several irregular dikes south of Clear Creek, and three northeast-trending dikes north of Clear Creek.

The relative ages of the biotite quartz monzonite plug and the leucocratic monzonite of the Empire stock are not known. The contact between the quartz monzonite and the southern body of leucocratic monzonite is sharp and no evidence of relative age was observed. The quartz monzonite is separated from the northern exposure of leucocratic monzonite by a zone of intrusion breccia. This breccia is intensely altered and contains rounded fragments of Precambrian rocks including Silver Plume Granite and fragments resembling fine-grained parts of the leucocratic monzonite body to the north.

The biotite quartz monzonite is a porphyry and has a granular very fine grained to aphanitic groundmass of alkali feldspar, plagioclase, and quartz. Phenocryst are plagioclase and subordinate sanidine, quartz, and biotite. The biotite-quartz monzonite is commonly highly altered; plagioclase is either sericitized or replaced by clay minerals; biotite is bleached or chloritized, and abundant secondary calcite replaces groundmass minerals.

The plagioclase phenocrysts are slightly to moderately zoned and range in composition from An_{18} to An_{27}. The sanidine phenocrysts are weakly perthitic to nonperthitic; $2V_x$ is 40°; they commonly contain inclusions of plagioclase. The quartz phenocrysts are subhedral to rounded and commonly embayed by groundmass minerals. In many thin sections the quartz phenocrysts have quartz overgrowths that enclose the fine-grained matrix feldspars.

The chemical composition of one sample of altered biotite quartz monzonite is shown in table 11. This sample, although the least altered that could be found, contains abundant secondary calcite.

BOSTONITE PORPHYRY

The bostonite porphyry is composed principally of alkali feldspars and minor to moderate amounts of quartz and is characterized by a distinctive groundmass texture in which elongate feldspars show mutually sutured contacts against each other and are arranged in a divergent (bostonitic) to subparallel (trachytic) pattern. Commonly the bostonites are pale lilac, but they may also be gray, yellow, or reddish.

The bostonites form nearly vertical straight dikes throughout the eastern part of the quadrangle and one thick sill-like body north of Lawson. Bostonite porphyry dikes cut dikes and plugs of biotite granodiorite at several localities. The best exposure of this relation is 0.7 mile north of the center of the town of Empire where an east-northeast-trending dike of bostonite porphyry crosscuts a small plug of biotite granodiorite (pls. 1 and 2).

The bostonite group has been subdivided by Wells (1960, p. 245) and Phair (1952) on the basis of the amount of modal quartz and the types of feldspar phenocrysts. This author has found that neither of these classifications can be used because no simple relation seems to exist between the type of feldspar phenocryst and the amount of quartz in the rock. Furthermore, because of the fine grain size and common extensive alteration, the quartz content of the rocks cannot be accurately determined. In this report the bostonites are not divided.

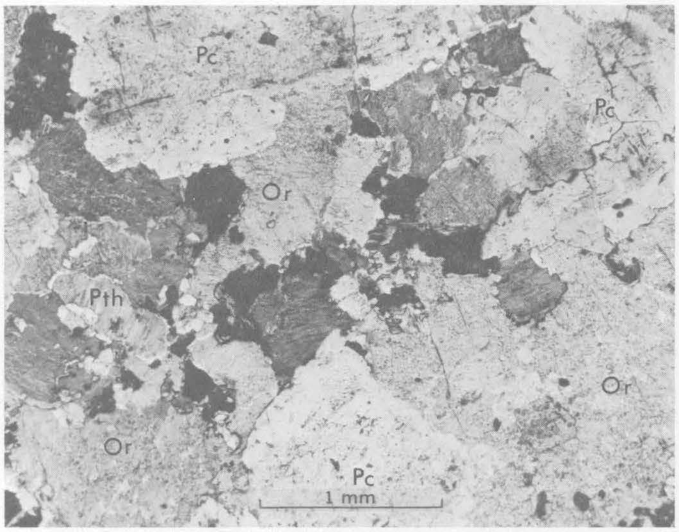
Pc
Pc
Or
Pth
Or
Or
Pc
1 mm

A

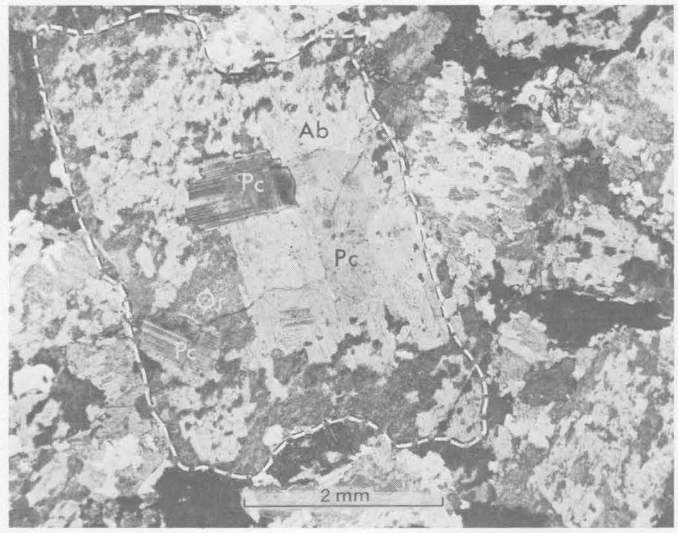
Ab
Pc
Pc
Or
Pc
2 mm

B

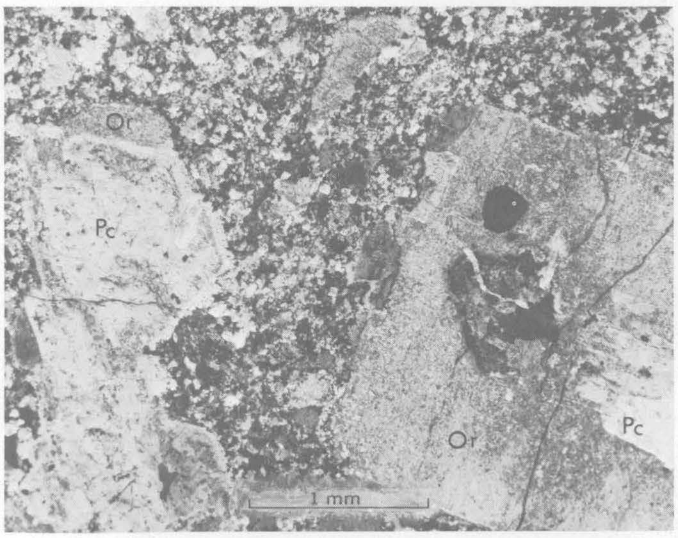
Or
Pc
Or
Pc
1 mm

C

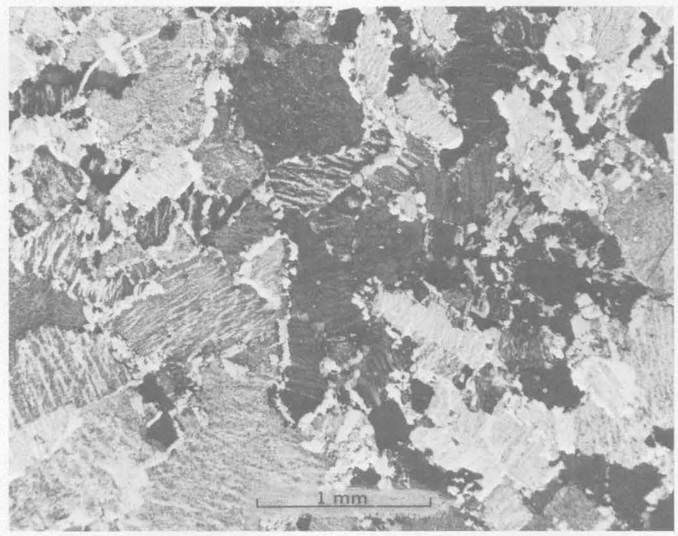
1 mm

D

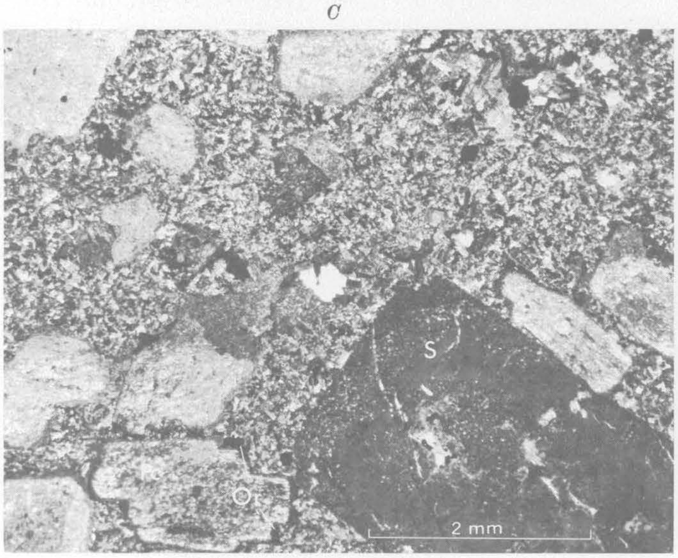
S
2 mm

E

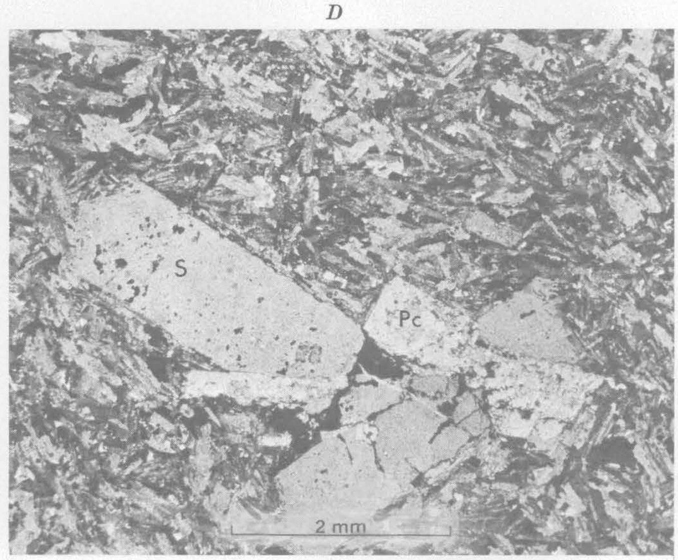
S
Pc
2 mm

F

FIGURE 15.—Photomicrographs of leucocratic monzonite, bostonite porphyry, and sanidinite porphyry. *A*, Leucocratic monzonite. Subhedral zoned phenocrysts of oligoclase (Pc) and anhedral phenocrysts of orthoclase (Or) are enclosed in a finer grained matrix of perthitic alkali feldspar (Pth). The smaller grains of alkali-feldspar perthite are rimmed by very fine grained albite (white). Crossed nicols. *B*, Leucocratic monzonite. Large composite phenocryst is outlined. This phenocryst consisted of three subindividuals of oligoclase (Pc) mantled by alkali feldspar. The alkali-feldspar mantle has been recrystallized and consists of a patch perthite of albite (Ab) and orthoclase (Or). The smaller grains of the matrix of the rock have also been recrystallized to a patch perthite of albite and orthoclase. Crossed nicols. *C*, Leucocratic monzonite porphyry. Phenocrysts are zoned oligoclase (Pc at left) with partial mantles of alkali feldspar (Or), and alkali-feldspar perthite (Or at right) with inclusions of oligoclase. The groundmass is made up of granular albite-oligoclase, potassium feldspar, and minor amounts of quartz. Crossed nicols. *D*, Syenite facies of leucocratic monzonite. Rock consists of alkali-feldspar perthite separated by rims of granular albite (white). Crossed nicols. Analyzed rock E-84, table 16. *E*, Bostonite porphyry. Phenocrysts are sericitized albite (Pc) and have thin mantles of potassium feldspar (Or) and sanidine (S). Groundmass is complex intergrowth of albite and potassium feldspar and has a bostonitic texture. Crossed nicols. Analyzed rock 8-2, table 17. *F*, Sanidinite porphyry. Phenocrysts are cloudy sanidine (S) and sericite pseudomorphs after plagioclase (?) (Pc). Groundmass is tabular twinned potassium feldspar with composition > 95 percent (Or) and minor amounts of very fine grained quartz. Crossed nicols.

Most of the feldspar phenocrysts are sodic plagioclase, but in many rock samples the feldspar is too altered to sericite for accurate identification. In many samples the sodic plagioclase has a thin mantle of potassium-rich alkali feldspar. In some samples phenocrysts are sanidine and sodic plagioclase (fig. 15*E*); in others all phenocrysts are sanidine. The composition of the feldspar phenocrysts in the chemically analyzed bostonites is summarized as follows:

Sample	*Normative quartz*	*Type of feldspar phenocryst*
1-51	20.3	Predominantly albite(?), minor sanidine(?).
1-111	19.9	Sanidine ($Or_{83}Ab_{17}$).
4-108	17.3	Albite ($Ab_{85}An_{10}Or_{5}$) with thin potassium-rich mantles.
10-21	14.1	Albite(?).
4-32	12.7	Albite(?) with thin potassium-rich mantles.
1-134	5.2	Albite ($Ab_{80}An_{10}Or_{10}$) with thin potassium-rich mantles.
8-2	5.2	Albite(?) with thin potassium-rich mantles and sanidine ($Or_{60-65}Ab_{35-40}$).

Aggregates of unidentified oxides that make up a few percent of the rock occupy the positions of former ferromagnesian phenocrysts. The octagonal outline of these aggregates indicates that pyroxene was once present. Wells (1960, p. 247) reported aegirine-augite in unaltered garnetiferous bostonite. In some rocks biotite may have been present.

The groundmass of the bostonites consists predominantly of tabular feldspar crystals and of minor to moderate amounts of quartz. The quartz was clearly a late mineral to crystallize for it forms small anhedral grains that fill angular spaces between the feldspar crystals. At low magnification the groundmass appears to consist of a single feldspar forming tabular crystals arranged in a bostonitic to trachytic texture. However, staining of the thin sections and X-ray study of unheated samples indicate that the groundmass contains two feldspars, one nearly pure albite and one nearly pure potassium feldspar. At higher magnifications, the areas occupied by the two feldspars do not seem to coincide with the tabular boundaries of the feldspars seen at low magnification. The potassium feldspars are concentrated along the margins of tablets or are patchily distributed through the interior parts of tablets. In some places the potassium feldspar may occupy most of an albite twin lamella in a multiple-twinned tablet. This fabric suggests that the groundmass initially contained one homogeneous alkali feldspar and that this feldspar has since been recrystallized to the nearly pure end members. In a few samples the two feldspars form completely discrete grains indicative of primary precipitation of the two feldspars. In the thin sections, however, the texture of the ground mass is granular, and recrystallization may have been more extensive. My belief that the groundmass of the bostonites was originally by a single homogeneous alkali feldspar is contrary to the opinion expressed by Phair and Fisher (1962, p. 512).

Accessory minerals are sphene, apatite, zircon, and opaque oxides. Calcite, fluorite, and quartz occur between feldspar crystals in one sample of quartz-poor bostonite.

The chemical and spectrographic analyses and CIPW norms of seven bostonites are shown in table 17.

SANIDINITE PORPHYRY

Sanidinite porphyry, composed predominantly of potassium feldspar, forms only two dikes in the Empire quadrangle: one is on the west side of the Washoe Gulch branch of Cumberland Gulch, and the other is 0.3 mile south-southwest of Lawson.

The sanidinite porphyry consists of sparse subhedral feldspar phenocrysts, which are dominantly cloudy sanidine ($Or_{95}Ab_{5}$, $2V_{x}45-50°$), in a very fine grained groundmass of tabular potassium feldspar and minor quartz (fig. 15*F*). Another mineral which was apparently present at one time in minor amounts is represented by tabular pseudomorphs of sericite (fig.

TABLE 17.—*Chemical and spectrographic analyses and CIPW norms of bostonite porphyry and sanidinite porphyry, in weight percent*

[----, constituent was not analyzed. Sample localities shown on pl. 2]

	Bostonite porphyry							Sanidinite porphyry
Field No.	[1] 1-51	[1] 1-111	[1] 1-134	[1] 4-32	[2] 4-108	[1] 8-2	[1] 10-21	[1] 4-83
Lab. No.	158279	158281	158282	158283	H3249	158292	158293	158284
Chemical analyses								
SiO_2	65.4	70.8	63.2	61.1	65.99	60.2	61.2	62.4
Al_2O_3	17.8	16.5	18.4	17.3	17.42	19.0	17.2	18.5
Fe_2O_3	3.3	.85	3.1	2.8	2.96	2.1	2.5	2.9
FeO	.58	.14	1.1	.32	.13	.97	2.1	.10
MgO	.58	.14	.62	.33	.26	.52	1.0	.21
CaO	.14	.28	.59	2.9	.75	2.7	2.6	.10
Na_2O	4.9	4.6	6.9	4.3	5.86	6.0	4.4	.30
K_2O	4.3	6.2	4.2	6.0	3.68	4.6	4.9	13.5
H_2O+ / H_2O-	2.6	.78	1.4	1.5	1.04 / .45	1.2	1.4	1.4
TiO_2	.43	.10	.44	.32	.34	.40	.52	.31
P_2O_5	.15	.02	.17	.11	.14	.10	.24	.10
MnO	.02	.01	.10	.14	.15	.14	.16	.08
CO_2	.01	0	.01	2.2	.36	1.4	1.6	0
Cl	.01	.01	.01	----	0.	.01	.01	.01
F	.16	.09	.04	.10	.08	.09	.08	.06
S	.02	----	----	----	.02	----	----	----
SO_3	----	----	----	.27	----	----	----	----
Subtotal	----	----	----	----	99.63	----	----	----
Less O=F, Cl	----	----	----	----	.04	----	----	----
Total	100	100	100	99	99.59	99	100	100
Spectrographic analyses [3]								
Ba	0.2	0.03	0.2	0.5	0.15	0.3	0.3	0.1
Be	.05	.003	.001	.005	.0002	.001	.0002	.0007
Ce	.02	0	.02	.02	.02	.02	.03	.02
Co	0	0	.0007	.0007	.0007	0	.0007	.0007
Cr	.001	0	.0005	.0005	.0003	0	.0003	.0003
Cu	.005	.001	.001	.001	.0007	.0005	.01	.005
Ga	.003	.005	.003	.003	.003	.003	.003	.003
La	.015	0	.015	.015	.01	.015	.02	.015
Nb	.007	.007	.007	.005	.005	.005	.005	.005
Ni	.001	0	.0007	0	.0015	0	.0005	.0007
Pb	.02	.005	.005	.007	.002	.007	.003	.07
Sc	.001	0	0	0	0	0	.0007	0
Sr	.05	.007	.15	.07	.05	.3	.2	.03
V	.01	.002	.01	.01	.007	.007	.007	.01
Y	.005	.003	.005	.005	.003	.002	.005	.005
Yb	.0005	.0005	.0005	.0005	.0005	.0003	.0005	.0005
Zn	0	0	0	0	0	0	.05	.05
Zr	.03	.05	.02	.015	.02	.015	.02	.015
Nd	.015	----	.015	.015	.015	.015	.015	.015
CIPW norms								
Q	20.3	19.9	5.5	14.1	17.5	5.6	14.6	8.5
or	26.1	36.6	24.8	35.4	21.7	27.2	29.0	80.1
ab	42.4	38.8	58.3	34.6	49.6	50.7	37.1	2.6
an	0	.6	1.5	0	0	3.3	.7	0
C	5.2	2.0	2.0	4.1	3.8	3.0	4.4	3.3
hy	1.4	.4	1.5	.4	.6	1.3	3.7	.5
mt	.7	.2	2.6	.6	0	2.4	3.6	0
hm	2.9	.7	1.3	2.4	3.0	.4	0	2.9
il	.8	.2	.8	.6	.6	.8	1.0	.2
ru	0	0	0	0	.1	0	0	.2
ap	.3	0	.4	.3	.3	.2	.6	.3
fr	.3	.2	.1	.2	.2	.2	.1	----
cc	0	0	0	4.7	.8	3.2	3.6	0
$MgCO_3$	0	0	0	.3	0	----	----	----

[1] Chemical analyses are rapid-rock analyses by P. L. D. Elmore, I. H. Barlow, S. D. Botts, G. W. Chloe, 1961. Separate analysis for F, Cl, S, SO_3 by V. C. Smith, 1961.

[2] Chemical analyses are standard rock analyses by C. L. Parker, 1961.

[3] Analyst, J. C. Hamilton, 1961. Looked for but not detected: Ag, As, Au, B, Bi, Cd, Ge, Hf, Hg, In, Li, Mo, Pd, Pt, Re, Sb, Sn, Ta, Te, Th, Tl, U, W, Pr, Sm, Eu, Gd, Tb, Dy, Ho, Er, Tm.

15*F*). The groundmass consists principally of subhedral tabular potassium feldspar ($Or_{95}Ab_5$) arranged in a trachytic to bostonitic texture. Small anhedral grains of quartz make up 5–10 percent of the matrix.

The chemical composition and CIPW norm of one sample of sanidinite porphyry are given in table 17.

AGE AND SEQUENCE OF INTRUSION

No radiometric age determinations have been made on rocks described in this report, but radiometric ages of several Tertiary porphyries in the Colorado mineral belt have been reported. The age of the Audubon-Albion stock west of Ward, Colo., is about 66 million years (Hart, 1960, p. 131) and that of a large stock near Eldora, Colo., is about 54 million years (Tilton and Hart, 1963, p. 359). Reported ages of two porphyries near Leadville, Colo., are 70 and 64 million years (Pearson and others, 1962, p. C79).

Figure 16 shows what is known about the sequence of intrusion of the Tertiary igneous rocks in the Empire quadrangle. Neither the author nor Wells (1960, p. 228) has found any evidence to indicate the relative ages between major members of the granodiorite group. The biotite quartz monzonite is shown as a relatively young rock for the following reason: The albite granodiorite porphyry and alkalic syenite porphyry of Wells (1960, p. 237–239) probably are equivalent to the leucocratic monzonite, and the biotite quartz monzonite is younger than both of those porphyries (Wells, 1960, p. 229).

Feldspathoidal hornblende-pyroxene monzonite has been intruded by hornblende-pyroxene monzonite, and hornblende-pyroxene monzonite is cut by both porphyritic hornblende-pyroxene monzonite and leucocratic monzonite. The relative ages of the latter two rocks are unknown.

Bostonite porphyry cuts biotite granodiorite porphyry in the Empire quadrangle and biotite quartz monzonite porphyry to the east (Wells, 1960, p. 229).

PETROLOGY

The Tertiary igneous rocks of the Empire quadrangle form a relatively complex array of rock types in close spatial association and in apparent close time relation. It seems that the gross chemical characteristics of the rocks must have been established by processes acting at depth, and that batches of magma periodically rose to the level now exposed where they completed crystallization to form the observed rocks. In the following sections the chemical data are evaluated with the aim of determining what processes most likely produced the rocks observed.

DEFINITION OF ROCK SERIES

For an understanding of the origin of diverse Tertiary igneous rocks, it is necessary to determine whether all the rock types are genetically related or whether they belong to several separate series.

Three series of igneous rocks can be distinguished on the basis of their contents of normative anorthite and normative quartz or normative nepheline (fig. 17). The normative contents were determined from chemical analyses of 37 rocks from the Empire quadrangle presented in preceding tables and from published chemical analyses of five other rocks from the general vicinity (table 18). One series is characterized by the abundance of nepheline; the second series is characterized by a

Rock type	Position in sequence unknown	Position in sequence known: Older				Younger
Hornblende granodiorite porphyry	X					
Biotite granodiorite porphyry	X (Older than bostonite porphyry)					
Granite aplite	(Younger than hornblende granodiorite and biotite granodiorite porphyries)					
Biotite quartz monzonite porphyry					X	
Feldspathoidal hornblende-pyroxene monzonite		X				
Hornblende-pyroxene monzonite			X			
Porphyritic hornblende-pyroxene monzonite				X		
Quartz-bearing monzonite porphyry	X				Relative age unknown	
Leucocratic monzonite				X		
Bostonite porphyry						X
Sanidinite porphyry	X					

FIGURE 16.—Known sequence of intrusion of Tertiary igneous rocks in the Empire quadrangle.

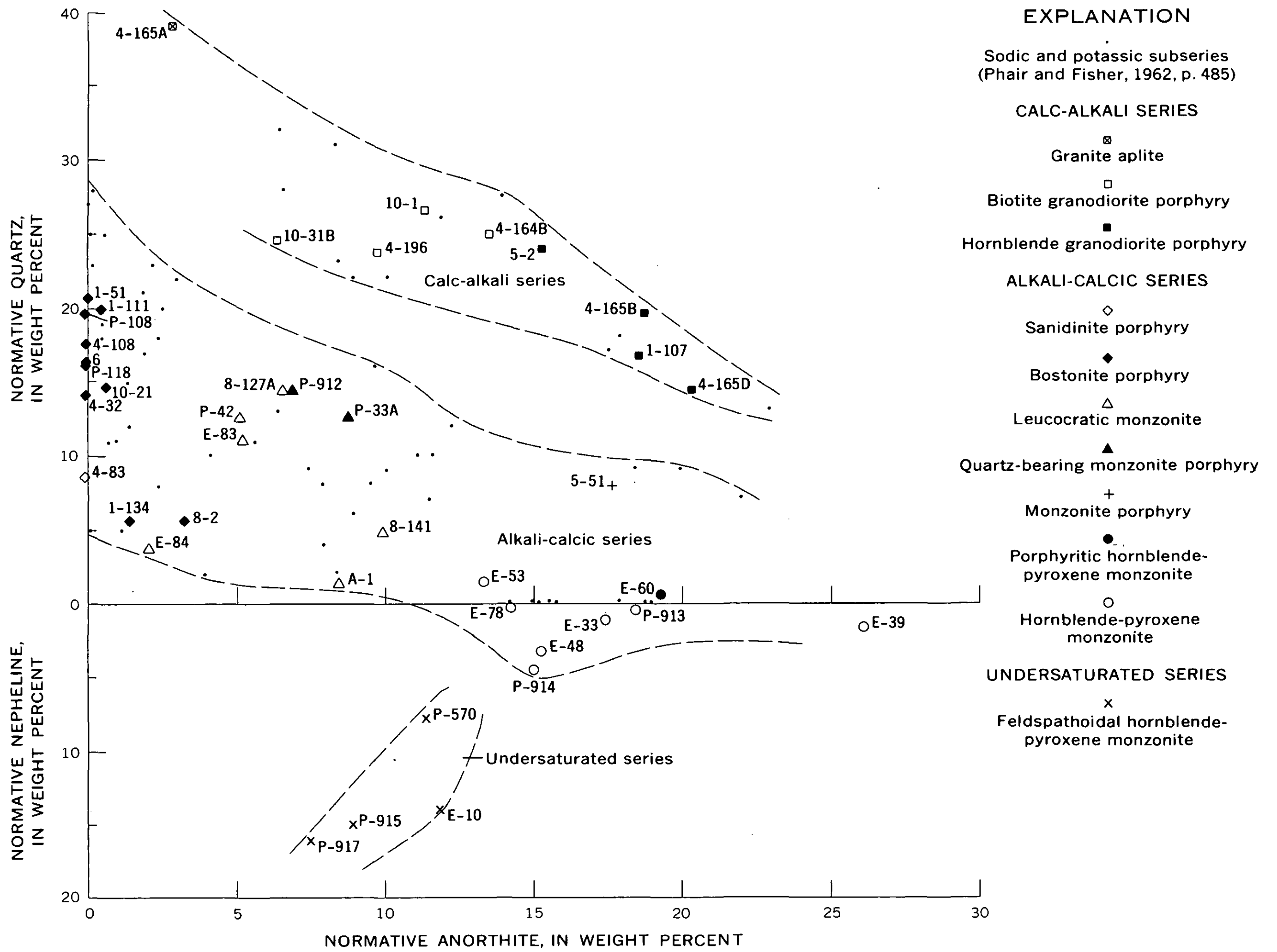

FIGURE 17.—Relation between normative anorthite and normative quartz or nepheline in Tertiary igneous rocks. The numbered points are analyzed samples in tables 11–13, 16–18.

low normative quartz content except at low anorthite contents; and a third series is characterized by a high normative quartz content at all values of anorthite. These series are referred to hereafter as the undersaturated series, the alkali-calcic series, and the calc-alkali series respectively. When the alkali-calcic and calc-alkali series are plotted on a standard Harker plot (Harker, 1909, p. 118), the silica percentage at which the total alkalies become equal to CaO is about 52 percent for the alkali-calcic series and about 57 percent for the calc-alkali series. Thus, these two series names are used in the manner defined by Peacock (1931).

Further chemical comparisons between series are shown on the Larsen (1938) plot in figure 18. It is apparent that the leucocratic monzonite and bostonite porphyry of the alkali-calcic series are very similar chemically; the principal difference seems to be the lower CaO content of the bostonites. The calc-alkali series has a higher SiO_2 content and lower K_2O and Na_2O contents than does the alkali-calcic series.

As shown in figure 17, the undersaturated series is made up of the feldspathoidal hornblende-pyroxene monzonite; the alkali-calcic series consists of hornblende-pyroxene monzonite, porphyritic hornblende-pyroxene monzonite, leucocratic monzonite, quartz-bearing monzonite porphyry, monzonite porphyry, bostonite porphyry, and sanidinite porphyry; and the calc-alkali series consists of hornblende granodiorite porphyry, biotite granodiorite porphyry, and granite aplite. The biotite quartz monzonite porphyry also probably belongs to the calc-alkali series, although no samples found of this rock were fresh enough for a definitive chemical analysis.

Additional reasons for placing the listed rocks together as the alkali-calcic series are: Their relative ages, that is, hornblende-pyroxene monzonite is older

TABLE 18.—*Chemical analyses and CIPW norms of various Tertiary rocks from the Idaho Springs and Central City areas, in weight percent*

[Tr., trace; ...., constituent was not analyzed]

Sample No.	A-1	P-42	6	P-118	P-108
Chemical analyses					
SiO_2	60.30	66.78	67.41	68.10	68.56
Al_2O_3	18.12	16.05	16.23	15.89	15.88
Fe_2O_3	2.45	1.69	.85	1.43	3.06
FeO	1.25	2.09	1.14	2.49	1.19
MgO	.28	.46	.15	.08	.10
CaO	3.89	1.65	.14	.22	0
Na_2O	5.83	5.49	3.95	4.95	4.80
K_2O	5.01	4.74	7.19	5.65	5.44
H_2O+	.77	.32	.88	.70	.64
H_2O-	.75	.10	.67	.18	.20
TiO_2	.55	.32	.16	.10	.14
P_2O_5	.25	.13	.05	.14	.04
MnO	.12	.09	.16	.12	.03
CO_2	----	.04	.56	.21	.01
SO_3	.06	----	----	----	----
BaO	.26	----	Tr.	----	----
ZrO_2	.01	----	.11	----	----
Total	99.90	99.95	99.65	100.26	100.09
CIPW norms					
Q	1.1	12.5	16.2	16.1	19.7
or	29.6	28.0	42.5	33.4	32.1
ab	49.3	46.4	33.4	41.9	40.6
an	8.5	5.2	0	0	0
zr	Tr.	0	.2	0	0
C	0	0	2.0	1.6	2.1
wo	3.2	0	0	0	0
di	1.5	1.6	0	0	0
hy	0	2.4	1.4	3.5	.2
ap	.6	.3	.1	.3	Tr.
il	1.0	.6	.3	.2	.3
mt	2.8	2.4	1.2	2.1	3.5
hm	.5	0	0	0	.6
cc	0	.1	.1	.2	Tr.

SAMPLE DESCRIPTIONS

A-1. Alkali syenite porphyry from south side of Clear Creek, near Soda Creek (S. H. Ball, in Spurr and Garrey, 1908, p. 83. Analyst, George Steiger).
P-42. Monzonite, station 68, Gilson Gulch (Phair, 1952, p. 13, 14. Analyst W. J. Blake.) The dike from which this sample was collected was classified as albite granodiorite porphyry by Wells (1960).
6. Bostonite, Red Lyon lode, Idaho Springs (Spurr and Garrey, 1908, p. 134. Analyst W. T. Schaller).
P-118. Quartz bostonite, station 23, Main Wood dike (Phair, 1952, p. 13, 14. Analyst W. J. Blake).
P-108. Quartz bostonite, station 2, Nigger Hill dike (Phair, 1952, p. 13, 14. Analyst, W. J. Blake).

than leucocratic monzonite which is older than bostonite porphyry; the ferromagnesian minerals are similar throughout the series, that is, clinopyroxene is replaced by amphibole; and their spatial relations, that is, composite stocks contain representatives of the monzonites, leucocratic monzonites, and bostonitic rocks at four separate localities in the Front Range. These stocks are at Jamestown, at Bryan Mountain west of Eldora, at Apex, and the Empire stock (Phair and Fisher, 1962, p. 481). This spatial relation would seem to support

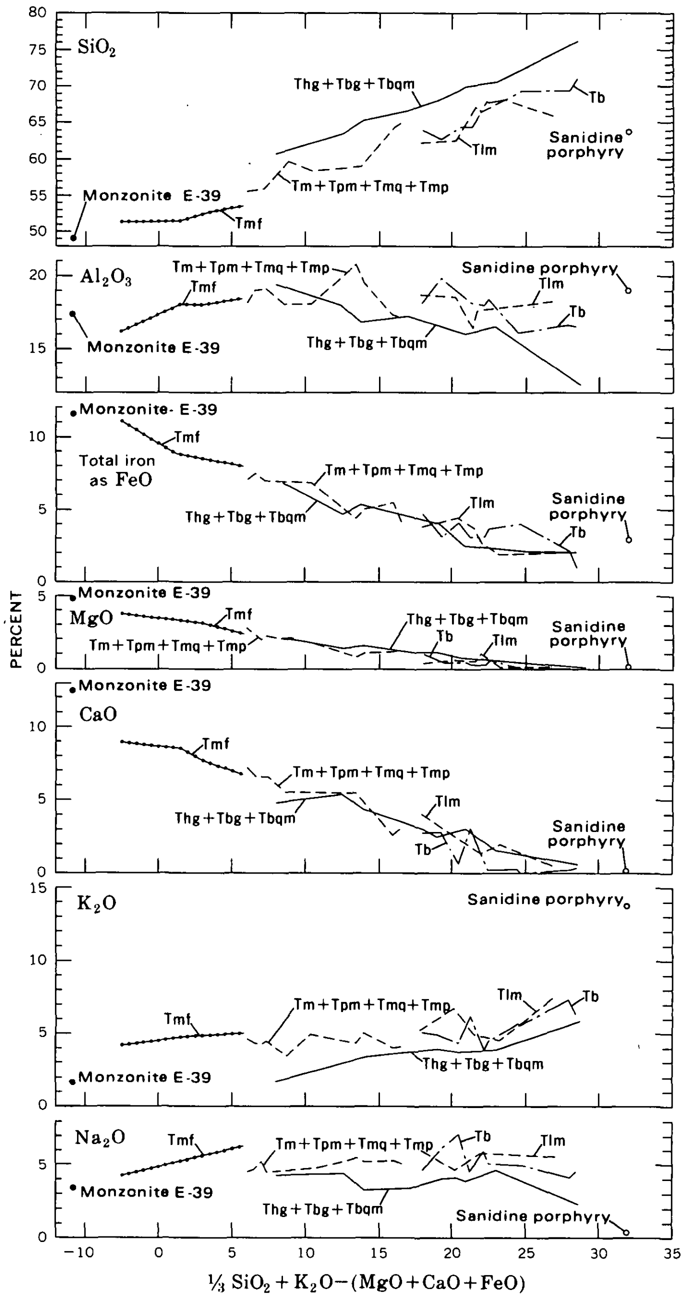

FIGURE 18.—Larsen plot of analyses of Tertiary igneous rocks. Solid line joins calc-alkali series; dashed line, alkali-calcic series; dotted line, undersaturated series. Tb, bostonite porphyry; Tbqm, biotite quartz monzonite porphyry; Tlm, leucocratic monzonite; Tmq, quartz-bearing monzonite porphyry; Tmp, monzonite porphyry undivided; Tpm, porphyritic hornblende-pyroxene monzonite; Tm, hornblende-pyroxene monzonite; Tmf, feldspathoidal hornblende-pyroxene monzonite; Thg, hornblende granodiorite porphyry; Tbg, biotite granodiorite porphyry.

the contention that the rocks of the alkali-calcic series are genetically related.

The age relationships shown in figure 16 seem to justify the conclusion that one of the earliest magmas to invade the level of the crust now exposed was the undersaturated one, and then successive alkali-calcic magmas and calc-alkali magmas were emplaced in two overlapping sequences.

Phair and Fisher (1962, p. 483) indicated that the Tertiary igneous rocks of the Front Range porphyry belt can be classified into a sodic subseries and a potassic subseries. They published partial norms for 68 of these rocks, and these norms have been plotted in figure 17. It seems reasonable to conclude that Phair and Fisher's sodic subseries corresponds to the alkali-calcic series plus the undersaturated series and that their potassic subseries corresponds to the calc-alkali series. It would also appear that the chemical series defined here are valid with respect to an area much larger than the Empire quadrangle.

CALC-ALKALI SERIES

In many ways the calc-alkali series is the simplest of the rock series. A triangular plot of the normative anorthite, albite, and orthoclase for the analyzed rocks of this series (fig. 19) shows the manner in which the feldspar constituents of the group change from the hornblende granodiorite to the granite aplite. The analyzed rocks of the Empire quadrangle do not show a continuous change from the biotite granodiorite to the granite aplite, but rocks listed by Phair and Fisher (1962, p. 485) that the author would class as calc-alkali do fill this gap. These rocks are shown by dots in figure 19. The

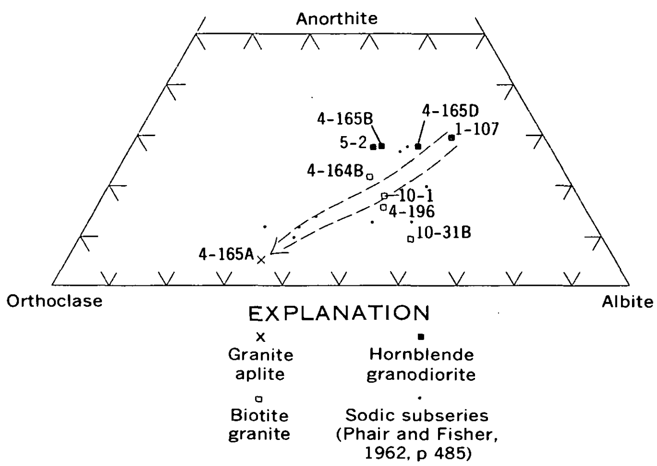

FIGURE 19.—Triangular plot of the calc-alkali series. Normative anorthite, albite, and orthoclase recalculated to 100 percent. Dashed arrow indicates postulated differentiation trend. Numbers refer to analyses in table 11.

progressive trend of change of feldspar components is shown in figure 19, and is accompanied by an increase in the normative quartz content (fig. 17) and by the change of the ferromagnesian mineral from hornblende to biotite.

The manner in which successive liquids would change during the crystallization differentiation of a granitic magma can be only roughly approximated because there has been little experimental work on systems of appropriate composition. Some data have been collected concerning crystallization in the anorthite-albite-orthoclase system (Yoder and others, 1957; Tuttle and Bowen, 1958, p. 130–135). Figure 20 shows two partial phase diagrams for the ternary feldspar system. Figure 20*A* refers to synthetic melts that are completely saturated with water at a pressure of 5,000 bars. These melts crystallize at relatively low temperatures. The probable equilibrium crystallization path of liquid C has been inferred in figure 20 (Bowen, 1914, 1915, 1941; Osborn and Schairer, 1941). The fractional crystallization path for liquid C can not be drawn because the necessary tielines are not known. The trend of the calc-alkali series of rocks begins near the point *c* and nearly coincides with the inferred equilibrium path. The data shown in figure 20*B* were deduced by Tuttle and Bowen (1958, p. 133) from a consideration of the composition of feldspars and groundmass in trachytic rocks, and they represent the dry system in which crystallization occurs at a high temperature. The rotation of the tielines from the cotectic *dk* is noticeable when 20*A* and *B* are compared. The trend of the calc-alkali rocks (fig. 19) does not correspond to the equilibrium crystallization path from C (fig. 20*B*) and would not coincide with any fractional crystallization trend.

SiO_2 is not a component of the systems just described. If silica in excess of that needed for the formation of feldspars was present, the temperature of crystallization in both the wet and the dry systems would presumably be lowered and consequently the positions of the tielines would change. Therefore, detailed comparison of the calc-alkali trend with the experimental data does not seem warranted, and no conclusion regarding probable water content of the magmas will be drawn on the basis of such a comparison. The trend in composition of the calc-alkali series, however, is close enough to the trend that would be deduced for the crystallization of feldspar melts at low to moderate temperatures to suggest that the different members of the calc-alkali series could have originated from a granodioritic or more basic magma by crystallization differentiation controlled primarily by removal of plagioclase.

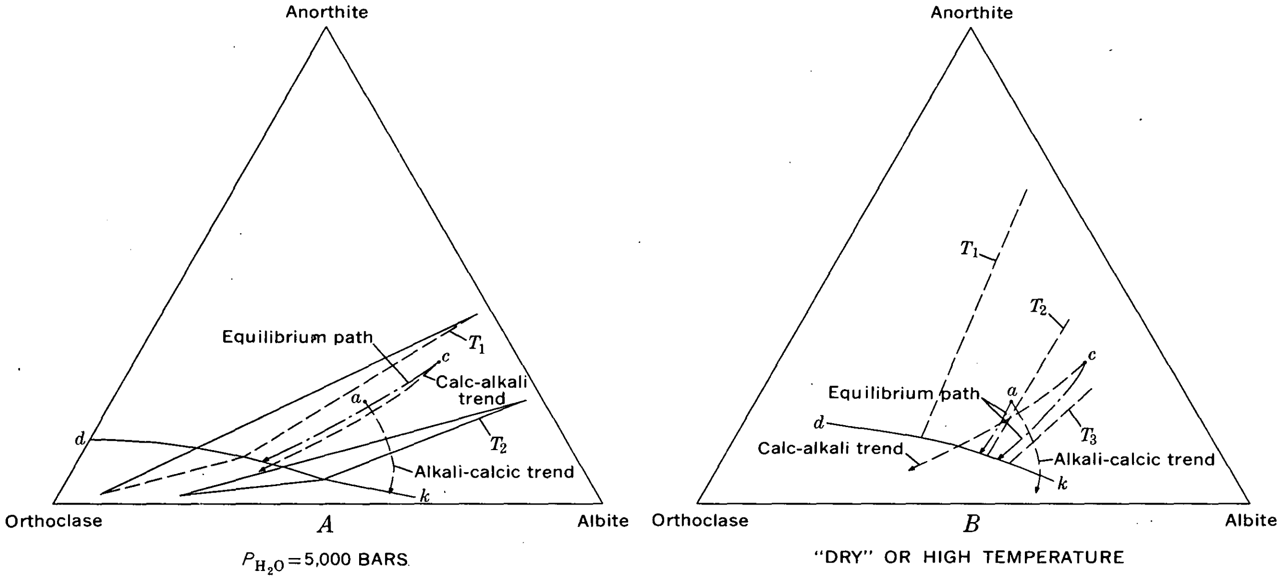

FIGURE 20.—Phase diagrams for the anorthite-albite-orthoclase system compared with the trends of the alkali-calcic and calc-alkali series. *dk* is the cotectic between plagioclase and alkali feldspar, T_1, T_2, and T_3 are tielines joining plagioclase in equilibrium with liquid on the cotectic. Dashed tielines inferred by author. (*A*, Yoder and others, 1957, p. 211–212; *B*, Tuttle and Bowen, 1958, p. 133.)

Hess (1960, p. 185) discussed the possibility that a series of rocks could be produced entirely by partial fusion:

> A series of liquids formed by partial fusion at varying depths within the crust, and hence varying compositions of the rocks fused, could, it appears, produce the calc-alkaline magma series. * * * Here then is a process which is relatively simple in operation and capable of producing rocks of the compositions required. There can be little doubt that it is the explanation for some calc-alkaline rocks, and the writer is inclined to believe that it is the major means by which such rocks are produced.

To duplicate by partial melting the trend that would be produced by equilibrium crystallization of a granodiorite, one of two conditions would have to prevail; either the rock being melted is granodiorite, or the rocks which are being melted would have to lie on the differentiation trend of granodiorite—that is the rocks to be partially melted are granite, quartz monzonite, granodiorite. If one conceives of a rather simple structure of the lower crust that involves layers chemically and mineralogically similar to the calc-alkaline magma series, then the equilibrium crystallization trend could be closely paralleled by a fractional melting trend. However, if the portion of the crust undergoing melting is heterogeneous and contains rocks that are mineralogically very different from the calc-alkaline rock series, then the partial melts would not be expected to fall on the granodiorite differentiation trend.

In considering whether the calc-alkali series of rocks of the Empire quadrangle has resulted from a process of differentiation or from a process of partial melting, one must consider how closely the indicated trend compares to the hypothetical trend of differentiation. As the calc-alkali trend shown in figure 19 is based on somewhat scattered data, a firm conclusion does not seem warranted, but probably the calc-alkali series originated through the classic process of crystallization differentiation.

ALKALI-CALCIC SERIES

A triangular plot (fig. 21*A*) of the normative anorthite, albite, and orthoclase for the analyzed rocks of the alkali-calcic series shows an apparent trend that is very different from the trend of the calc-alkali series. The trend for the alkali-calcic rocks has been drawn from the center of points representing the monzonites of the Empire stock through the points representing the leucocratic monzonites. This trend has also been plotted on the theoretical phase diagrams in figure 20 beginning at point *a*. It is obvious from examination of these phase diagrams that the apparent trend of the alkali-calcic series cannot be explained as a simple crystallization trend, controlled by the removal of plagioclase, because the trend line is nearly perpendicular to the tielines.

The hornblende-pyroxene monzonite contains a large amount of ferromagnesian minerals, whereas the leucocratic monzonite contains a small amount. The removal of pyroxene from the hornblende-pyroxene monzonite magma would produce residual liquids that would be approximately equivalent to the leucocratic monzonite.

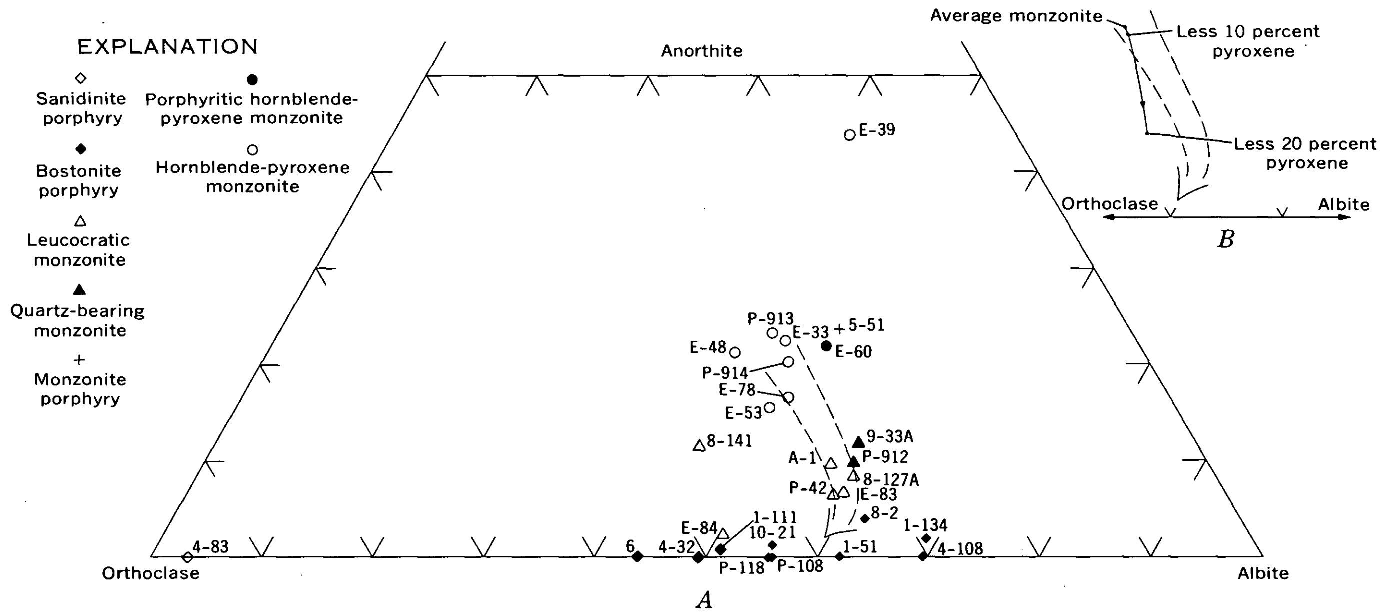

Figure 21.—Triangular plot of alkali-calcic series. Normative anorthite, albite, and orthoclase recalculated to 100 percent. The inset *B* shows the effect of the removal of pyroxene from average monzonite. Dashed arrow indicates postulated differentiation trend. The numbers refer to analyses in tables 13, 15, 16–18.

Table 19 shows the compositions and norms for average hornblende-pyroxene monzonite, and residual liquids resulting from the removal of 10 and 20 weight percent of a pyroxene like E–119 of table 14. The normative feldspar components are plotted in figure 21*B* from which it can be seen that the removal of pyroxene results in a trend which approaches that of the alkali-calcic series.

The normative alkali feldspar and quartz contents of the leucocratic monzonite, bostonite porphyry, and sanidinite porphyry are shown in figure 22. With the exception of the sanidinite porphyry, these rocks plot in or near the minimum troughs for the albite-orthoclase-quartz system as determined by Tuttle and Bowen (1958, p. 54–56). The leucocratic monzonite and bostonite contain small amounts of normative anorthite. Tuttle and Bowen (1958, p. 135–137) and Stewart and Roseboom (1962) showed that anorthite-poor magmas may solidify at high temperatures as hypersolvus rocks containing a single homogeneous alkali feldspar or at low temperatures as subsolvus rocks containing two feldspars. The temperature of solidification is controlled largely by the content of water dissolved in the melt. Samples of leucocratic monzonite are composed either entirely of moderately to strongly perthitic alkali feldspar or of sodic plagioclase phenocrysts surrounded by a groundmass of perthitic alkali feldspar. Thus it would appear that the water content of the leucocratic monzonite magma was low enough and temperatures of crystallization were high enough that crystallization of a single homogeneous feldspar occurred. The extensive

Table 19.—*Chemical compositions and CIPW norms of average hornblende-pyroxene monzonite and two hypothetical magmas that would be produced by the removal of pyroxene, in weight percent*

	Hornblende-pyroxene monzonite [1]	Residual magma after removal of— 10 percent pyroxene [2]	20 percent pyroxene [2]
Chemical composition			
SiO_2	55.4	56.4	57.4
Al_2O_3	18.3	19.8	21.5
Fe_2O_3	3.6	3.4	3.2
FeO	3.1	2.8	2.4
MgO	2.0	1.1	0
CaO	6.1	4.3	2.1
Na_2O	4.7	5.1	5.6
K_2O	4.5	5.0	5.6
H_2O	.70	.77	.85
TiO_2	.81	.72	.61
P_2O_5	.42	.42	.42
MnO	.18	.13	.07
CO_2	.08	.09	.10
Total	99.89	100.03	99.85
CIPW norms			
or	26.7	29.5	33.4
ab	36.4	40.9	47.2
an	15.3	16.4	7.5
ne	1.8	1.1	0
C	0	0	3.5
di	9.6	1.5	0
ol	1.5	2.4	.4
mt	5.3	4.9	4.6
il	1.5	1.4	1.2
ap	1.0	1.0	1.0
cc	.2	.2	.2

[1] Average of samples P-913, P-914, E-33, E-48, E-53, E-78, table 13.
[2] Pyroxene composition used in calculations is that of sample E-119, table 14.

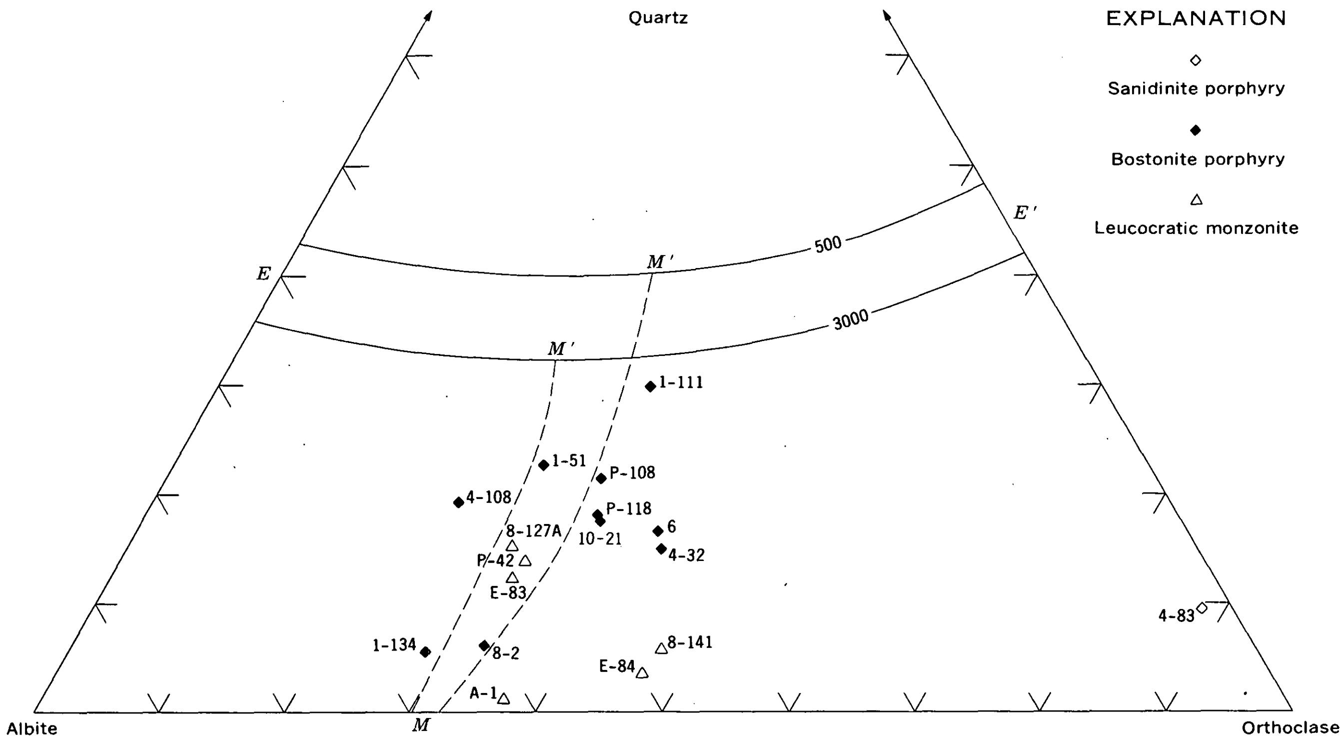

FIGURE 22.—Triangular plot of the anorthite-poor members of the alkali-calcic series with normative albite, orthoclase, and quartz recalculated to 100 percent. Lines *E–E'* are quartz-alkali feldspar cotectics at p_{H_2O}=500 and 3,000 kg/cm². Lines *M–M'* are centers of minimum troughs on liquidus surfaces. Liquidus data from Tuttle and Bowen (1958, p. 54–56). Numbers refer to analyses in tables 16–18.

development of perthite in the leucocratic monzonite indicates, however, that there may have been sufficient water available following crystallization to facilitate the partial exsolution and recrystallization of the feldspar. The bostonites contain even less normative anorthite than the leucocratic monzonite, and many of the bostonites have groundmass textures indicative of the initial formation of one homogeneous alkali feldspar. The groundmass of the bostonites now consists of albite and orthoclase in a very fine grained complex intergrowth indicating that there has been extensive postsolidification recrystallization.

UNDERSATURATED SERIES

The origin of the undersaturated series and its relation to other series are problematical. The undersaturated series is most nearly like the hornblende-pyroxene monzonite, and the question naturally arises whether the two may be related. The crystallization differentiation of silica undersaturated magmas tends to produce feldspathoidal-alkali-feldspar rocks. Thus, whether differentiation of the slightly oversaturated to slightly undersaturated hornblende-pyroxene monzonite could give rise to the feldspathoidal rock should be considered. Examination of the position of the feldspathoidal hornblende-pyroxene monzonite and monzonite on the Larsen plot (fig. 18) shows that this suggested line of descent is backward with respect to FeO, MgO, and CaO. Comparison of the total normative femic minerals in each rock type (tables 12 and 13) indicates a similar relation—the feldspathoidal monzonite contains 25–35 percent femic normative minerals, but the monzonite contains only 13–23 percent. Therefore, differentiation of a monzonitic magma probably could not have given rise to the undersaturated group.

It is generally believed that crystallization of a silica undersaturated magma cannot give rise to saturated differentiation products except where an early formed mineral, such as olivine or leucite, has failed to react. In the quaternary nepheline-anorthite-kalsilite-silica system (fig. 23), the plane joining albite, anorthite, and orthoclase is the critical silica saturation plane. As can be seen from figure 17, the hornblende-pyroxene monzonites would plot on or close to the albite-anorthite-orthoclase plane whereas the feldspathoidal hornblende-pyroxene monzonites would plot on the nepheline side of the plane. Crystallization of feldspars and feldspathoids (except leucite) from an undersaturated magma will produce residual liquids at some point in the tetrahedron on the nepheline side of the saturation plane.

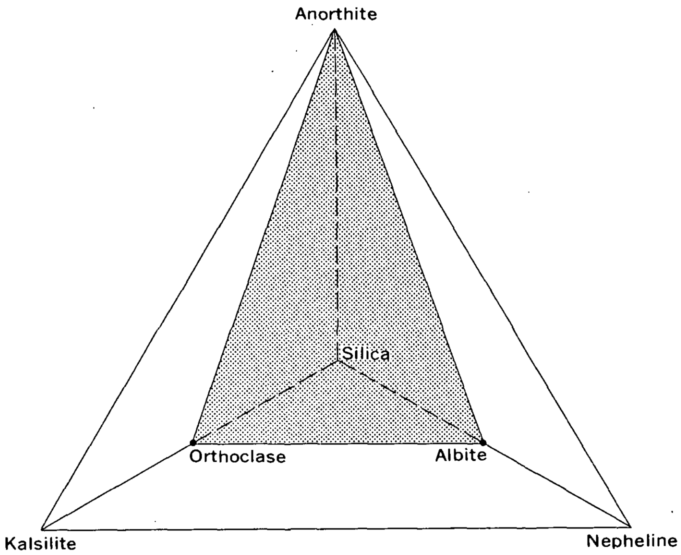

FIGURE 23.—Quaternary nepheline-anorthite-kalsilite-silica system showing the position of the ternary feldspar plane.

Removal of pyroxene from the feldspathoidal hornblende-pyroxene monzonite results in a decrease in FeO, MgO, and CaO as the values for the hornblende-pyroxene monzonite are approached, but the alkalis are increased to such an extent that the resulting rocks are even more undersaturated in silica than the starting feldspathoidal rock (table 20). Consequently, it does not seem possible to relate the monzonite to the feldspathoidal monzonite by any normal process of fractional crystallization.

In the Empire stock irregular bodies of pyroxenite occur at the contact between feldspathoidal hornblende-pyroxene monzonite and hornblende-pyroxene monzonite. The pyroxenite could represent altered inclusions of Precambrian hornblendic rocks such as the hornblendite that occurs west of the stock. Possibly small amounts of feldspathoidal monzonite magma could have formed as a result of the reaction occurring between monzonite magma and hornblendic rock. The process hypothesized is that masses of hornblendite became surrounded by monzonite magma, that through mutual exchange of chemical constituents the hornblendite was converted to pyroxenite of a composition that would be in equilibrium with the magma, and that the chemistry of the monzonite magma was changed such that the composition approached the composition of the feldspathoidal monzonite. To test this theory the addition and subtraction diagram in figure 24 was constructed. On the left-hand side of this diagram is the average composition of two samples of hornblende (table 4) from Precambrian rocks in the Empire quadrangle, and this average is used as the approximate composition of the postulated hornblendite inclusions prior to reaction with the magma. On right-hand side is the average composition of hornblende-pyroxene monzonite based on the analyses of samples P–913, P–914, E–33, and E–48 in table 13, and this average is used as the approximate composition of the postulated uncontaminated monzonite magma. Complete incorporation of hornblendite by magma would result in a mixture lying somewhere along the straight line joining hornblende and monzonite (such as line *AB* for CaO). A mixture of about 35 weight percent hornblende and 65 percent monzonite would have an SiO_2 content equivalent to the average feldspathoidal hornblende-pyroxene monzonite (average composition of samples in table 12), but the amounts of the other major oxides in the mixture would not be the same as in the feldspathoidal rocks. If a larger amount of hornblende was incorporated—for example 50 weight percent as represented by the vertical dashed line—then the SiO_2 content of the mixture would be less than that of the feldspathoidal hornblende-pyroxene monzonite. Then, if the constituents of the residual pyroxenite (represented by the average of the pyroxene in table 14) were removed from the mixture, the composition of the contaminated magma would be shifted as shown by the arrows (such as line *CD* for CaO). The shift of all constituents except FeO and Fe_2O_3 is in the right direction. Thus, the small bodies of feldspathoidal hornblende-pyroxene monzonite may have originated by assimilative reaction between monzonite magma and Precambrian hornblendic rocks.

TABLE 20.—*CIPW norms of feldspathoidal hornblende-pyroxene monzonite and two hypothetical magmas that would be produced by the removal of pyroxene, in weight percent*

	Feldspathoidal hornblende-pyroxene monzonite [1]	Residual magma after removal of—	
		10 percent pyroxene [2]	20 percent pyroxene
or	27.5	30.6	34.5
ab	15.2	13.6	15.2
an	11.8	11.1	11.7
ne	14.0	17.9	19.3
hl	.2	0	0
di	18.7	14.0	5.0
ol	2.1	2.4	3.7
mt	5.9	5.8	5.6
il	1.8	1.7	1.5
ap	1.6	1.7	2.0
fr	.2	0	0
cc	.2	.2	.2

[1] Sample E–10, table 12.
[2] Like sample E–119, table 14.

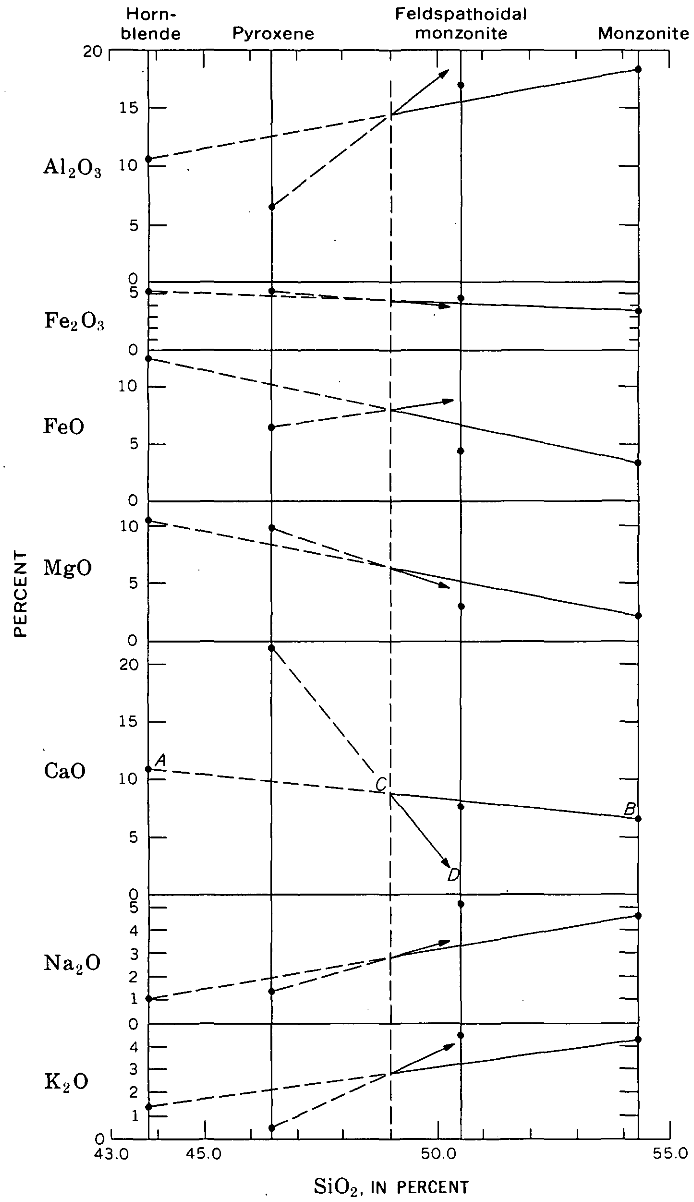

FIGURE 24—Addition and subtraction diagram used in testing a theory about the origin of feldspathoidal hornblende-pyroxene monzonite. See text for explanation of lines.

SUMMARY OF PETROLOGIC INTERPRETATIONS

The field, petrographic, and chemical relations seem to indicate that during the early part of the Tertiary, granodiorite magma and monzonite magma were generated beneath the central Front Range. Both magmas underwent processes causing diversification at depth, and secondary magmas resulting from the diversification were emplaced at the level now exposed in an overlapping time sequence. The granodiorite magma gave rise to the rocks of the calc-alkali series primarily as a result of fractional crystallization of plagioclase. The monzonite magma gave rise to small amounts of undersaturated feldspathoidal monzonite by assimilative reaction with Precambrian hornblendic rocks, and removal of pyroxene from the monzonite magma resulted in the leucocratic monzonite magma of the alkali-calcic series.

None of these interpretations can be proved, but they seem to best explain the data available.

QUATERNARY DEPOSITS

About one-third of the bedrock of the Empire quadrangle is completely covered by unconsolidated deposits of Pleistocene and Recent age. These deposits, which were not subdivided during mapping, consist of glacial moraines, glacial outwash, talus, solifluction debris and alluvium.

STRUCTURE

The structure of the Precambrian gneisses of the Empire quadrangle conforms in general to that of the rocks just to the east (Sims, 1964; Sims and Gable, 1964; Harrison and Wells, 1956, 1959; Moench, 1964; Moench and others, 1962). There, two periods of Precambrian deformation are recognized—an older, plastic, gneiss-forming deformation that produced large, north- to northeast-trending folds (B_o) throughout the area, and a younger deformation that produced east-northeast-trending folds (B_y) and cataclasis that are most pronounced along the Idaho Springs–Ralston shear zone (Tweto and Sims, 1963). The rocks also might have been deformed prior to the recognized older B_o deformation, but, if so, the accompanying minor structures have been obliterated. According to Moench, Harrison, and Sims (1962), granodiorite (Boulder Creek Granite of this report) was emplaced during the B_o deformation and biotite-muscovite granite (Silver Plume Granite of this report) was emplaced toward the end of this deformation. More recent work, however, suggests that emplacement of the Silver Plume Granite might have been later than the B_o deformation (Moench, 1964, p. A40).

Faults of considerable horizontal extent are abundant in the northwestern part of the quadrangle. The material within individual fault zones is mostly gouge and cemented breccia but includes well-developed mylonite along parts of several of the faults. The contrast between types of fault zone material suggests that the faults have been active during at least two widely separated periods.

OLDER DEFORMATION (B_o)

The major folds in the Empire quadrangle trend north to northeast, parallel to the trend of the B_o folds of Moench, Harrison, and Sims (1962). The Lawson syncline and the Loch Lomond anticline are the main folds in the eastern part of the quadrangle. The Lawson syncline, which passes through the extreme southeast corner of the quadrangle, is a broad open fold that has been traced for about 3½ miles north-northeastward into the Central City quadrangle (Sims, 1964). The Loch Lomond anticline is a broad asymmetric fold in the central part of the quadrangle but appears to become more complex toward the northeast (pl. 1 sections *A–A′* and *B–B′*). The anticline probably extends several miles northward into the East Portal quadrangle.

The fold structure differs east and west of the Loch Lomond anticline. In the Central City area east of this anticline, the structure is dominated by long folds spaced from 1 mile to several miles apart (fig. 25). By contrast, west of the Loch Lomond anticline the folds are closely spaced and individual axial planes can be traced only short distances. The metasedimentary rocks in these closely spaced folds do not contain distinctive horizon markers, and much of the area west of the Continental Divide has poor bedrock exposure. Thus, the amplitude of the folds or the extensions of their axial planes are difficult to determine.

The Rogers Pass anticline and syncline pair is asymmetric to overturned, and thus, although the axes plunge north, the traces of the axial planes trend about N. 35° E. The fold pair appears to have an amplitude of about 2,000 feet in the vicinity of Rogers Pass, but the fold must be very disharmonic, for it appears to die out southward (downward) in the valley of Jim Creek.

The Mount Eva anticline-syncline pair is shown on plate 1 as extending about 3½ miles southwestward from James Peak; the folds change from open at the north to overturned at the south. The existence of the overturned parts of the folds southwest of Fall River is quite speculative. The overturned structure of the anticline is inferred from the occurrence of a zone of well-developed minor folds near the crest of Mount Eva and southwestward. These minor folds range in amplitude from about 1 to 10 feet, and if they are interpreted as drag folds they have symmetry that suggests that the northwest-dipping foliation (pl. 1) is overturned.

The Witter Peak syncline is delineated by the outcrop pattern of the Bancroft microcline gneiss layer and its associated hornblende gneiss. The syncline apparently plunges under the hanging wall of the Bancroft fault to the northeast. Southwestward the syncline and the anticline that lies west of the syncline die out rapidly into a structural terrace. This change in shape probably indicates that the folds are disharmonic. (See pl. 1, section D–D′.)

The characteristics of the deformation that produced the B_0 folds can be deduced from the geometry of the major folds and from the features seen in outcrops and thin sections. Many of the major folds are open in the sense that opposing limbs have low dips. Parts of some folds are overturned, and the axial planes may dip either southeast or northwest; no large recumbent folds have been found. The major folds trend north-northeast, and the major direction of the compression which formed them was presumably west-northwest and nearly horizontal.

Many small folds, and probably some large folds in places, are noticeably disharmonic, and extreme attenuation of many fold limbs has occurred. These features indicate that there has been intense plastic flow of the rocks modified by the presence of thin to thick layers of relatively more competent rocks. From outcrop observations it appears that the hornblende gneiss and amphibolite were the most competent major rock types and that microcline gneiss, biotite gneiss, and migmatite were decreasingly less competent.

The metasedimentary gneisses in the Empire quadrangle characteristically contain only one foliation. It is defined by the parallel alinement of platy micas, lensoid grains and clusters of grains of quartz and feldspar, and layers of different mineral composition. The foliation is parallel to contacts between metamorphic rock bodies. These characteristics suggest that the foliation developed parallel to the bedding of the original sediments from which the gneisses were derived and is called bedding foliation in this report.

Locally, younger foliation planes cut across the bedding foliation. On the ridge between the south branch of Parry Creek and Eva Creek some of the outcrops of biotite gneiss contain slip-cleavage planes that cut across and deform the bedding foliation. The slip cleavage appears to form two sets: one that strikes northwest and dips gently to the north, and one that strikes northeast and dips southeast. Because of the very limited areal extent of this slip cleavage, no interpretation of its significance can be made.

Nearly all exposures of the metasedimentary rocks contain a variety of measurable linear structures. These linear structures, in the approximate order of abundance, include the axes of small folds that have amplitudes of a few inches to several feet, the axes of crinkles that have amplitudes of a fraction of an inch, alined crystals of elongate shape, slickenside striations, and boudinage structures.

The metamorphic rocks affected only by the B_0 folding typically have a crystalloblastic texture in which granoblastic quartz and feldspar grains surround mica plates that tend to have a parallel alinement. Platy biotite and acicular sillimanite or hornblende tend to be alined and produce mineral lineations. Plates of biotite

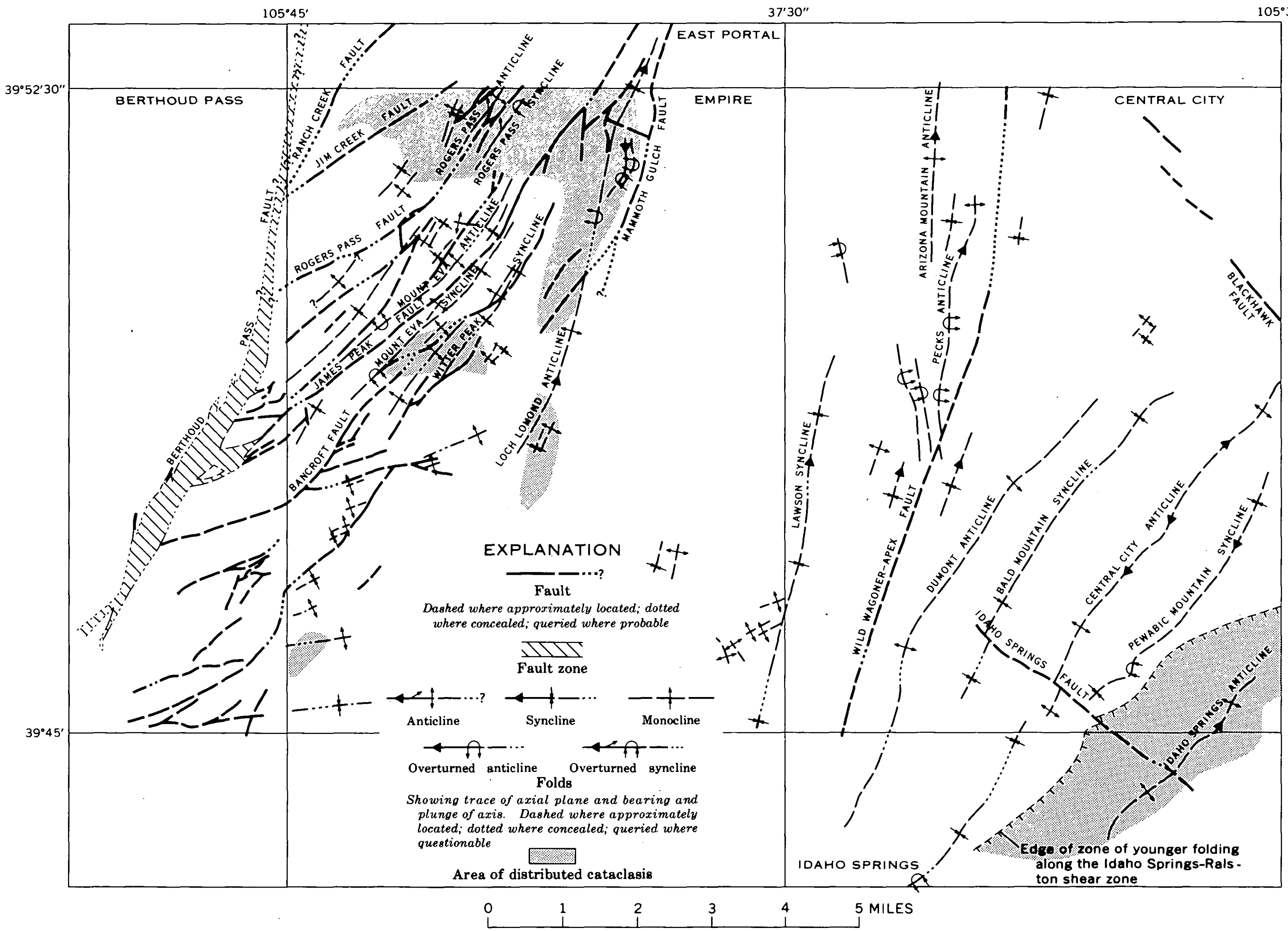

FIGURE 25.—Folds and faults in the Empire and Central City quadrangles and adjacent areas. Sources of data: Berthoud Pass quadrangle (Theobald, 1965); East Portal (reconnaissance mapping, 1962); Empire (this report); Central City (Sims, 1964); Idaho Springs (Moench and others, 1962).

that statistically tend to be parallel to the foliation deviate somewhat from the foliation plane; thus, the edges of some biotite plates are visible on the foliation surfaces, and the edges also tend to be parallel and produce a mineral alinement. Sillimanite forms lensoid to elongate clots within which the individual sillimanite crystals tend to be roughly alined, but many randomly oriented needles occur. There is no evidence of granulation of quartz or feldspar, of bending of mica plates or sillimanite needles, or of rotation during growth of garnet porphyroblasts. These features suggest either that metamorphism occurred after folding ceased or that metamorphic fabrics produced during folding have been obliterated by recrystallization after the folding. Possibly, much of the mineral alinement is the result of mymetic recrystallization.

The foliation and lineation data collected during the field study are shown in the projections on plate 3. The positions of the major foliation and lineation maxima for all areas except 4, 10, and 14 on plate 3 are shown in figure 26. Clearly most foliation maximums are distributed approximately along a great circle girdle that lies between the limiting girdles shown. This distribution of foliation maximums shows that throughout much of the quadrangle the bedding foliation has been rotated about fold axes that plunge 10°–40°, N. 30°–35° E. The distribution of the major lineation maximums in figure 26 indicates that many of the lineations tend to be parallel to the fold axes deduced from the foliation data. The major fold direction in the Empire quadrangle is parallel to the direction of the older folds (B_o) described by Moench, Harrison, and Sims (1962).

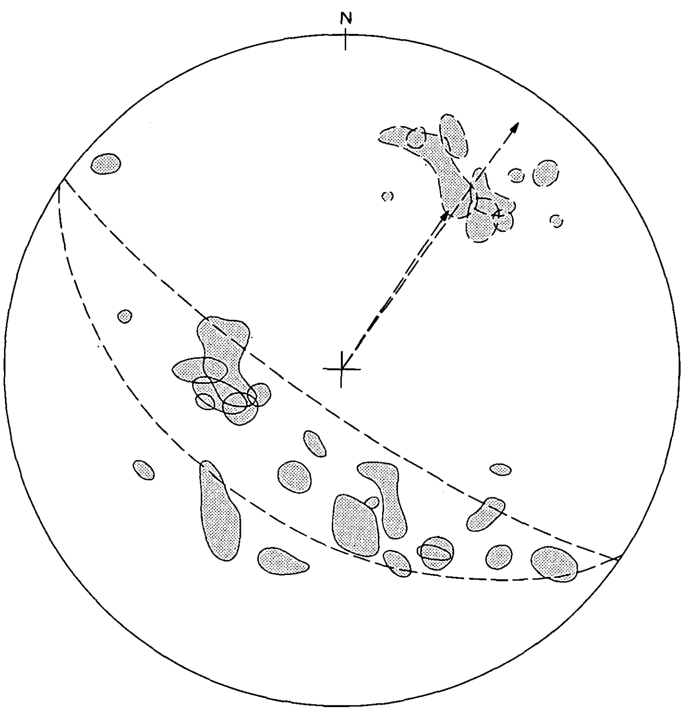

FIGURE 26.—Synoptic diagram showing major maximums of foliation (solid) and lineation (dashed), Empire quadrangle. Areas 4, 10, and 14 on plate 3 not included. Two dashed girdles and their axes are shown to indicate the limits within which the average girdle must lie.

Although the structure of the Empire quadrangle seems to be dominated by folds (B_o) that plunge gently northeast, the lineation and foilation data shown on plate 3 indicate that there are complexities that cannot be explained by the assumption of one fold direction. These complexities manifest themselves as complex foliation distributions, as multiple lineation directions, and as major lineation directions that diverge at large angles from the average direction.

In areas 1, 2, 3, 6, and 7, the bedding foliation strikes generally northwest and dips northeast. This region is the limb between the Lawson syncline and the Loch Lomond anticline. Within areas 8 and 9 the bedding foliation trends northeast and dips steeply northwest along the northwest limb of the Loch Lomond anticline. The individual bedding-foliation plots for these areas contain a maximum or partial girdles which indicate the large size of the anticline-syncline pair. By contrast, the bedding-foliation diagrams for areas 10, 11, 12, and 13 show nearly complete girdles which reflect the close spacing of the axial surfaces in these regions. In area 10 the distribution of poles of bedding foliation is more complex but can be interpreted as being dominated by a girdle about an axis plunging about 50° N. Probably the major fold axes (B_o), which trend about N. 40° E. in areas 11, 12, and 13, swing gradually to trend of N. 15° E. to north within area 10.

Moench, Harrison, and Sims (1962, p. 44) have observed that there are lineations (A_o) oriented at about right angles to the direction of the older folds (B_o) in the Idaho Springs–Central City area. The A_o lineations consist primarily of small fold axes with minor alined minerals and boudinage structure, while the B_o lineations consist dominantly of small fold axes and alined minerals. Within several areas (1, 2, 5, 8, 10, 12, pl. 3) of the Empire quadrangle there are also minor concentrations of lineations that are about at right angles to the dominant B_o lineations. The A_o lineations in the Empire quadrangle consist primarily of small folds and minor crinkles, alined minerals, and slickenside striations. Folding about A_o is also reflected by partial girdles in the foliation plots of areas 7 and 8 and perhaps area 5. Mutually perpendicular lineations may develop virtually simultaneously during a single folding episode. However, in the simplest case, the B lineations would be different in kind from the A

lineations: for example, folds and boudinage in B, and slickenside striations, streaking, and elongate pebbles in A. In the present case the B_o and A_o lineations are virtually the same type and relating them genetically is more hypothetical. Moench, Harrison, and Sims (1962) believe that the A_o lineations formed late in the period in which B_o folds formed and that the A_o lineation formed as a result of warping of the axial surfaces of the B_o folds.

YOUNGER DEFORMATION (B_y)

The younger deformation is most strongly developed along the Idaho Springs-Ralston shear zone, which is southeast of the Empire quadrangle (fig. 25). Near Idaho Springs (Moench and others 1962, p. 35), the younger deformation was dominantly cataclastic, but small folds were formed locally in the relatively incompetent rocks. The folds, which are very straight, trend N. 55° E. and plunge at various angles depending upon their position on the older folds. Associated with these folds are two lineations, one (B_y) parallel to the fold axes and one (A_y) at about 80° to the fold axes.

Effects of cataclasis have been observed in the western and northwestern parts of the Empire quadrangle (fig. 25). Areas of intense cataclasis can be recognized in outcrop where quartzofeldspathic rocks such as microcline gneiss have been so crushed that closely spaced slickensided shear planes are abundant. Less intense cataclasis can be recognized in thin sections of microcline gneiss, Boulder Creek Granite, and Silver Plume Granite where initial granulation has produced extreme undulatory extinction in quartz and a mortar texture along grain boundaries (fig. 27*A*). Mechanical deformation of micaceous rocks has produced undulatory extinction in quartz and pronounced kink banding of biotite and coarse poikiloblastic muscovite (fig. 27*B*.)

In areas 8, 9, and 10 (pl. 3), many outcrops contain two, three, or four different lineations. Two lineations are most common: the dominant B_o lineation that trends northeast and a lineation trending N. 20°–30° W. or one trending about N. 60° E. All three lineations can be found together in some outcrops. The relative ages of crossing lineations can be deduced in especially favorable outcrops: the northwest lineations and the east-northeast lineations are younger than the B_o lineations. In the Idaho Springs area Moench, Harrison, and Sims (1962, p. 45) found that the lineations related to the zone of younger folding trend N. 55° E. (B_y) and N. 25° W. (A_y). The east-northeast lineations in the Empire quadrangle probably are equivalent to B_y and the northwest lineations equivalent to A_y. A_y and B_y lineations are most abundant in areas 8, 9, and 10, but they also occur in areas 1, 2, and 12. In areas 1 and 2, however, intersecting lineations are not common. Lineations in the B_y direction in the Empire quadrangle consist, in order of decreasing abundance, of small folds, crinkles, and alined minerals; whereas lineations in A_y consist of slickenside striations, small folds, and crinkles. Comparison of figure 25 and plate 3 shows that the areas of cataclastic deformation coincide with the areas in which B_y and A_y lineations are abundant; indeed, many of the A_y lineations are slickenside striations formed during the catalastic deformation of quartzofeldspathic rocks.

RELATIONS OF INTRUSIVE ROCKS TO DEFORMATIONS

The Boulder Creek Granite and the quartz diorite and hornblendite form bodies that are conformable to the structure in the metamorphic rocks produced during the period of B_o folding. These igneous rocks have also been foliated and recrystallized, and this foliation and recrystallization are clearly related in time to the period of B_o folding. The Silver Plume Granite characteristically forms highly discordant bodies that cut across B_o folds and that show no evidence of refoliation or recrystallization. The Silver Plume Granite thus appears to be younger than the period of B_o folding. This last conclusion is contrary to that expressed by Moench, Harrison, and Sims (1962, p. 56). These authors indicated that in a few places small phacolithlike bodies of Silver Plume occur on the crests of B_o folds, and they concluded that the Silver Plume was emplaced late in the period of B_o folding. The Silver Plume phacoliths possibly are sills intruded into already folded rocks. In the northern part of the Empire quadrangle, Silver Plume Granite, granite porphyry, and pegmatite have all been affected by the pervasive cataclastic deformation that occurred during the younger period of deformation.

It is interesting to note that the lineation and foliation plots for areas 11, 12, and 13 on plate 3 are very similar even though area 13 has been extensively invaded by discordant Silver Plume Granite. In particular the bearing and plunge of the B_o lineation maximums are very nearly the same. Thus the emplacement of the Silver Plume stocks in the southwestern part of the quadrangle did not result in any appreciable tilting or deformation of the wallrocks, and stoping must have been the principal mechanism of emplacement.

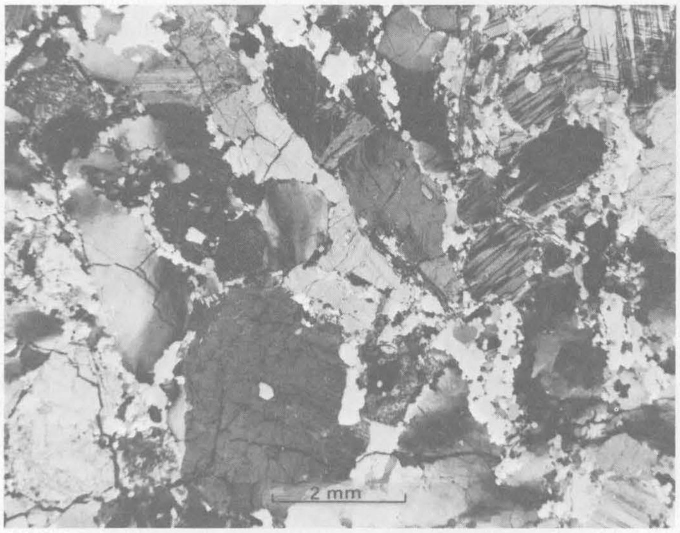

A

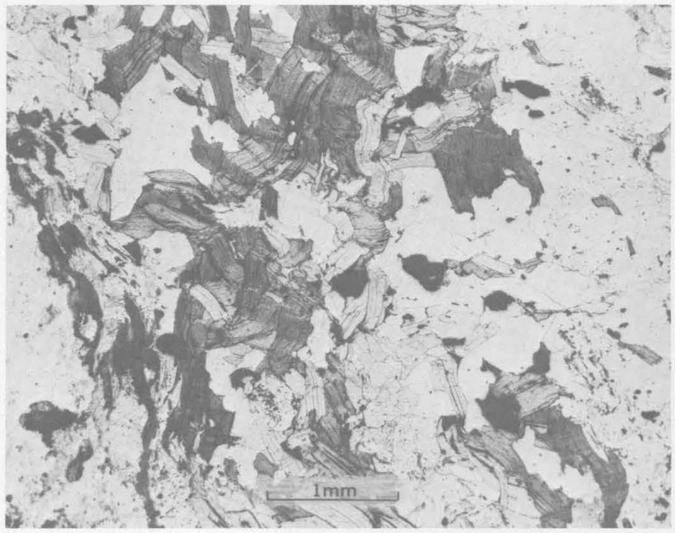

B

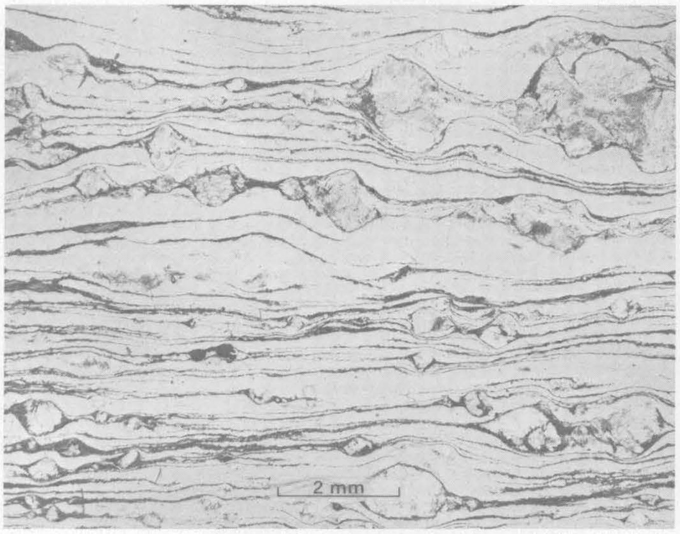

C

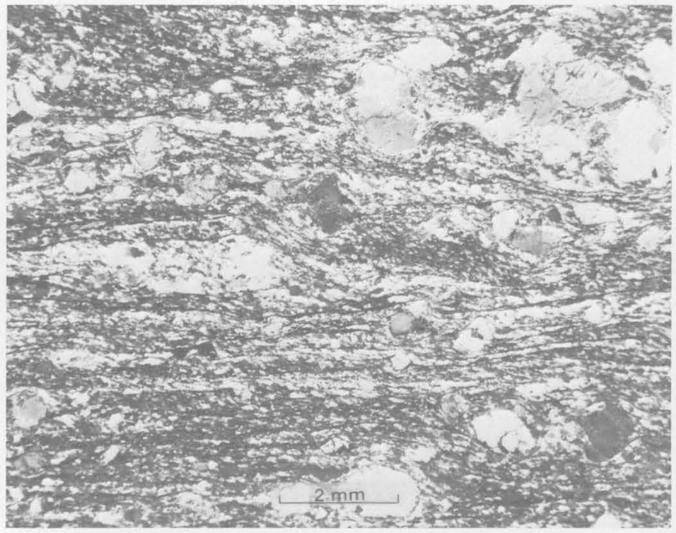

D

E

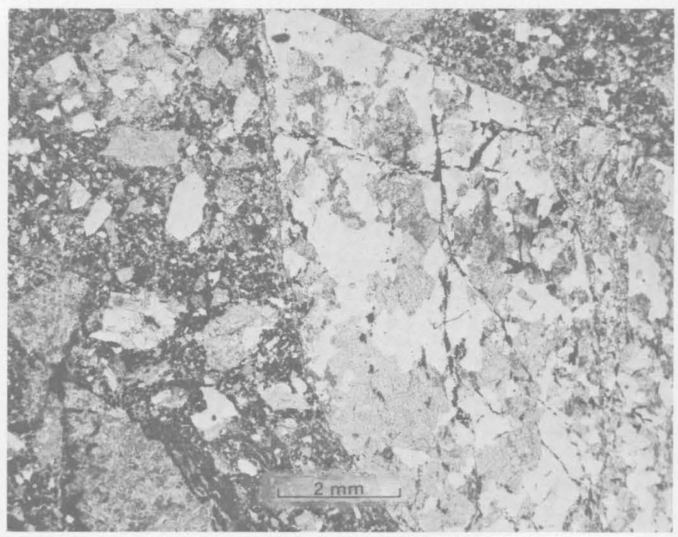

F

FIGURE 27.—Photomicrographs of cataclastically deformed rocks. *A*, Weakly deformed Boulder Creek Granite showing mortar texture and undulatory quartz. Crossed nicols. *B*, Biotite-muscovite gneiss. Both the biotite and the muscovite are kink banded. Plain light. *C*, Mylonite from the Bancroft fault zone showing a well-developed fluxion structure that is marked by streamers of finely comminuted biotite and showing porphyroclasts of quartz and feldspar. Plain light. *D*, Same specimen as *C*. Crossed nicols. *E*, Flaser gneiss from northwest-trending flat fault north of Mammoth Gulch. Lenses of strongly granulated gneiss alternate with seams of mylonite. Plain light. *F*, Microbreccia from Bancroft fault zone. Angular fragments of microcline gneiss are enclosed in a very fine grained matrix that is cemented by hematite. Plain light.

EAST-NORTHEAST-TRENDING FOLDS OF UNKNOWN ORIGIN

The lineation and foliation data (pl. 3) show that areas 4 and 14 are dominated by folds that trend east-northeast. In area 4, which in part covers the trough of the Lawson syncline, moderate-sized folds and abundant small folds and other lineations trend east-northeast. In this area also, some moderate-sized folds trend north-northwest. In area 14 steeply dipping beds along the canyon of the North Fork of Clear Creek mark the limb between a large anticline and syncline that plunges about 30° N. 80° E. (pl. 1, section *F–F′*).

As these structures trend east-northeast, they are subparallel to the trend of the B_y folds elsewhere in the area, and for this reason, they could be interpreted as having been produced during the period of younger folding. Hawley and Moore (1967, p. 43) have made such an interpretation in area 4.

The character of the deformation in these areas, and the relations of the folds to the Silver Plume Granite, however, are not consistent with this interpretation. There is no evidence of postmetamorphic mechanical deformation of the rocks in these areas except on the extreme west side of area 14, where the Silver Plume Granite is locally granulated. Furthermore, the evidence is clear in area 14 that the Silver Plume Granite was emplaced after the major and minor folds of east-northeast trend had formed. Elsewhere in the region where Silver Plume is associated with B_y folds, it is older than the folds and has been granulated during the B_y deformation. For these reasons, Moench, Harrison, and Sims (1962, p. 44) considered the east-northeast-trending minor folds in area 4 to be "a local manifestation" of the older deformation.

Formation of the east-northeast-trending folds appears to be explainable in three ways, and no firm choice can be made among them. (1) The folds may be of the same age as the B_o folds and represent a local divergence of this direction of folding. (2) The folds may be of the same age as the B_y folds but formed in a place where the rocks were more plastic than elsewhere. If true, the Silver Plume Granite would have to be of the same general age as B_y folding so that in some places (area 14) it was emplaced after folding ceased whereas in others it was emplaced before folding ceased. (3) The folds are remnants of a fold set older than B_o folds. Moench, Harrison, and Sims (1962, p. 45) briefly considered the possibility of the existence of a large anticline trending about east near Idaho Springs that was older than the B_o folds. Areas 4 and 14 could possibly contain remnants of this very old fold set.

FAULTS

Many extensive faults are exposed in the northwestern part of the quadrangle, and numerous short faults and veins are exposed in the southeastern part (pl. 1). This apparent difference in the nature of fracturing is in part real and is in part due to the technique of mapping. It is true that large faults occur only in the northwest. The distribution of short faults as mapped is biased, however, because they are easily recognized within the mineral belt where they have been mineralized and prospected.

Most of the small faults and veins dip steeply, and trend N. 25° E. to N. 75° E. (fig. 28). In the southeast corner of the quadrangle and the adjacent area to the east, however, faults and veins have many different trends: a few old faults (apparently Precambrian) trend northwest and northeast; many small early Tertiary faults and veins trend east, east-northeast to northeast, and west-northwest; and a set of minor younger Tertiary faults trend north to north-northeast (Hawley and Moore, 1967, p. 49).

The faults in the northwestern part of the quadrangle trend dominantly northeast, generally have very steep dips, and appear to branch from the Berthoud Pass fault in the adjacent Berthoud Pass quadrangle (fig. 25). The fault zones are characterized by gouge, breccia, and oxidized and argillized wallrocks. The fault zones range in thickness from a few tens of feet to 200 feet. Although critical evidence of the direction or amount of movement could not be found, the position of rock units adjacent to the Ranch Creek, Jim Creek, and Bancroft faults can probably best be explained by assuming that the northwest sides of these faults have a component of uplift relative to the southeast sides.

Most commonly the material within fault zones consists of gouge or breccia, and in some place the breccia is cemented with iron oxide (fig. 27*F*), silica, or carbonate minerals. At a few places, however, well-indurated cataclastic rocks ranging from flaser gneiss to mylonite

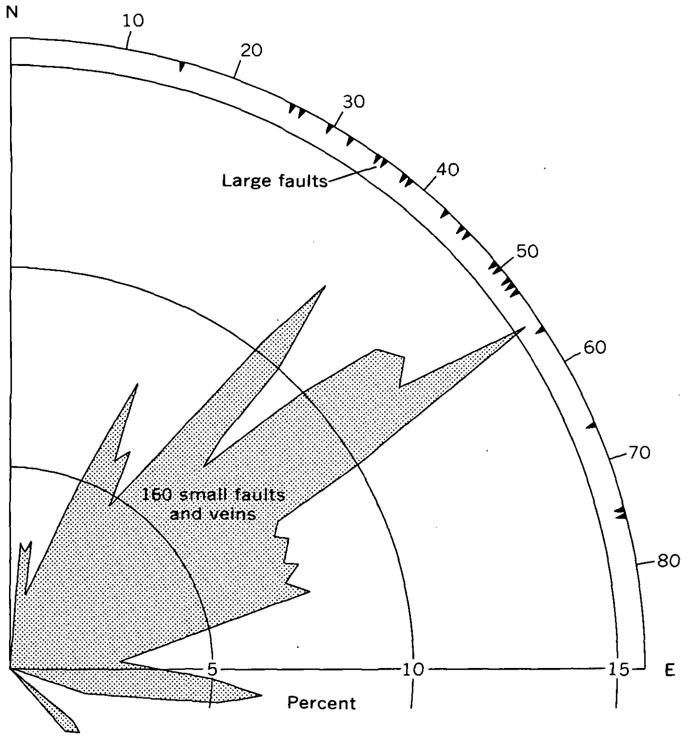

FIGURE 28.—Strike of large faults and small faults and veins, Empire quadrangle.

occur along faults (figs. 27*C*, *D*, *E*). Mylonite has been observed along the Berthoud Pass fault where it has been mapped in the East Portal quadrangle (fig. 25) and along the Bancroft fault between Lake Caroline and Mount Eva. Flaser gneiss and mylonite comprise the only fault zone material along the two faults that extend northwest from the Mammoth Gulch fault north of Mammoth Gulch.

The contrasting types of fault zone materials are evidence that there has been more than one period of movement along the faults. The formation of gouge and breccia probably occurred as a result of young faulting at relatively shallow depths, whereas the mylonite and flaser gneiss were probably formed during older faulting at greater depth. The dominant period of younger faulting is almost certainly Laramide, whereas the period of older faulting is probably Precambrian.

Because cataclasis characterizes the B_y period of Precambrian folding, the period of older faulting possibly is of the same age. Tweto and Sims (1963, p. 1001) concluded that many presumed Precambrian faults are younger than the period of deformation that produced the B_y fold zones. In particular, there are north-northeast faults in the Idaho Springs–Central City area that apparently are younger than the period of B_y folding. Thus the period of older faulting in the Empire quadrangle could be the same general age as the B_y folding, or it could be younger.

REFERENCES

Barth, T. F. W., 1962, Theoretical petrology [2d ed.]: New York, John Wiley & Sons, Inc., 416 p.

Bastin, E. S., and Hill, J. M., 1917, Economic geology of Gilpin County and adjacent parts of Clear Creek and Boulder Counties, Colorado: U.S. Geol. Survey Prof. Paper 94, 379 p.

Bergendahl, M. H., 1963, Geology of the northern part of the Tenmile Range, Summit County, Colorado: U.S. Geol. Survey Bull. 1162–D, 19 p.

Boos, M. F., and Boos, C. M., 1934, Granites of the Front Range—the Longs Peak–St. Vrain batholith: Geol. Soc. America Bull,. v. 45, no. 2, p. 303–322.

Bowen, N. L., 1914, The ternary system; diopside-forsterite-silica: Am. Jour. Sci., v. 38, 4th ser., p. 207–264.

——— 1915, The crystallization of haplobasaltic, haplodioritic, and related magmas: Am. Jour. Sci., v. 40, 4th ser., p. 161–185.

——— 1941, Certain singular points on crystallization curves of solid solutions: Natl. Acad. Sci. Proc., v. 27, p. 301–309.

Evans, B. W., 1965, Application of a rate method to the breakdown equilibria of muscovite and muscovite plus quartz: Am. Jour. Sci., v. 263, p. 647–667.

Guidotti, C. V., 1963, Metamorphism of the pelitic schists in the Bryant Pond quadrangle, Maine: Am. Mineralogist, v. 48, p. 772–791.

Harker, Alfred, 1909, Natural history of igneous rocks: London, Methuen, 384 p.

Harrison, J. E., and Moench, R. H., 1961, Joints in Precambrian rocks, Central City–Idaho Springs area, Colorado: U.S. Geol. Survey Prof. Paper 374–B, 14 p.

Harrison, J. E., and Wells, J. D., 1956, Geology and ore deposits of the Freeland-Lamartine district, Clear Creek County, Colorado: U.S. Geol. Survey Bull. 1032–B, p. 33–127.

——— 1959, Geology and ore deposits of the Chicago Creek area, Clear Creek County, Colorado: U.S. Geol. Survey Prof. Paper 319, 92 p.

Hart, S. R., 1960, A study of mineral ages in a contact metamorphic zone: U.S. Atomic Energy Comm. 8th Ann. Prog. Rept. NYO 3941, 1960, p. 131–154.

Hawley, C. C., and Moore, F. B., 1967, Geology and ore deposits of the Lawson–Dumont–Fall River district, Clear Creek County, Colorado: U.S. Geol. Survey Bull. 1231, 92 p.

Hedge, C. E., Peterman, Z. E., and Braddock, W. A., 1967, Age of the major Precambrian metamorphism in the northern Front Range, Colorado: Geol. Soc. America Bull., v. 78, p. 551–558.

Hess, H. H., 1960, Stillwater igneous complex, Montana—a quantitative mineralogical study: Geol. Soc. America Mem. 80, 230 p.

Larsen, E. S., 1938, Some new variation diagrams for groups of igneous rocks: Jour. Geology, v. 46, p. 505–520.

Lovering, T. S., 1935, Geology and ore deposits of the Montezuma quadrangle, Colorado: U.S. Geol. Survey Prof. Paper 178, 119 p.

Lovering, T. S., and Goddard, E. N., 1950, Geology and ore deposits of the Front Range, Colorado: U.S. Geol. Survey Prof. Paper 223, 319 p.

Luth, W. C., Jahns, R. H., and Tuttle, O. F., 1964, The granite system at pressures of 4 to 10 kilobars: Jour. Geophys. Research, v. 69, no. 4, p. 759–773.

Moench, R. H., 1964, Geology of Precambrian rocks, Idaho Springs district, Colorado: U.S. Geol. Survey Bull. 1182–A, 70 p.

Moench, R. H., Harrison, J. E., and Sims, P. K., 1962, Precambrian folding in the Idaho Springs–Central City area, Front Range, Colorado: Geol. Soc. America Bull., v. 73, no. 1, p. 35–58.

Newton, R. C., 1966, Kyanite-sillimanite equilibrium at 750°C: Sicence, v. 151, p. 1222–1225.

Nockolds, S. R., 1954, Average chemical compositions of some igneous rocks: Geol. Soc. America Bull., v. 65, no. 10, p. 1007–1032.

Nutalaya, P., 1966, Metamorphic petrology of a part of the northeastern Front Range, Larimer County, Colorado: Boulder, Univ. Colorado Ph. D. thesis.

Orville, P. M., 1958, Feldspar investigations, *in* Annual report of the director of the Carnegie Geophys. Lab. for 1957–1958: p. 206–209.

Osborn, E. F., and Schairer, J. F., 1941, The ternary system pseudowollastonite-akermanite-gehlenite: Am. Jour. Sci., v. 239, no. 10, p. 715–763.

Peacock, M. A., 1931, Classification of igneous rock series: Jour. Geology, v. 39, no. 1, p. 54–67.

Pearson, R. C., Tweto, Ogden, Stern, T. W., and Thomas, H. H., 1962, Age of Laramide porphyries near Leadville, Colorado, *in* Short papers in geology and hydrology: U. S. Geol. Survey Prof. Paper 450–C, p. C78–C80.

Peterman, Z. E., Hedge, C. E., and Braddock, W. A., 1968 Age of Precambrian events in the northeast Front Range, Colorado: Jour. Geophys. Research, v. 73, no. 6, p. 2277–2296.

Pettijohn, F. J., 1949, Sedimentary rocks: New York, Harper & Bros., 526 p.

———1957, Sedimentary rocks [2d ed.]: New York, Harper & Bros., 718 p.

———1963, Chemical composition of sandstones—excluding carbonate and volcanic sands: U.S. Geol. Survey Prof. Paper 440–S, 21 p.

Phair, George, 1952, Radioactive Tertiary porphyries in the Central City district, Colorado, and their bearing upon pitchblende deposition: U.S. Geol. Survey TEI–247, 53 p., issued by U.S. Atomic Energy Comm. Tech. Inf. Service, Oak Ridge, Tenn.

Phair, George, and Fisher, F. G., 1962, Laramide comagmatic series in the Colorado Front Range—The feldspars, *in* Engel, A. E. J., James, H. L., and Leonard, B. F., eds., Petrologic studies (Buddington volume): Geol. Soc. America, p. 479–521.

Segnit, R. E., and Kennedy, G. C., 1961, Reactions and melting relations in the system muscovite-quartz at high pressures: Am. Jour. Sci., v. 259, no. 4, p. 280–287.

Shaw, D. M., 1956, Major elements and general geochemistry, pt. 3 *of* Geochemistry of pelitic rocks: Geol. Soc. America Bull., v. 67, no. 7, p. 919–934.

Sheridan, D. M., Maxwell, C. H., Albee, A. L., and Van Horn, R., 1958, Preliminary map of bedrock geology of the Ralston Buttes quadrangle, Jefferson County, Colorado: U.S. Geol. Survey Mineral Inv. Map MF–179.

Sims, P. K., 1964, Geology of the Central City quadrangle, Colorado: U.S. Geol. Survey Geol. Quad. Map GQ–267.

Sims, P. K., Drake, A. A., Jr., and Tooker, E. W., 1963, Economic geology of the Central City district, Gilpin County, Colorado: U.S. Geol. Survey Prof. Paper 359, 231 p.

Sims, P. K., and Gable, D. J., 1964, Geology of Precambrian rocks, Central City district, Colorado: U.S. Geol. Survey Prof. Paper 474–C, 52 p.

———1967, Petrology and structure of Precambrian rocks, Central City quadrangle, Colorado: U.S. Geol. Survey Prof. Paper 554–E, 56 p.

Smith, J. V., and Sahama, T. G., 1954, Determination of the compositions of natural nephelines by an X-ray method: Mineralogy Mag., v. 30, p. 439–449.

Spurr, J. E., and Garrey, G. H., 1908, Economic geology of the Georgetown quadrangle, Colorado, *with a section on* General geology, by S. H. Ball: U.S. Geol. Survey Prof. Paper 63, 422 p.

Stewart, D. B., and Roseboom, E. H., Jr., 1962, Lower temperature terminations of the three-phase region plagioclase–alkali feldspar–liquid: Jour. Petrology, v. 3, no. 2, p. 280–315.

Taylor, R. B., and Sims, P. K., 1962, Precambrian gabbro in the central Front Range, Colorado, *in* Short papers in geology, hydrology, and topography: U.S. Geol. Survey Prof. Paper 450–D, p. D118–D122.

Theobald, P. K., 1965, Preliminary geologic map of the Berthoud Pass quadrangle, Clear Creek and Grand Counties, Colorado: U.S. Geol. Survey Misc. Geol. Inv. Map I–443.

Tilton, G. R., and Hart, S. R., 1963, Geochronology: Science, v. 140, p. 357–366.

Tourtelot, H. A., 1962, Preliminary investigation of the geologic setting and chemical composition of the Pierre Shale, Great Plains region: U.S. Geol. Survey Prof. Paper 390, 74 p.

Turner, F. J., and Verhoogen, John, 1960, Igneous and metamorphic petrology [2d ed.]: New York, McGraw-Hill Book Co., 694 p.

Tuttle, O. F., and Bowen, N. L., 1958, Origin of granite in the light of experimental studies in the system $NaAlSi_3O_8$–$KAlSi_3O_8$–SiO_2–H_2O: Geol. Soc. America Mem. 74, 153 p.

Tweto, Ogden, and Sims, P. K., 1963, Precambrian ancestry of the Colorado mineral belt: Geol. Soc. America Bull., v. 74, p. 991–1014.

Wells, J. D., 1960, Petrography of radioactive Tertiary igneous rocks, Front Range mineral belt, Colorado: U.S. Geol. Survey Bull. 1032–E, p. 223–272.

———1967, Geology of the Eldorado Springs quadrangle, Boulder and Jefferson Counties, Colorado: U.S. Geol. Survey Bull. 1221–D, 85 p.

Wells, J. D., Sheridan, D. M., and Albee, A. L., 1964, Relationship of Precambrian quartzite-schist sequence along Coal Creek to Idaho Springs Formation, Front Range, Colorado: U.S. Geol. Survey Prof. Paper 454–O, 23 p.

Yoder, H. S., Jr., Stewart, D. B., and Smith, J. R., 1957, Ternary feldspars: Carnegie Inst. Washington Year Book 56, p. 206–214.

INDEX

[Italic page numbers indicate major references]

A — Page

Alkali-calcic series, Tertiary intrusive rocks 38, *41*
Alkali feldspar, monzonite group 25
Amphibole, monzonite group, analyses 29
Amphibolite *8*
modal analyses 9
origin 13
Analyses, chemical, feldspar, bostonite porphyry 35
chemical, hornblende-pyroxene monzonite 42
chemical and spectrographic, bostonite porphyry 36
granodiorite group 21
hornblende, amphibolite 10
monzonite group 26, *27*, 29, 32, 44
sanidinite porphyry 36
Tertiary intrusive rocks 39
modal, amphibolite 9
Brancroft layer 9
Boulder Creek Granite 17
Lawson layer 9
microcline gneiss 9
quartz diorite of St. Marys Lake 15
Silver Plume Granite 19
Archean quartz monzonite 15
Argillite, mesonorm 11
Arkose, mesonorm 11
Audubon-Albion stock, age 37

B

Bancroft fault 46, 51
Bancroft layer 7, 9
modal analyses 9
Berthoud Pass fault 51
Biotite, Boulder Creek Granite 17
monzonite group 28
quartz diorite 17
quartz diorite of St. Marys Lake 15
Biotite gneiss *3*
origin *10*
sedimentary parents 13
Biotite granodiorite porphyry, granodiorite group 22
Biotite quartz monzonite porphyry 33
Bostonite porphyry *33*
chemical and spectrographic analyses 36
Boulder Creek Granite *15*
age 3
deformation 49
modal analyses 17
Boulder Creek granite gneiss 15

C

Calc-alkali series, Tertiary intrusive rocks 38, *40*
Calc-silicate gneiss 6
origin 12

D

Dikes, biotite quartz monzonite porphyry 33
bostonite porphyry 33
granodiorite group 20, 22
monzonite group 29, 32, 33
Precambrian igneous rocks 18
sanidinite porphyry 35
Dioritic rock, monzonite group 29

E — Page

Elk Creek pluton 18
Empire stock, biotite quartz monzonite porphyry 33
contact metamorphism 29
monzonite group 22, 26, 31

F

Faults 46, *51*
Feldspar, bostonite porphyry, chemical analysis 35
Feldspathoidal hornblende-pyroxene monzonite, chemical analyses 44
monzonite group *22*
Folds *45*
trending east-northeast 51
Front Range mineral belt 1

G

Garnet, biotite gneiss 3
Glaciers 3
Granite aplite, granodiorite group 22
Granite porphyry 18
Graywacke, mesonorm 11

H

Harrison, J. E., Sims, P. R., and Moench, R. H., quoted 12
Hess, H. H., quoted 41
Hornblende, amphibolite, analyses 10
hornblende gneiss 9
monzonite group 22, 28
quartz diorite of St. Marys Lake 15
Hornblende diorite 18
Hornblende gneiss *8*
origin 13
Hornblende granodiorite porphyry, granodiorite group *20*
Hornblende-pyroxene monzonite, chemical analyses 42
monzonite group *26*
Hornblendite *17*

I, J

Idaho Springs Formation 3
Idaho Springs–Ralston shear zone 45, 49

Jim Creek fault 51

L

Laramide orogeny 3
faulting 52
Lawson layer 7, 9, 13
modal analyses 9
Lawson syncline 15, 46
Leucocratic monzonite, monzonite group 32
Linclon Mountain stock, monzonite group 22, 32
Location 1
Loch Lomond anticline 46

M, N

Magmatic differentiation, Tertiary intrusive rocks *40*
Mesonorms, calculation methods *10*
sedimentary rocks *11*

Page

Metamorphic rocks, origin 3
Metamorphism, pressure-temperature range 14
regional 3
Microcline, biotite gneiss 5
microcline gneiss 6
Silver Plume Granite 19
Microcline gneiss *6*
modal analyses 9
origin *12*
Migmatite, biotite gneiss 6
Mineral assemblages, biotite gneiss *4*
metamorphic rocks 13
Moench, R. H., Harrison, J. E., and Sims, P. R., quoted 12
Monzonite porphyry, monzonite group 32
Mount Eva anticline and syncline 46
Muscovite, biotite gneiss 4
Boulder Creek Granite 17
Muscovite plus quartz, stability limits 14
Mylonite, fault zones 52

Nepheline, monzonite group 25

P

Pegmatite 19
quartz diorite of St. Marys Lake 14
Plagioclase, biotite gneiss 6
Boulder Creek Granite 17
granodiorite group 20, 22
hornblende gneiss 9
microcline gneiss 6
monzonite group 22, 28, 31, 32
quartz diorite 17
quartz diorite of St. Marys Lake 15
Silver Plume Granite 19
Porphyritic hornblende-pyroxene monzonite, monzonite group *31*
Precambrian deformation, faults 52
folds *45*
Precambrian intrusive rocks *14*
Protoquartzite, mesonorm 11
Pyroxene, monzonite group 22, 28, 29
monzonite group, analyses 29

Q

Quartz, Boulder Creek Granite 17
hornblende gneiss 9
microcline gneiss 6
quartz diorite 17
quartz diorite of St. Marys Lake 15
Silver Plume Granite 19
Quartz-bearing monzonite porphyry, monzonite group 32
Quartz diorite *17*
Quartz diorite of St. Marys Lake *14*
modal analyses 15
Quartz monzonite gneiss 3
Quartz plus muscovite, stability limits 14
Quartzite, mesonorm 11
Quartzo-feldspathic rocks, stability limits 14
Quaternary deposits 45

R

Ranch Creek fault 51
Red Elephant Hill, microcline gneiss 7, 9
References *52*
Rogers Pass anticline and syncline 46

S

Page

Sinidinite porphyry ... *35*
Shale, mesonorm ... 11
Sillimanite, biotite gneiss ... 3
  stability limits ... 14
Sills, Precambrian intrusive rocks ... 15, 17, 18, 19
Silver Plume Granite ... 19
  age ... 3
  deformation ... 49
  modal analyses ... 19
Sims, P. R., Moench, R. H., and Harrison, J. E., quoted ... 12
Slate, mesonorm ... 11
Sodalite, monzonite group ... 25
Structural formulas, hornblende, amphibolite ... 9
  pyroxene, monzonite group ... 28
Subarkose, mesonorm ... 11
Subgraywacke, mesonorm ... 11
Swandyke Hornblende Gneiss ... 3

T

Tectonism ... 3
Tertiary intrusive rocks ... *19*
  age ... 37, *38*
  correlation ... 20
  magmatic differentiation ... *40*
  series of rock types ... *37*

U, W

Undersaturated series, Tertiary intrusive rocks ... 38, *43*
Witter Peak syncline ... 46

U.S. GOVERNMENT PRINTING OFFICE: 1969 O—332-862